Department for
Business, Energy
& Industrial Strategy

Primary Store Geomechanical Model & Report

Key Knowledge Document

NS051-SS-REP-000-00012

August 2021

Acknowledgements

Any enquiries regarding this publication should be sent to us at:
enquiries@beis.gov.uk

Contents

Foreword 5
Executive Summary 7
1.0 Introduction 9
1.1 Geomechanics Study Scope 9
2.0 Input Data 11
2.1 Regional Information 11
2.2 Surfaces and Faults 11
2.3 Well Data 13
2.3.1 Sonic and Density Logs 14
2.3.2 Well 42/25d-3 Geomechanical Data 17
2.3.2.1 Röt Halite 1 19
2.3.2.2 Röt Clay 19
2.3.2.3 Bunter Sandstone Formation 19
2.3.2.4 Image Logs and Sonic Scanner 20
2.3.3 Regional in-situ Stress Data 20
3.0 Input Grids 22
3.1 Gridding Process 22
3.1.1 Simulation Grid 23
3.1.2 Overburden Grids 26
4.0 Geomechanical Modelling 31
4.1 Geomechanical Grids 32
4.2 Geomechanical Property Modelling 35
4.2.1 P-sonic and Density 35
4.2.2 Upscaling to Geomechanical (GM) Grids 39
4.2.3 Key Property Creation and Clean-up 40
4.2.4 Pore Pressure Properties 44
4.2.5 Matrix Geomechanical Properties 45
4.3 Faults 48
4.4 Stress Initialisation 52
4.4.1 Salt Influence 53

4.4.2 Stress Initialisation Process 53
4.4.3 Stress Initialisation Checks 54
5.0 Simulation Cases 55
5.1 Scenario Tree 56
5.2 Reference Cases – 3.5,5.0 and 10 Mtpa Injection 58
5.2.1 3.5 Mpta no Brine Production 58
5.2.2 5.0 Mtpa with Brine Production 62
5.2.3 10.0 Mtpa with Brine Production 67
5.3 Seabed Iplift and Tilts – All Cases 69
5.3.1 Seabed Uplift 69
5.3.2 Seabed Tilts 70
6.0 Conclusions and Recommendations 71
7.0 References 73
Annex A – VISAGE Simulation Output Property Key 74

Foreword

The Net Zero Teesside (NZT) project in association with the Northern Endurance Partnership project (NEP) intend to facilitate decarbonisation of the Humber and Teesside industrial clusters during the mid-2020s. Both projects will look to take a Final Investment Decision (FID) in early 2023, with first CO2 capture and injection anticipated in 2026.

The projects address widely accepted strategic national priorities – most notably to secure green recovery and drive new jobs and economic growth. The Committee on Climate Change (CCC) identified both gas power with Carbon Capture, Utilisation and Storage (CCUS) and hydrogen production using natural gas with CCUS as critical to the UK's decarbonisation strategy. Gas power with CCUS has been independently estimated to reduce the overall UK power system cost to consumers by £19bn by 2050 (compared to alternative options such as energy storage).

Net Zero Teesside Onshore Generation & Capture

NZT Onshore Generation & Capture (G&C) is led by bp and leverages world class expertise from ENI, Equinor, and TotalEnergies. The project is anchored by a world first flexible gas power plant with CCUS which will compliment rather than compete with renewables. It aims to capture ~2 million tonnes of CO2 annually from 2026, decarbonising 750MW of flexible power and delivering on the Chancellor's pledge in the 2020 Budget to "support the construction of the UK's first CCUS power plant." The project consists of a newbuild Combined Cycle Gas Turbine (CCGT) and Capture Plant, with associated dehydration and compression for entry to the Transportation & Storage (T&S) system.

Northern Endurance Partnership Onshore/Offshore Transportation & Storage

The NEP brings together world-class organisations with the shared goal of decarbonising two of the UK's largest industrial clusters: the Humber (through the Zero Carbon Humber (ZCH) project), and Teesside (through the NZT project). NEP T&S includes the G&C partners plus Shell, along with National Grid, who provide valuable expertise on the gathering network as the current UK onshore pipeline transmission system operator.

The Onshore element of NEP will enable a reduction of Teesside's emissions by one third through partnership with industrial stakeholders, showcasing a broad range of decarbonisation technologies which underpin the UK's Clean Growth strategy and kickstarting a new market for CCUS. This includes a new gathering pipeline network across Teesside to collect CO2 from industrial stakeholders towards an industrial Booster Compression system, to condition and compress the CO2 to Offshore pipeline entry specification.

Offshore, the NEP project objective is to deliver technical and commercial solutions required to implement innovative First-of-a-Kind (FOAK) offshore low-carbon CCUS infrastructure in the UK, connecting the Humber and Teesside Industrial Clusters to the Endurance CO2 Store in the Southern North Sea (SNS). This includes CO2 pipelines connecting from Humber and Teesside compression/pumping systems to a common subsea manifold and well injection site

at Endurance, allowing CO2 emissions from both clusters to be transported and stored. The NEP project meets the CCC's recommendation and HM Government's Ten Point Plan for at least two clusters storing up to 10 million tonnes per annum (Mtpa) of CO2 by 2030.

TEESSIDE (NZT)

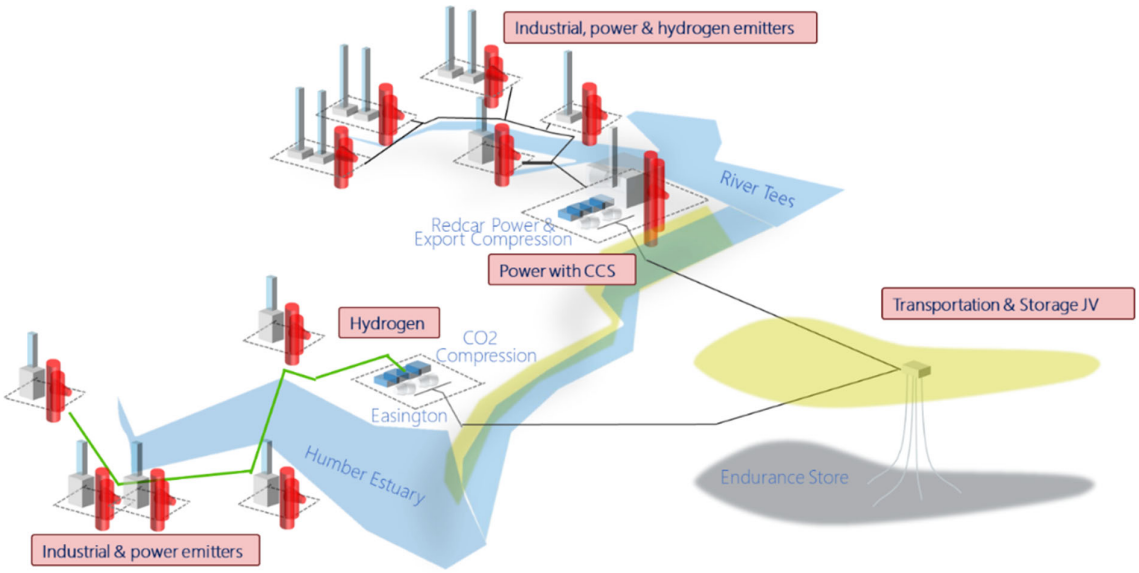

HUMBERSIDE (ZHC) NEP

The project initially evaluated two offshore CO2 stores in the SNS: 'Endurance', a saline aquifer formation structural trap, and 'Hewett', a depleted gas field. The storage capacity requirement was for either store to accept 6+ Mtpa CO2 continuously for 25 years. The result of this assessment after maturation of both options, led to Endurance being selected as the primary store for the project. This recommendation is based on the following key conclusions:

- The storage capacity of Endurance is 3 to 4 times greater than that of Hewett
- The development base cost for Endurance is estimated to be 30 to 50% less than Hewett
- CO2 injection into a saline aquifer is a worldwide proven concept, whilst no benchmarking is currently available for injection in a depleted gas field in which Joule-Thompson cooling effect has to be managed via an expensive surface CO2 heating solution.

Following selection of Endurance as the primary store, screening of additional stores has been initiated to replace Hewett by other candidates. Development scenarios incorporating these additional stores will be assessed as an alternative to the sole Endurance development.

Executive Summary

Geomechanical models and simulation in VISAGE were used to assess the stress / strain changes resulting from injection-induced pressure increases and determine the potential for failure of the primary sealing units (Röt Clay and Röt Halite) at the Endurance store for the Net Zero Teeside CCUS project. The geomechanical properties and initial in-situ stresses were defined within a Petrel 3D geomechanical grid using all available data from the Endurance area (seismic interpretations of horizons and faults, well logs, geomechanical core data, fracture tests, etc.) for all the stratigraphy from seabed down to base Zechstein Salt (Top Rotliegend).

The Röt Clay initial in-situ stress is predicted from the VISAGE modelling to be approximately 0.15 psi/ft lower at the crest just north of well 43/21-1 (~0.71 psi/ft) compared to the flank location at 42/25d-3 (0.86 psi/ft). Because of the likely crestal reduction in Röt Clay initial in-situ stress values, the Röt Halite 1, modelled with high lithostatic in-situ stresses, is also treated as part of the seal system over Endurance.

Three key pressure cases (3.5, 5 and 10 Mtpa) from the NEXUS dynamic model were simulated in VISAGE for 25 years injection, utilising different combinations of fault and matrix properties. None of the simulations using these key pressure cases displayed any plastic failure, including reactivation of faults.

The Bunter Sandstone unit displays a clear poroelastic response with the total horizontal principal stresses increasing during CO2 injection. This reduces the likelihood of failure in this unit by reducing the differential stress and keeping it below the modelled failure envelopes despite the effective stresses decreasing.

Horizontal in-situ stress reductions above the Bunter Sandstone are expected from the elastic inflation and stretching of the Bunter Sandstone during injection. The VISAGE modelling indicated a slight decrease in the Röt Clay Shmin (-0.01 to -0.03 psi/ft) reducing to a maximum change of -0.078 psi/ft in the Quaternary over the Endurance crest. These shallow stress reductions are not regarded as a significant issue for Endurance, as they are likely to be largely absorbed by the overburden, although surface facility and monitoring system designs should account for them.

Modelled maximum uplift at seabed occurs over the Endurance structure crest and ranges from 0.17m to 0.19m. These uplift values are regarded as toward the high end of expectation as they are similar to the uplift values at Top Bunter Sandstone. It is likely more uplift will be absorbed within the overburden.

Tilting of the seabed calculated from the gradient of vertical uplift was also evaluated. Modelled maximum tilt values in all cases reported here were below 0.002° and generally found on the flanks of the structure. Seabed tilting is unlikely to cause significant issues with the planned Hornsea 4 windfarm and other infrastructure.

The geomechanical model provides a useful exploration of the possible rock mechanics properties and in-situ stresses expected within and above Endurance, including the overburden fault system. With planned injection schemes of up to 10 Mtpa (with brine production where necessary) coupled with a comprehensive data gathering and monitoring program, risks of seal breach or adverse seabed uplift and tilting effects are regarded as low.

1.0 Introduction

The purpose of this document is to summarize the work program completed on geomechanical aspects of the integrated subsurface description of the Endurance store. This follows previous studies such as those completed as part of the White Rose project. Early analysis of previous studies highlighted a number of key areas to further advance understanding, which were drawn together and used in the development of the geomechanical model used to test subsurface uncertainties and assess risk.

Subsurface storage risks can be broadly classified as those relating to containment, capacity, injectivity and monitorability, with those covered by this document focussing on containment. Key areas to advance geomechanical understanding to assess containment uncertainties and risks at the Endurance store were identified as:

Stress / strain changes from injection-induced pressure increases and potential for failure of primary sealing units (Röt Clay and Röt Halite)

This was investigated via geomechanical numerical modelling and simulation studies.

1.1 Geomechanics Study Scope

Containment is a fundamental component of successful long-term storage of CO2. Building on earlier geomechanical modelling completed as part of the White Rose project, VISAGE numerical geomechanics simulation on a field scale was completed by TRACS International Limited. This sought to obtain best estimates honouring available data, applying engineering judgement to sense check results where appropriate and testing sensitivity to key parameters.

This report describes the construction, initialization and simulation of a suite of numerical geomechanical models that capture the potential impact of injecting CO2 into the Bunter Sandstone of the Endurance structure (**Figure 1**). The primary focus has been to assess the stress / strain changes from the injection pressure increases and the potential for failure of the primary sealing units (Röt Clay and Röt Halite). A list of key screening criteria is given below:

1. Failure of Röt Halite 1 and Röt Clay sealing units via tensile or shear failure.
2. Tensile or shear reactivation of faults mapped in the overburden of Endurance down to Top Röt Halite 3
3. Uplift and tilt of seabed
4. Tensile or shear failure of Bunter Sandstone

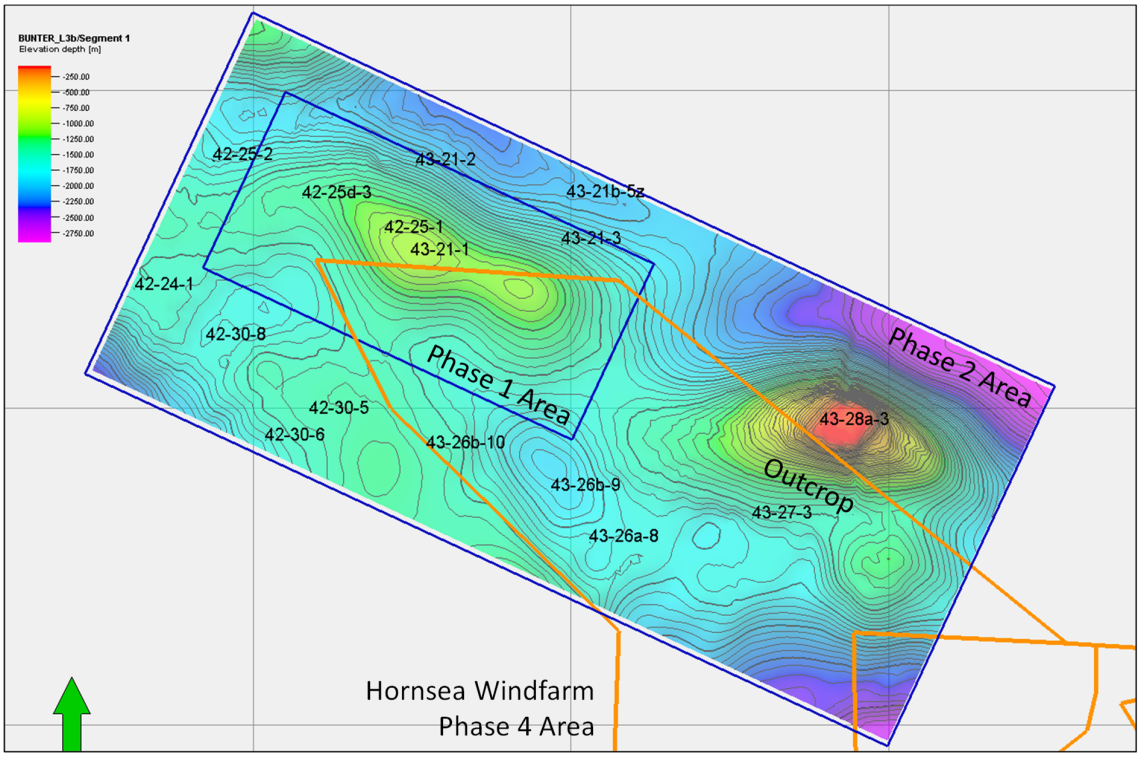

Figure 1 - Endurance structure location map. Surface is Top Bunter Sandstone.

A number of sensitivities to injection pressure scenarios, matrix rock properties, downward fault extents and fault properties have been performed to map out the potential for plastic failure under different injection schemes. In addition to the results of specific numerical simulation cases, other possibilities of potential failure are discussed that augment the numerical modelling results.

The work has been performed using the Petrel Reservoir Geomechanics software (version 2019.4) and VISAGE numerical geomechanics simulator software (versions 2019.2 and 2020.1). It should be noted that this modelling has been carried out as a one-way coupled process. This is where VISAGE uses the output from a reservoir simulator with changes in pressure at particular time steps and calculates the stresses and strains (elastic and plastic). After a solution is reached, VISAGE then takes the next pressure step and recalculates the stresses and strains until all steps have been simulated (or the job fails to converge due to extreme gradients in stress, strain or displacement). Updating of properties such as permeability after the VISAGE calculations and re-exporting to the reservoir simulator in a two-way coupled model has not been undertaken in this study. In addition, thermal effects have also not been modelled during this work but have been captured in separate modelling exercises (please see Well Injectivity Thermal Fracturing Study with Reveal™ KKD).

The phase of work detailed in this report covers a rebuild of the property grid over Endurance and outcrop area including the overburden sequence to seabed and a geomechanical model derived from that property grid but built over the Endurance structure only. Both models utilised all the available well data in the area plus horizons and faults derived from seismic interpretation (please see Geophysical Model KKD). Later phases of work will be carried out as

new data is integrated (for example, Phase 2+ area marked on map below. Please note this nomenclature in this report addresses phases of modelling and not the phased development of the store). The Phase 1 area in **Figure 1** shows the area covering the main Endurance structure, that is the focus of this report.

2.0 Input Data

2.1 Regional Information

The CO2 store unit is the thick Triassic Bacton Group Bunter Sandstone. This high quality, aeolian and fluvial sandstone was deposited on the Bunter Shale, which occurs above the Stassfurt Halite of the Zechstein Supergroup. The immediate sealing units above the Bunter Sandstone are the Bacton Group Röt Clay and the Röt Halite. These are overlain by Triassic Dowsing Formation and Haisborough Group mudstones and evaporites and Lower Jurassic (Liassic) clay and silt mudstones. Younger, Middle Jurassic to Tertiary sediments onlap the flanks of Endurance which have been eroded over the crest during various pulses of Mesozoic to Cenozoic diapirism and inversion. Variable thickness Quaternary sediments occur over the crest of Endurance, which are deposited directly on eroded Lower Jurassic. In the outcrop location close to seabed, a thin veneer of Quaternary was deposited directly on steeply dipping Liassic to Bacton Group sediments, including the Bunter Sandstone and Bunter Shale. Following earlier White Rose project interpretation, the Zechstein halites are also currently interpreted sub-cropping at Base Quaternary in the centre of the outcrop. New ultra-high resolution seismic over the outcrop may provide further information on this.

The Petrel project is setup with all distance units in metres, pressures in bar and the following coordinate system:

- Coordinate reference system X, Y: ED50 * UKOOA-CO / UTM zone 31N [23031*1311] (ED50 / UTM zone 31N assoc. with ED50 to WGS 84 (18)) [BP,62303118]

2.2 Surfaces and Faults

Key surface and fault interpretations were derived from 3 main seismic datasets: 2D seismic (of various vintages); the 1997 OBC 3D survey and the 2013 Polarcus towed streamer 3D survey (**Figure 2** and **Figure 3**). The faults have been picked as detailed in the Geophysical Model KKD. The faults over Endurance are not interpreted to extend below the Röt Halite 3 although further ESE in the saddle area and around the outcrop, the faults cut down into the Bunter Sandstone.

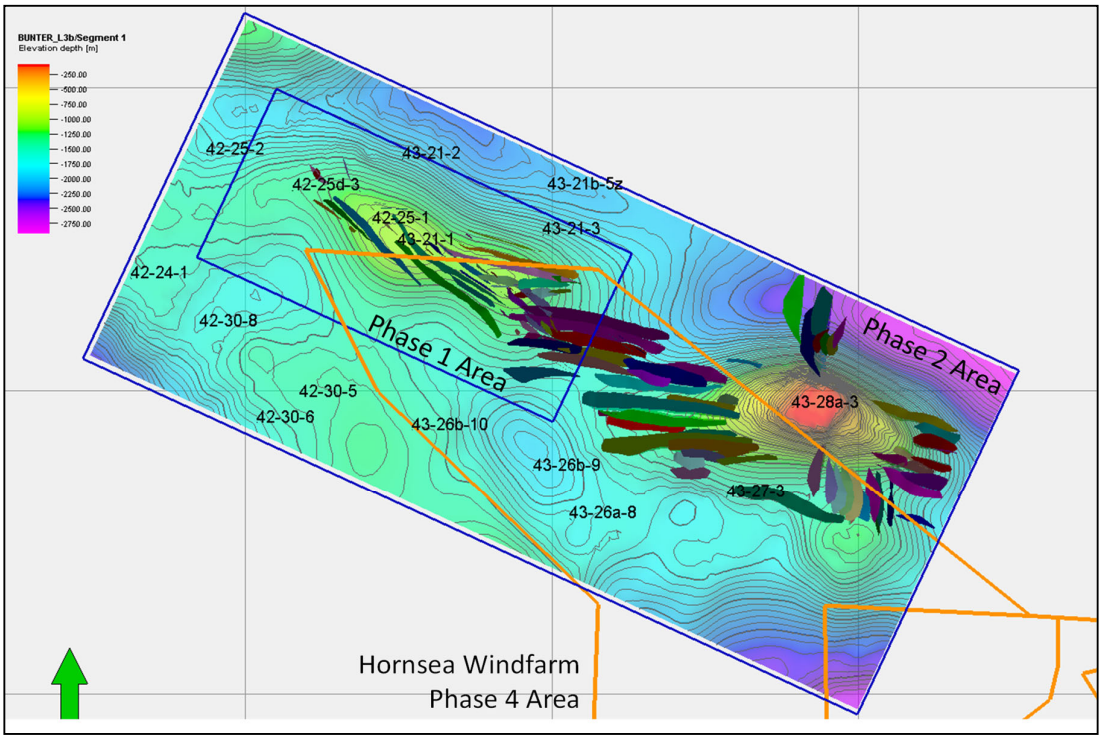

Figure 2 - Endurance overburden fault surfaces and Top Bunter Sandstone interpretation. Blue rectangle encompasses the Endurance structure. Orange polygon is planned Hornsea windfarm Phase 4 area.

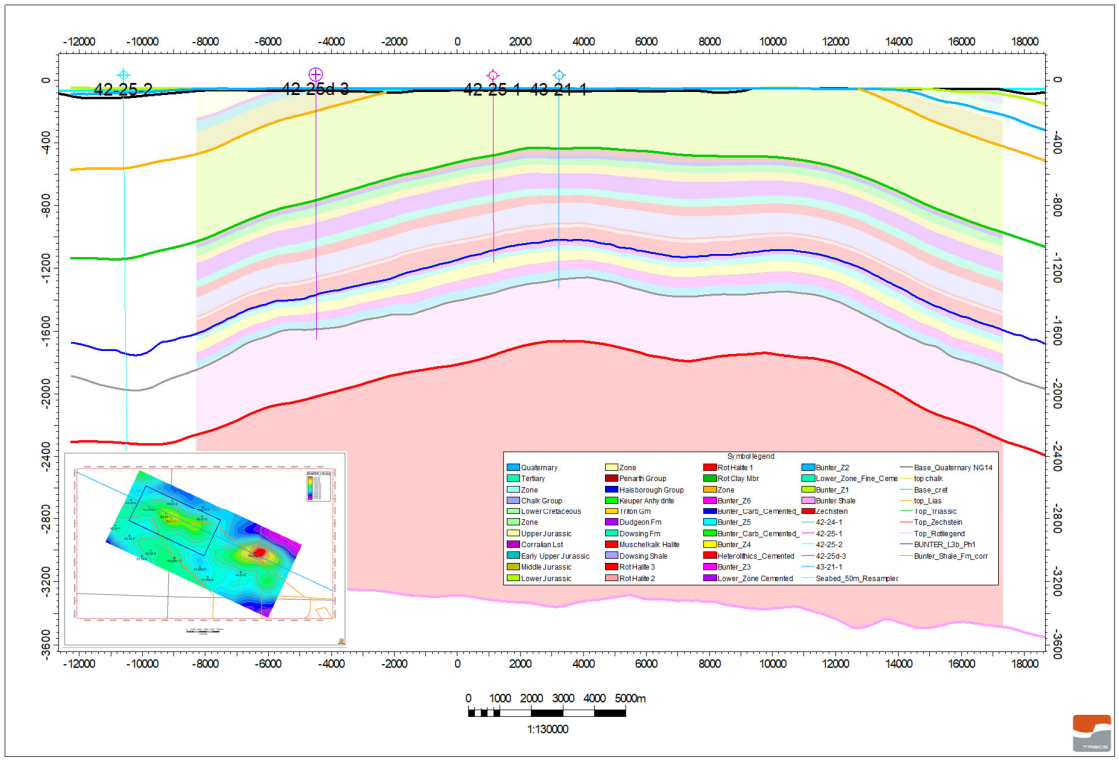

Figure 3 - Seismic input surfaces within Endurance structure area. Line of section shown on inset map.

2.3 Well Data

Wells used in the project are shown in **Figure 1** and listed in Table 1. Six wells are located within the Endurance structure/GM Phase 1 area and three contain key stress and geomechanical property data used during the modelling (Table 1).

Table 1 - Endurance project wells list.

Name	Surface X [m]	Surface Y [m]	TD (MD) [m]	Notes
42-24-1	352568.72	6007407.65	4145.30	
42-25-1	368291.58	6011023.82	1195.00	Key data well; Endurance WNW shallow flank
42-25-2	357477.70	6015578.40	3516.60	Endurance WNW deep flank
42-25d-3	363098.78	6013203.09	1693.80	Key data well; Endurance WNW mid flank
42-30-5	363536.59	5999616.83	3350.10	
42-30-6	360778.90	5997932.35	3295.00	
42-30-8	357031.59	6004254.82	3218.00	
43-21-1	369943.96	6009606.05	1362.50	Key data well; Endurance crest
43-21-2	370252.99	6015287.85	4954.00	Endurance NNE deep flank
43-21-3	379416.21	6010308.41	3565.00	Endurance E deep flank
43-21b-5z	379750.57	6013254.83	3535.70	
43-26a-8	381171.95	5991555.72	3376.30	
43-26b-9	378772.69	5994765.93	3546.30	

43-26b-10	370893.31	5997446.03	3246.10	
43-21b-5	379750.57	6013254.83	2711.20	
43-27-3	391404.40	5993008.24	4157.50	Outcrop S deep flank
43-28a-3	395649.75	5998916.42	3659.40	Outcrop W shallow flank

2.3.1 Sonic and Density Logs

Figure 4 and **Figure 5** show the distribution of P-sonic and density log data respectively within the Phase 2 Endurance area. It can be seen that the P-sonic data coverage is good in most wells, particularly below the 13 3/8" casing shoe set within the Lias. However, only well 42/25d-3 contains S-sonic data.

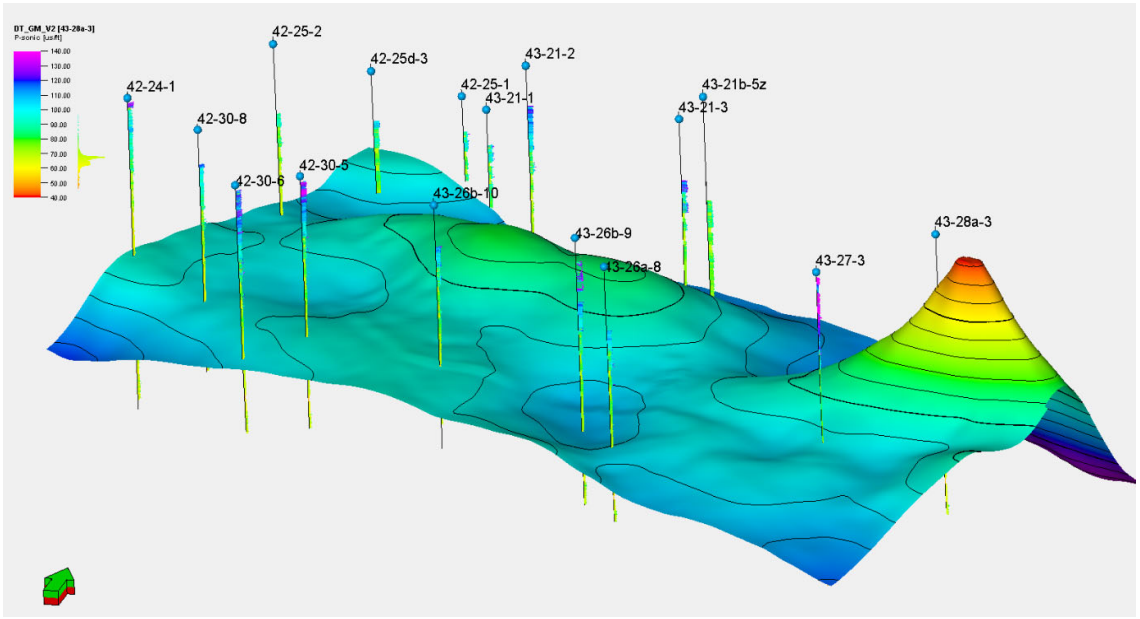

Figure 4 - Endurance area distribution of P-sonic log data. Surface is Top Zechstein.

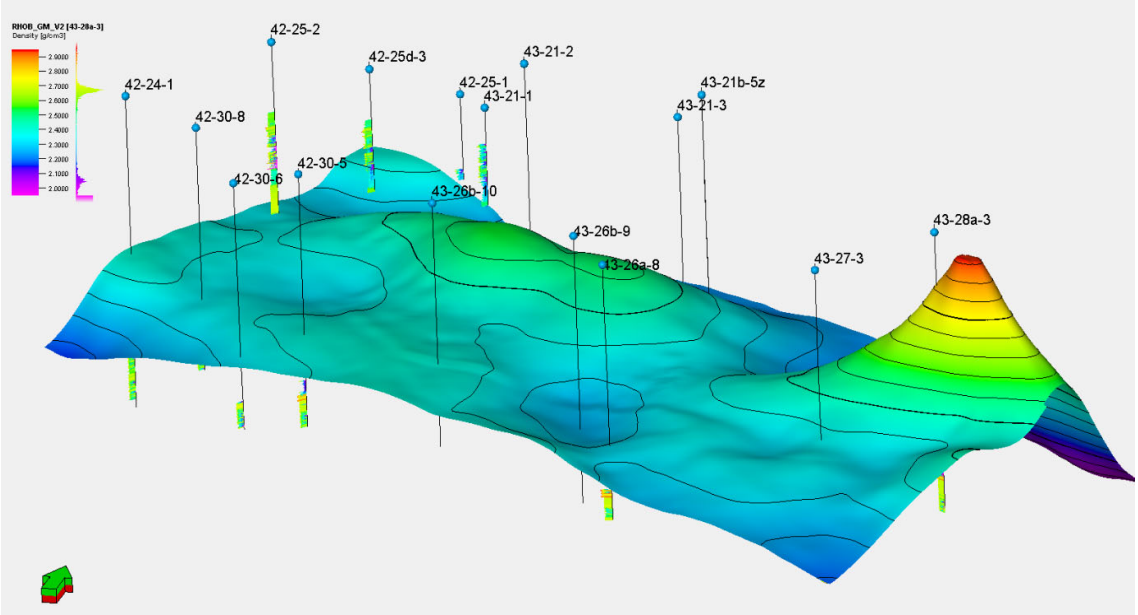

Figure 5 - Figure 29 Endurance area distribution of density log data. Surface is Top Zechstein.

The density log data is very sparse with most density logs taken within the Rötliegend sequence and only four wells have data above Top Zechstein. The best coverage is in well 42/25-2 on the deep WNW flank of Endurance just outside the Endurance structure area.

To address the shortcomings in density log availability, correlations were created to the P-sonic data to enable the creation of estimated density logs. Log density (RHOB_GM_V2) versus log P-sonic (DT_GM_V2) is shown in **Figure 6**. There is no overall trend but there are clear trends per lithology. These trends per lithology were used to create the DENS_DT_TREND log in all wells with P-sonic data. DENS_DT_TREND was then spliced with the real density data (RHOB_GM_V2) to create DENS_DTT_Cmb.

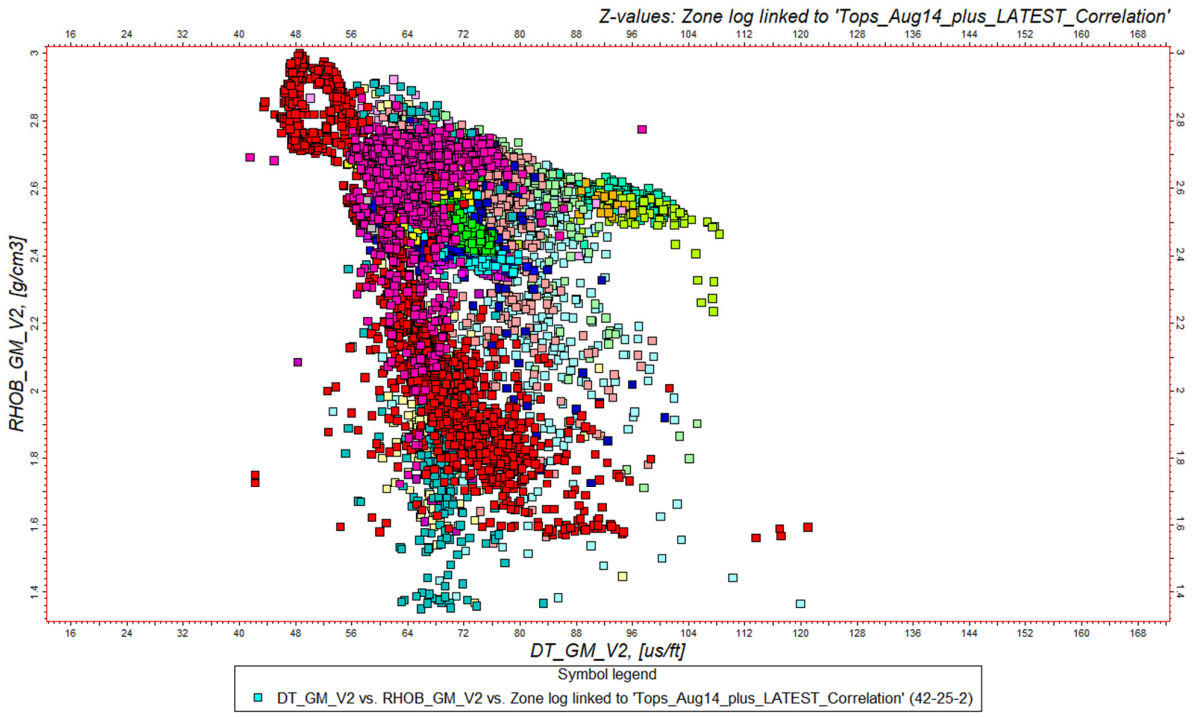

Figure 6 - Density versus P-sonic data coloured by unit.

Shear sonic also only exists in well 42/25d-3. **Figure 7** shows the correlation between S-sonic and P-sonic, which is good across all values. **Figure 7** also shows the correlation between Vs from S-sonic versus Vp from P-sonic. Two trends were defined – a linear trend valid at velocities below 3000 m/s and a curved trend valid from 3000 m/s. These Vs versus. Vp correlations were defined to minimise unrealistically low Vs values at low Vp values and to simplify the process by defining Vs estimates directly on the upscaled Vp properties. The final geomechanical grid Vs vs. Vp properties are shown by the red points in the lower part. These points are defined from a combination of the two trends described above.

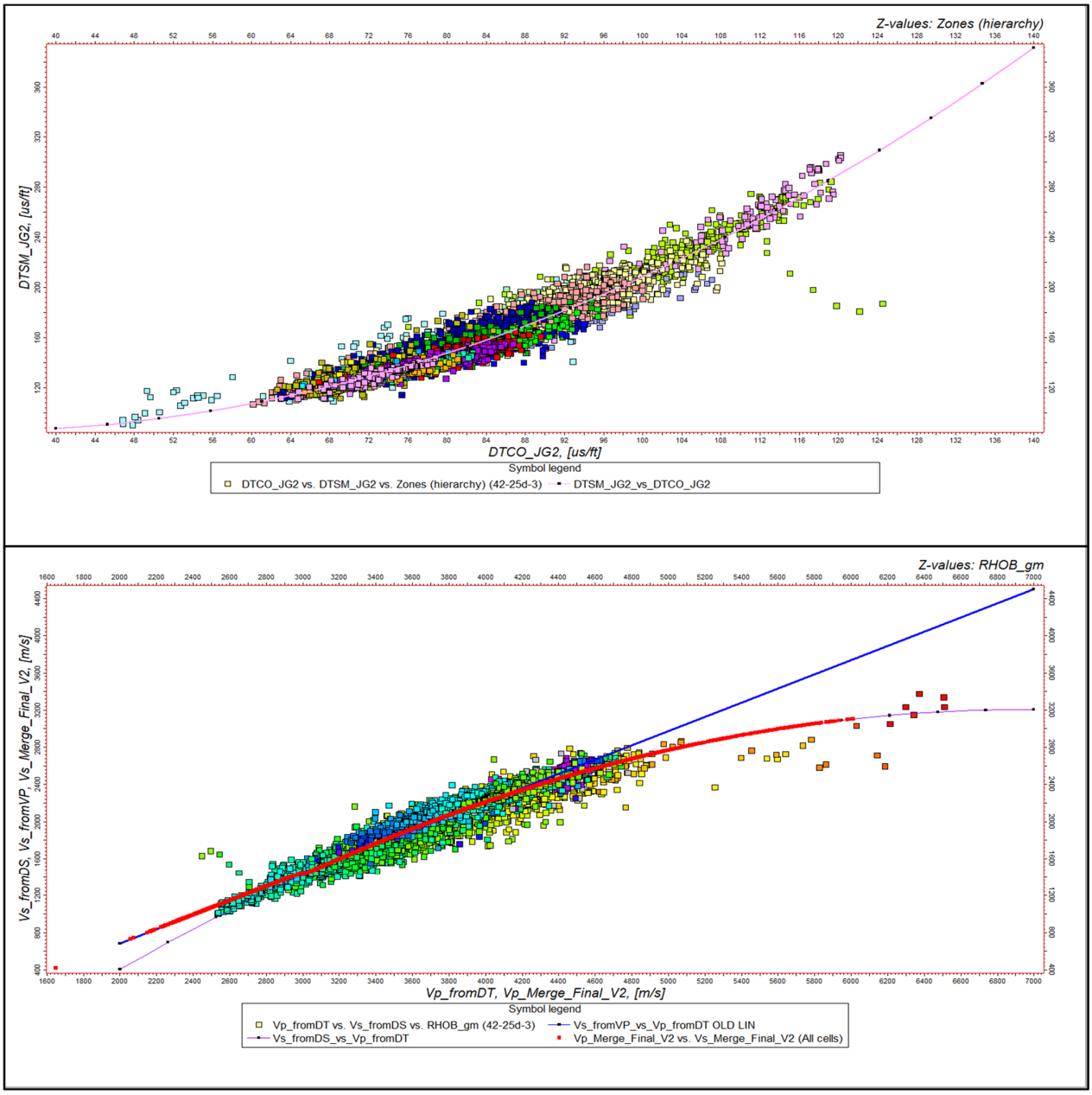

Figure 7 - Upper: S-sonic versus P-sonic in well 42/25d-3. Lower: Vs from S sonic versus. Vp from P-sonic in well 42/25d-3. Red points are calculated Vs versus. Vp from upscaled P-sonic.

2.3.2 Well 42/25d-3 Geomechanical Data

Well 42/25d-3 was drilled in 2013 by National Grid as part of the White Rose Carbon Capture and Storage (CCS) project. It was a dedicated appraisal well for that CCS project that included a significant amount of geological, reservoir engineering and geomechanical data gathering specifically designed for CCS store appraisal. The key elements of the geomechanical data acquisition and analysis program are listed below:

- Multiple confined core tests of static elastic parameters, static compressive strength and tensile strength plus acoustic velocities in the Röt Halite, Röt Clay and Bunter Sandstone. Tests performed on fresh state core and CO2 aged core by FracTech.
- Openhole logs, image logs and advanced sonic logs to determine in-situ dynamic elastic and strength parameters and in-situ stress azimuths and horizontal stress anisotropy
- Formation Integrity Test (FIT) in Röt Halite to determine minimum halite stress (regarded as lithostatic)
- MicroFrac tests in Röt Clay and Bunter Sandstone to obtain the minimum principal stress (regarded as Shmin)

It is beyond the scope of this work to describe these tests and further analyses in any detail. However, this data has been reviewed and used to constrain the Endurance model reported here and some of the results are described below with respect to how they have been used in the geomechanical model. **Figure 8** shows the core test data and log-derived properties (Reference Case model) in well 42/25d-3.

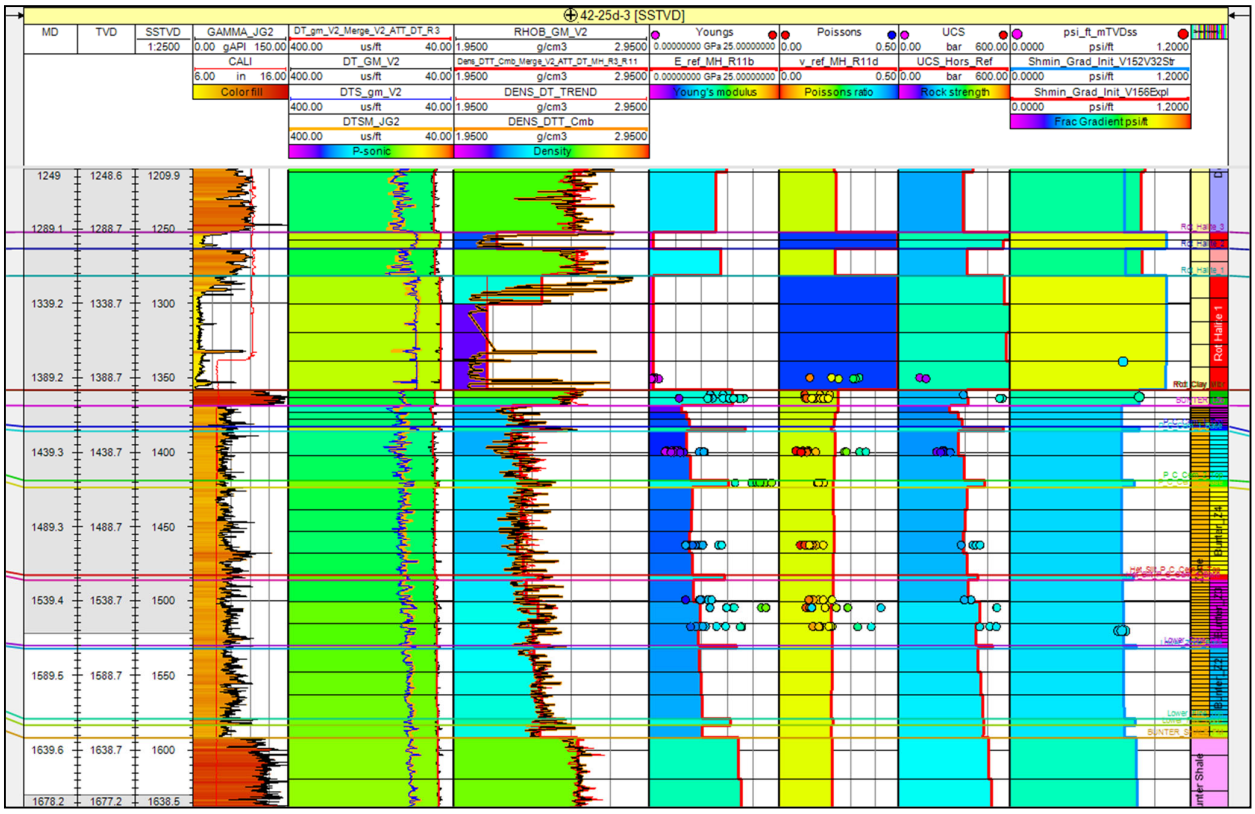

Figure 8 - Geomechanical data in well 42/25d-3.

Core derived elastic properties (Young's modulus and Poisson's ratio) and confined strengths were obtained at confining pressures of 20, 50 and 100 bar on separate plugs taken from the same depth. Plugs were prepared according to ISRM criteria. Some of the samples were also CO2 aged.

Note that all these core derived values represent ‘static’ estimates of elastic properties and strengths, which are taken under stable, usually drained conditions, over relatively long periods of hours or days. These are generally accepted as the values to use directly in geomechanical modelling with pressure changes of a similar to longer timeframe such as injection and/or production. Log or seismic derived values are regarded as ‘dynamic’ and effectively represent a stiffer response of the rock under short duration (acoustic frequency) timeframes with little or no movement of the pore fluid meaning they typically act as an undrained system.

2.3.2.1 Röt Halite 1

The Röt Halite 1 core data is highly uncertain, as the samples were coarsely crystalline so strength and elastic moduli values may not be representative. In addition, whilst halite is a relatively stiff material at surface conditions with short duration tests, on geological periods, halite behaves as a creeping material. Whilst creep tests were obtained for the Röt Halite, further analysis is required to ensure any derived creep parameters are appropriate for the Endurance modelling. Note that creeping behaviour was not modelled for the halites in the Endurance area model due to various computational issues. The details of how the halites were modelled are discussed in later sections.

2.3.2.2 Röt Clay

The elastic properties shown in **Figure 8** are from all confining pressures so some scatter is expected. There is no significant difference in the Young’s modulus values between different confining pressures although the highest values occur at the lower confining pressures. Most are in the range of 11 to 17 GPa. Poisson’s ratio shows a trend of increasing values with increasing confining pressure with most values in the range of 0.12 to 0.20.

For each group of confining pressures, Unconfined Compressive Strength (UCS) and friction angle (FA) estimates were made by FracTech by linear regression of the confined strength samples. Most estimated UCS values are in the range of 552 to 689 bar. However, the lowest value is approximately 348 bar and the highest approximately 896 bar. Only two groups of samples were CO2 aged and the results do not appear to be significantly different to the fresh state samples. The lower value of 348 bar was used for matching the log-derived values at 42/25d-3. This was to provide some conservatism to the Röt Clay frictional strength model.

Tensile strength was obtained from Brazilian tests. The fresh state samples have a range between 22 and 72 bar with an average of 45 bar. The samples with 30 days of CO2 ageing have a range from 23 to 47 bar with most values around 42 bar and an average of 38 bar. The average for all tests is 41 bar which is approximately 12% of the reference case 348 bar UCS. Tensile strengths were treated as a sensitivity in the Endurance geomechanical modelling but they range between 1 bar and 10% of UCS and are therefore similar to or lower than the CO2 aged samples.

2.3.2.3 Bunter Sandstone Formation

There is a large variability in elastic property values in the Bunter Sandstone. This is controlled by three main factors, particularly for Young’s modulus.

1. Confining stress. Tests at 20 bar confinement are typically lower than those at 50 and 100 bar which overlap significantly
2. Rock quality. Samples from intervals with lower porosity or greater clay content have higher Young's moduli. There is a general trend of decreasing porosity / increasing clay content with depth in 42/25d-3
3. Cementation. Very high Young's moduli occur in thin cemented intervals. Some of these are picked as discrete zones others occur within otherwise higher porosity intervals

From **Figure 8** it can be seen that Young's modulus generally has moderate to low values in non-cemented intervals and an overall trend of increasing values with depth. Poisson's ratio is more scattered with a weaker relationship with depth / rock quality and no relationship to confining pressure.

UCS values also show a moderate relationship with rock quality with values increasing with decreasing porosity / increased clay content.

The log showing the best correlation with Young's modulus and UCS is density. P-sonic is less sensitive.

2.3.2.4 Image Logs and Sonic Scanner

Schlumberger Dual OBMI and UBI logs were taken in the 8 ½" hole section. The hole was close to gun barrel so no breakouts are visible. No induced fractures were imaged either. A few minor natural fractures may occur in the Röt Clay and some cemented fractures in the Bunter Sandstone. Most features relate to bedding in the Bunter Sandstone.

A Schlumberger Sonic Scanner log was also taken in the 8 ½" hole section. The benefit of this log is that dispersion analysis allows different types of anisotropy (structure, near wellbore alteration / damage, in-situ stress) to be discriminated. The 8 ½" hole is near vertical, in good condition with few natural fractures. Some minor slowness anisotropy of 4–8% that was attributed to stress anisotropy was detected at 1417 mMD in the Bunter Sandstone Z6. The fast shear azimuth (assumed to be SHmax) was estimated at 92-105°. This direction is slightly different to the direction of 115° assumed for most of Endurance based on regional data and the Endurance pericline azimuth plus Rötliegend fault trend (Williams et al 2015). However, because the detected stress anisotropy is low, some local variability in SHmax is expected and the Endurance structure is locally oriented more E-W in the vicinity of 42/25d-3.

2.3.3 Regional in-situ Stress Data

Although a number of wells have been drilled in the area, most are focused on the pre-salt Rötliegend sequence and the Triassic sequence in this part of the Southern North Sea is not particularly well sampled in terms of in-situ stress data. In general, the Triassic is characterized by Permian Zechstein salt-cored periclinal features with occasional diapirs. Faulting associated with the structures in the Triassic may have occurred before or during one of the pulses of halokinesis. As a result, the in-situ stress system in the post Zechstein sequence is probably decoupled from the in-situ stresses in the Rötliegend in terms of both magnitudes and orientations.

Whilst the bulk of the dedicated in-situ stress tests were taken in well 42/25d-3, Formation Integrity Test (FIT) and Leak-off Test (LOT) data is also available in a number of other wells. MicroFrac data from the Röt Clay and Bunter Sandstone in 42/25d-3 were re-interpreted by BP as part of this project. These values are included in **Table 2** below.

Table 2 - Endurance area in situ stress data.

Well	Depth [mMD]	Shoe ins	MW [PPG]	Test Pres [bar]	Pres [psi/ft TVDss]	Pres [bar/m TVDss]	Test Type	Lithology	Unit
42-25d-3	751.64	13.38	11.00	140.13	0.869	0.197	FIT	Shale	Lias
42-25d-3	1378.31	12.25	10.00	226.89	0.749	0.169	FIT	Salt	Röt Halite 1
42-25d-3	1402.08	None	0.00	264.07	0.857	0.194	Microfrac	Shale	Röt Clay
42-25d-3	1559.66	None	0.00	247.73	0.720	0.163	Microfrac Low	Sandstone	Bunter Sst
42-25d-3	1559.66	None	0.00	254.69	0.741	0.168	Microfrac Mid	Sandstone	Bunter Sst
42-25d-3	1559.66	None	0.00	262.14	0.762	0.172	Microfrac High	Sandstone	Bunter Sst
42-25-1	565.00	13.38	10.92	93.26	0.775	0.175	FIT	Shale	Lias
43-21-1	565.40	13.38	9.70	92.09	0.766	0.173	FIT	Shale	Lias
43-21-3	886.00	20.00	-999.25	141.65	0.741	0.168	FIT	Shale	Lias
43-28a-3	487.68	20.00	10.20	110.12	1.078	0.244	FIT	Shale	Bunter Shale
43-28a-3	1065.28	13.38	10.70	225.52	0.969	0.219	FIT	Salt	Zechstein
43-27-3	652.88	13.38	8.60	120.45	0.865	0.196	FIT	Shale	Lias
43-27-3	2321.36	9.63	11.50	562.25	1.089	0.246	LOT	Shale	U Zechstein Z5
42-25-2	1000.66	20.00	10.50	175.27	0.802	0.182	LOT	Shale	Lias
42-25-2	2334.77	13.38	11.50	521.01	1.003	0.227	FIT	Salt	Zechstein Aller Halite
42-25-2	3124.20	9.63	13.00	498.93	0.715	0.162	FIT	Sandstone	Rötliegend

The most reliable data in terms of estimating the minimum principal total stress (S3) are the MicroFrac tests in well 42/2d-3 as they are specifically designed to determine S3. FITs provide a lower limit to S3 as they don't exceed the formation strength. LOT data does exceed the formation strength but the values are often less reliable than MicroFracs and similar tests due to near wellbore effects.

Despite these limitations, a number of conclusions can be drawn relating to S3 (Shmin) magnitudes relating to Endurance:

Halites generally have lithostatic stress magnitudes as expected from their long-term creep behaviour.

The Röt Clay has higher in-situ stress than the Bunter Sandstone. This is expected based on the differing elastic properties in these two units.

The shallow sequence above Röt Halite 3 to Seabed is poorly sampled by logs but FIT and LOT data indicates that an S3 (Shmin) value of 0.80 psi/ft or 0.182 bar/m is a reasonable estimate at base Lias Group levels of -530 to -713 mTVDss over Endurance.

Density log derived estimates of the vertical principal total stress (Sv) indicate values of 0.99 to 1.03 psi/ft from base Lias Group to Base Bunter Sandstone Formation respectively.

Based on the above analysis, the in-situ stress regime in Endurance is regarded as normally stressed with vertical stress (Sv) greater than maximum horizontal stress (SHmax) and minimum horizontal stress (Shmin). From the Sonic Scanner analysis in well 42/25d-3 and regional considerations, the SHmax/Shmin ratio within the Bunter Sandstone is estimated at around 1.05. In general, shales have higher SHmax/Shmin anisotropies than sandstones so a SHmax/Shmin of 1.10 is regarded as more reasonable for the Röt Clay. The Röt Halite and Zechstein halites are regarded as lithostatic where Sv = SHmax = Shmin.

3.0 Input Grids

This section describes the process to create the relevant base and grids that are used as the basis for the geomechanical grids.

3.1 Gridding Process

Figure 9 shows a summary of the entire gridding workflow involving various imported and derived grids leading to the final geomechanical grids. The process appears somewhat convoluted with multiple intermediate grids. However, this approach allowed the rapid exploration of different layering schemes, cells sizes and grid areas to optimise the geomechanical simulation run-times whilst still capturing the key characteristics of each lithology.

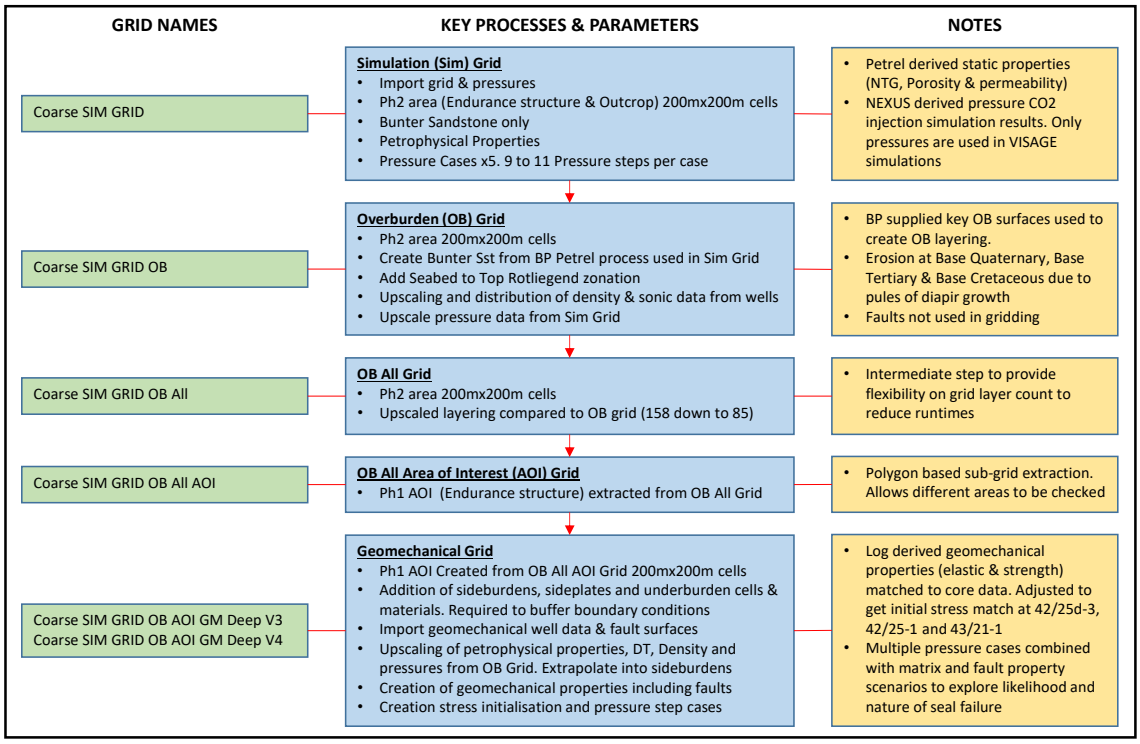

Figure 9 - Endurance Phase 1 geomechanical modelling workflow.

3.1.1 Simulation Grid

The Simulation Grid (Sim Grid) was imported into the working Petrel project from a BP Petrel project. This preserved all the processes and input data used to generate the grid. The Sim Grid was created over a relatively large area that encompasses the Endurance structure and the Bunter Sandstone outcrop to the ESE.

As part of the simulation, injectors and brine producers were placed on the flanks of Endurance to manage the CO2 migration pathway within the structure and pressures during injection. The Bunter Sandstone sub-crops at Base Quaternary or possibly Seabed on the flanks of the outcrop and it is believed to be hydraulically open at this location. Outcrop related brine outflow was modelled in NEXUS by a dummy wellbore. Whilst this outcrop related flow would have some minor impact on the Endurance pressures, the outcrop area was not modelled during this study.

The simulation results were exported from NEXUS and then imported into RMS. The simulated pressure and saturation properties for each case were imported into the Petrel Sim Grid. A number of cases were supplied which are listed in **Table 3**.

Table 3 - NEXUS injection cases used in Endurance geomechanical modelling.

Petrel Geomechanics Case Name	Description
3.5mtpa_case1	Low injection rate case, no brine production
5mtpa_case2	Moderate injection rate case with brine production. Reference Case
10mtpa_case3	High injection rate case with brine production.

The various simulated pressure steps are defined below in **Table 4**. The table also defines which steps were used in the VISAGE simulations. In all cases, the initial pressure + injection pressures + one post injection monitoring pressure were simulated. This provided the best distribution of pressure changes that captured the pressure trends modelled.

Table 4 - Details of imported pressure cases and VISAGE subset.

Date	Definition	Applicable Cases	Used in VISAGE
1st Jan 2024	Initial Pressure	All	Y
1st Jan 2025	Injection	All	N
1st July 2025	Injection	3.5, 5.0, 10.0,	N
1st Jan 2026	Injection	All	Y
1st Jan 2030	Injection	All	Y
1st Jan 2035	Injection	All	Y
1st Jan 2040	Injection	All	N
1st Jan 2045	Injection	3.5, 5.0, 10.0,	Y
1st Jan 2050	Injection	All	Y
1st Jan 2500	Monitoring	3.5, 5.0, 10.0,	Y

Figure 10 shows the Sim Grid porosity property and saturation and pressure from the 2050 5.0 Mtpa case. Note that the pressures vary much more smoothly in comparison to the saturations. This is primarily a function of the high permeability in the Bunter Sandstone.

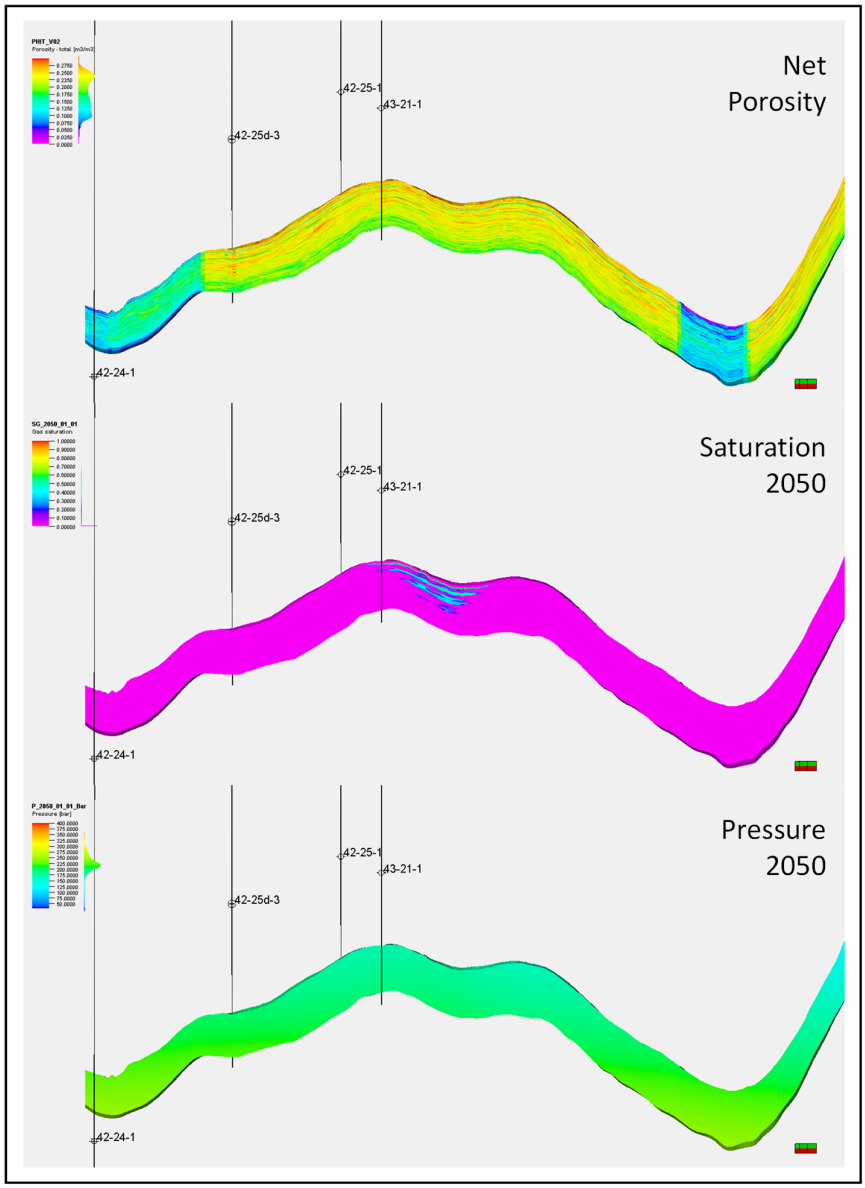

Figure 10 - Sim Grid porosity, saturation, and pressure at end injection in 2050 for the 5.0 Mtpa case. Section shown is Endurance crest viewed to the NNE.

The NEXUS simulations were all performed prior to, and in isolation from, the VISAGE simulations. Therefore, the pressure steps were used in one-way coupling mode. This means that the pressure steps are given inputs to the geomechanical model and the VISAGE simulations calculate the geomechanical responses of the Bunter Sandstone CO2 store, cap rocks and overburden to these pressure changes.

3.1.2 Overburden Grids

Three separate grids were created that incorporated the overburden section above Endurance. This is required to accurately model the stresses, strains and displacements occurring in the matrix and on the mapped faults from the Top of the Bunter Sandstone (the upper limit of the modelled injection pressures) to the Seabed. The processes adopted are described in more detail below.

3.1.2.1 Overburden Grid

This is essentially derived from the Sim Grid modelling process with the addition of extra surfaces in the overburden sequence. The steps followed are described below:

1. The AOI_New_Proposal_Final polygon object was used to create a simple grid aligned WNW-ESE with 200m x 200m cell dimensions. Faults are not included in the gridding. This is mainly because they are low throw entities with little or no expression on the interpreted surfaces. It is also because Petrel Geomechanics will remove gridded faults during the geomechanical gridding process and create a smoothed grid. Faults are added back in later as discontinuity objects.
2. Horizon modelling utilised seismic surfaces (**Figure 11**). Note that the well tops used are from Tops_Aug14_plus_LATEST_Correlation for all horizons except Top Bunter L3b and Top Bunter Shale, which are from Reservoir_Tops_Oct 19_Plus_Bunter_cemented_intervals. The former top set is inherited from the White Rose project work on Endurance. The latter set were re-interpreted by NZT/NEP project after an intra Bunter Sandstone repicking exercise with particular focus on the intra Bunter Sandstone cements. A few further edits were made to both top sets during this work. Note that the Seabed, Base Quaternary and Base Cretaceous Unconformity (BCU) were set as erosional. All other parameters are as per Petrel defaults.

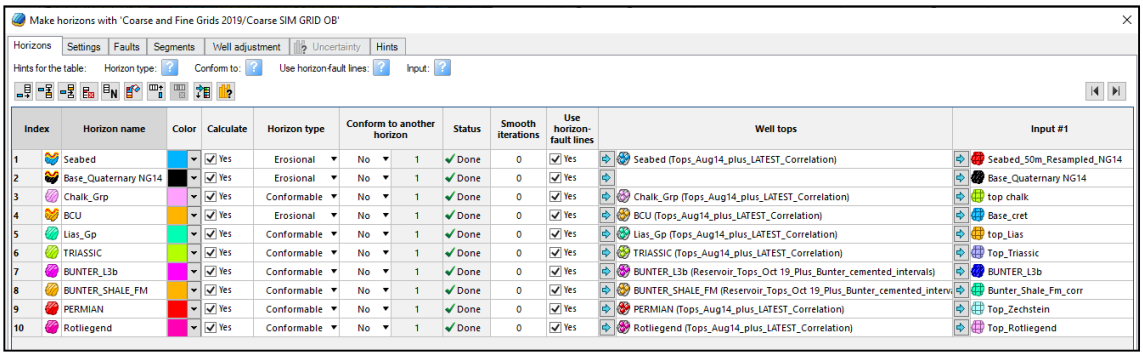

Index	Horizon name	Color	Calculate	Horizon type	Conform to another horizon		Status	Smooth iterations	Use horizon-fault lines	Well tops	Input #1
1	Seabed		Yes	Erosional	No	1	Done	0	Yes	Seabed (Tops_Aug14_plus_LATEST_Correlation)	Seabed_50m_Resampled_NG14
2	Base_Quaternary NG14		Yes	Erosional	No	1	Done	0	Yes		Base_Quaternary NG14
3	Chalk_Grp		Yes	Conformable	No	1	Done	0	Yes	Chalk_Grp (Tops_Aug14_plus_LATEST_Correlation)	top chalk
4	BCU		Yes	Erosional	No	1	Done	0	Yes	BCU (Tops_Aug14_plus_LATEST_Correlation)	Base_cret
5	Lias_Gp		Yes	Conformable	No	1	Done	0	Yes	Lias_Gp (Tops_Aug14_plus_LATEST_Correlation)	top_Lias
6	TRIASSIC		Yes	Conformable	No	1	Done	0	Yes	TRIASSIC (Tops_Aug14_plus_LATEST_Correlation)	Top_Triassic
7	BUNTER_L3b		Yes	Conformable	No	1	Done	0	Yes	BUNTER_L3b (Reservoir_Tops_Oct 19_Plus_Bunter_cemented_intervals)	BUNTER_L3b
8	BUNTER_SHALE_FM		Yes	Conformable	No	1	Done	0	Yes	BUNTER_SHALE_FM (Reservoir_Tops_Oct 19_Plus_Bunter_cemented_interv	Bunter_Shale_Fm_corr
9	PERMIAN		Yes	Conformable	No	1	Done	0	Yes	PERMIAN (Tops_Aug14_plus_LATEST_Correlation)	Top_Zechstein
10	Rotliegend		Yes	Conformable	No	1	Done	0	Yes	Rotliegend (Tops_Aug14_plus_LATEST_Correlation)	Top_Rotliegend

Figure 11- Overburden grid input surfaces and well tops used in grid construction.

3. The Make Zones Process added several additional zones throughout the overburden and within the Bunter Sandstone. The settings details are shown in **Figure 12** and **Figure 13**. Note that all zones are constructed as conformable to well tops using Tops_Aug14_plus_LATEST_Correlation except for the Röt Clay, which uses an isochore surface and well tops from Reservoir_Tops_Oct 19_Plus_Bunter_cemented_intervals.

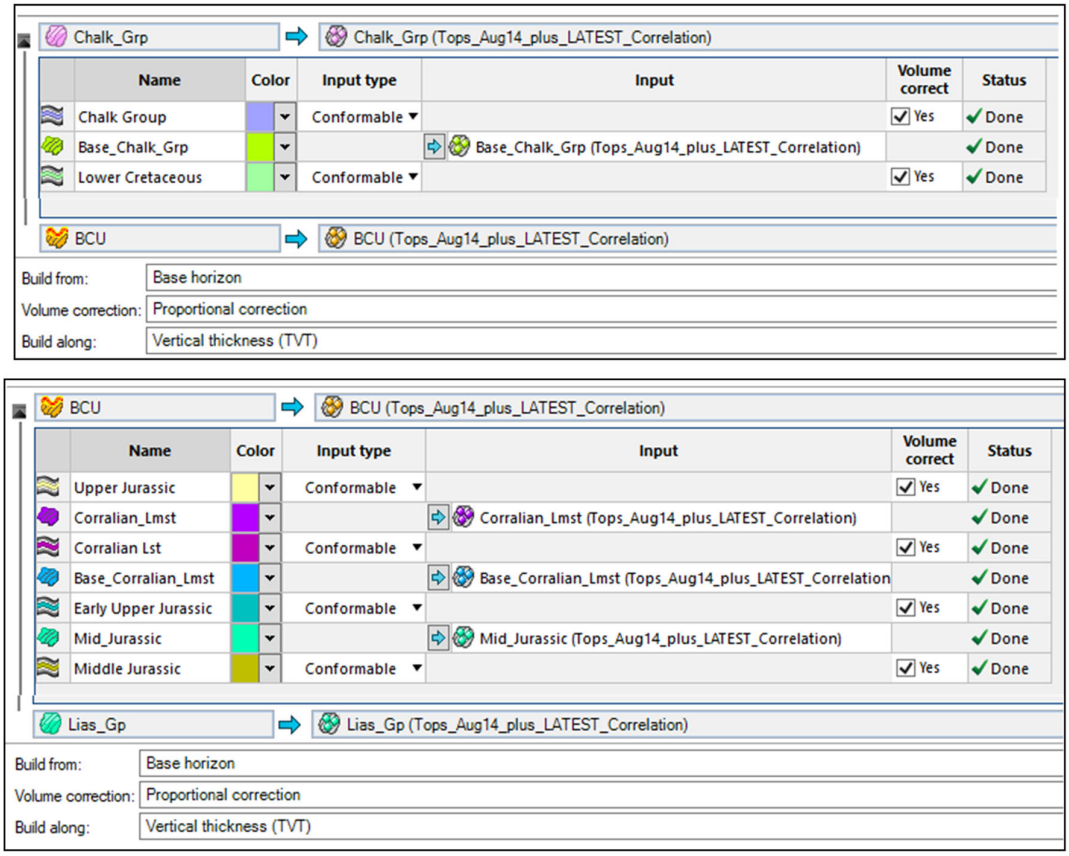

Figure 12 - Overburden Grid Make Zones process settings. Cretaceous and Upper to Middle Jurassic.

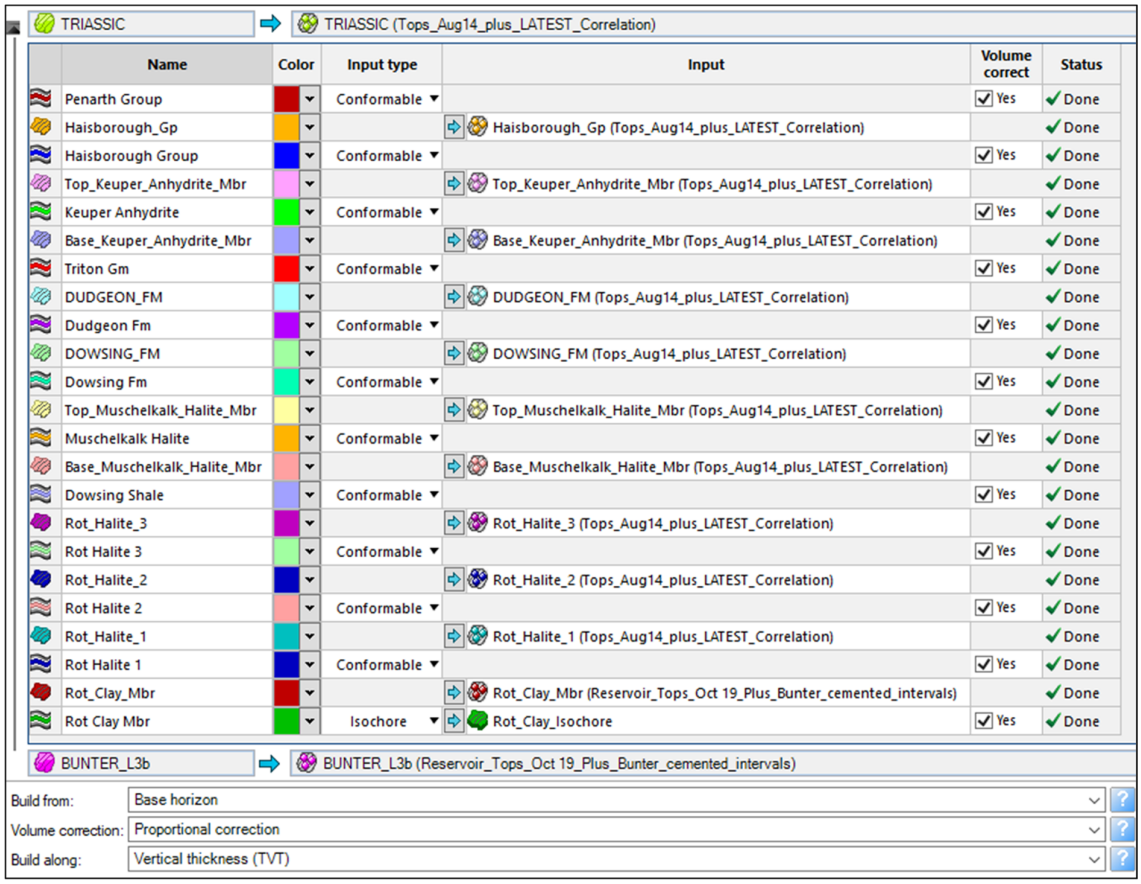

Figure 13 - Overburden Grid Make Zones process. Top Triassic to Top Bunter Sandstone.

4. The cell Layering process defined the K layering scheme. All zones were proportional with the exception of the Bunter Shale where fractions were used to provide a gradual change from the thin cells in the Bunter Sandstone to the thicker cells in the Zechstein Halites. The grid has 158 K layers and a total of 4,698,288 cells. Just over half of these cells are in the Bunter Sandstone, which has fine layering to capture the petrophysical heterogeneities and allow detailed tracking of the CO2 saturation changes. Pressure changes vary relatively smoothly over the Endurance area. The porosity variations whilst heterogeneous on a cell-to-cell scale are dominated by larger scale variations from Top to Base Bunter Sandstone and from the higher porosity crestal area to the cemented flank areas. Therefore, vertically coarser Bunter Sandstone cells will be able to adequately capture the geomechanical responses to the property variations and pressure changes.

3.1.2.2 Overburden All Grid

This grid is a copy of the Overburden Grid with coarser layering (particularly in the Bunter Sandstone) to reduce the cell count but still capture the key heterogeneities relevant to geomechanical modelling. All other settings are the same as described previously. **Figure 14** shows the layering settings and **Figure 15** shows zonation of the Overburden All Grid model. This grid and the layering scheme formed the basis for the subsequent AOI grid. No modelling was performed directly on this grid.

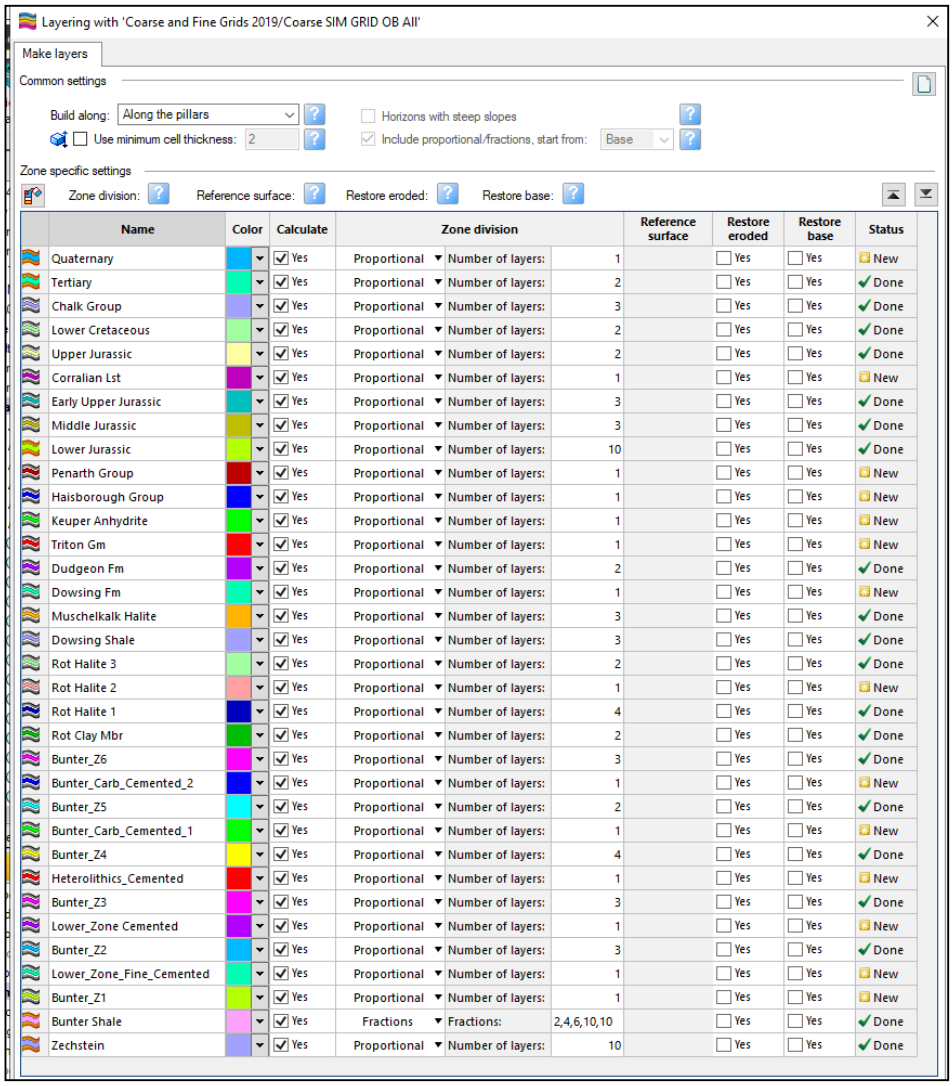

Name	Color	Calculate	Zone division			Reference surface	Restore eroded	Restore base	Status
Quaternary		Yes	Proportional	Number of layers:	1		Yes	Yes	New
Tertiary		Yes	Proportional	Number of layers:	2		Yes	Yes	Done
Chalk Group		Yes	Proportional	Number of layers:	3		Yes	Yes	Done
Lower Cretaceous		Yes	Proportional	Number of layers:	2		Yes	Yes	Done
Upper Jurassic		Yes	Proportional	Number of layers:	2		Yes	Yes	Done
Corralian Lst		Yes	Proportional	Number of layers:	1		Yes	Yes	New
Early Upper Jurassic		Yes	Proportional	Number of layers:	3		Yes	Yes	Done
Middle Jurassic		Yes	Proportional	Number of layers:	3		Yes	Yes	Done
Lower Jurassic		Yes	Proportional	Number of layers:	10		Yes	Yes	Done
Penarth Group		Yes	Proportional	Number of layers:	1		Yes	Yes	New
Haisborough Group		Yes	Proportional	Number of layers:	1		Yes	Yes	New
Keuper Anhydrite		Yes	Proportional	Number of layers:	1		Yes	Yes	New
Triton Gm		Yes	Proportional	Number of layers:	1		Yes	Yes	New
Dudgeon Fm		Yes	Proportional	Number of layers:	2		Yes	Yes	Done
Dowsing Fm		Yes	Proportional	Number of layers:	1		Yes	Yes	New
Muschelkalk Halite		Yes	Proportional	Number of layers:	3		Yes	Yes	Done
Dowsing Shale		Yes	Proportional	Number of layers:	3		Yes	Yes	Done
Rot Halite 3		Yes	Proportional	Number of layers:	2		Yes	Yes	Done
Rot Halite 2		Yes	Proportional	Number of layers:	1		Yes	Yes	New
Rot Halite 1		Yes	Proportional	Number of layers:	4		Yes	Yes	Done
Rot Clay Mbr		Yes	Proportional	Number of layers:	2		Yes	Yes	Done
Bunter_Z6		Yes	Proportional	Number of layers:	3		Yes	Yes	Done
Bunter_Carb_Cemented_2		Yes	Proportional	Number of layers:	1		Yes	Yes	New
Bunter_Z5		Yes	Proportional	Number of layers:	2		Yes	Yes	Done
Bunter_Carb_Cemented_1		Yes	Proportional	Number of layers:	1		Yes	Yes	New
Bunter_Z4		Yes	Proportional	Number of layers:	4		Yes	Yes	Done
Heterolithics_Cemented		Yes	Proportional	Number of layers:	1		Yes	Yes	New
Bunter_Z3		Yes	Proportional	Number of layers:	3		Yes	Yes	Done
Lower_Zone Cemented		Yes	Proportional	Number of layers:	1		Yes	Yes	New
Bunter_Z2		Yes	Proportional	Number of layers:	3		Yes	Yes	Done
Lower_Zone_Fine_Cemented		Yes	Proportional	Number of layers:	1		Yes	Yes	New
Bunter_Z1		Yes	Proportional	Number of layers:	1		Yes	Yes	New
Bunter Shale		Yes	Fractions	Fractions:	2,4,6,10,10		Yes	Yes	Done
Zechstein		Yes	Proportional	Number of layers:	10		Yes	Yes	Done

Figure 14 - Overburden All Grid layering settings.

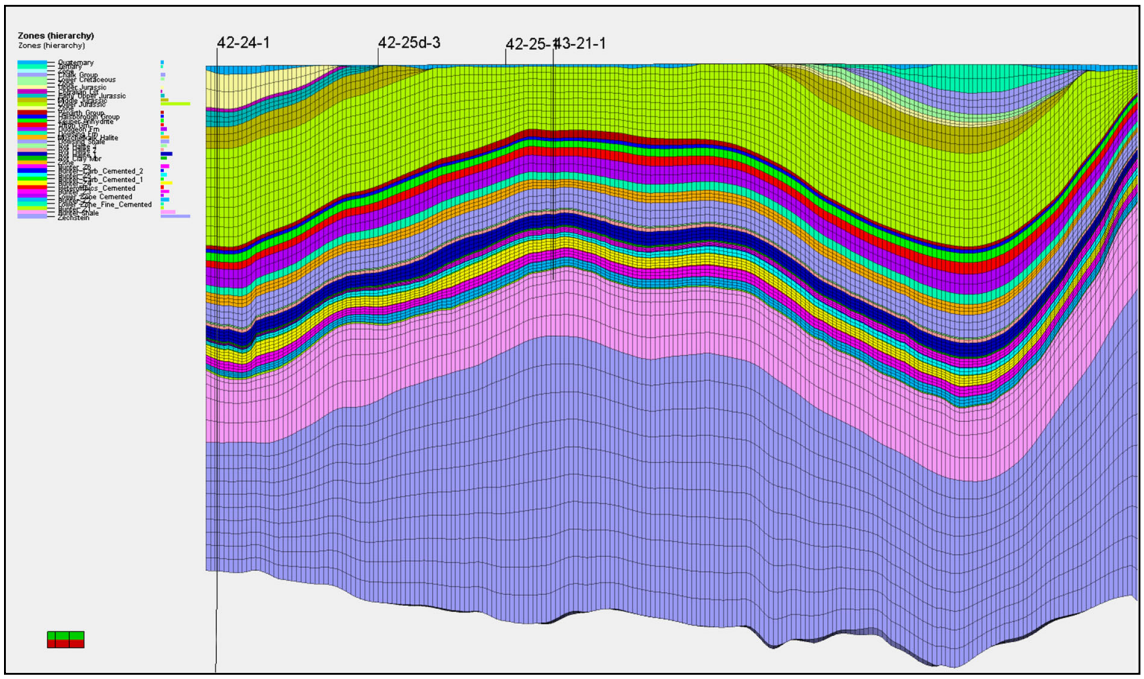

Figure 15 - Overburden All Grid zonation property.

3.1.2.3 Overburden All AOI Grid

This grid was created by extracting a sub area of the coarser Overburden All Grid using the AOI polygon that covers the Endurance structure only. This area is termed the Phase 1 (GM Ph1) modelling area. The area was selected to cover the Endurance structure closure at the Bunter L3b (Top Bunter Sandstone) level (**Figure 16**). This grid formed the basis for the subsequent geomechanical grids. No modelling was performed directly on this grid.

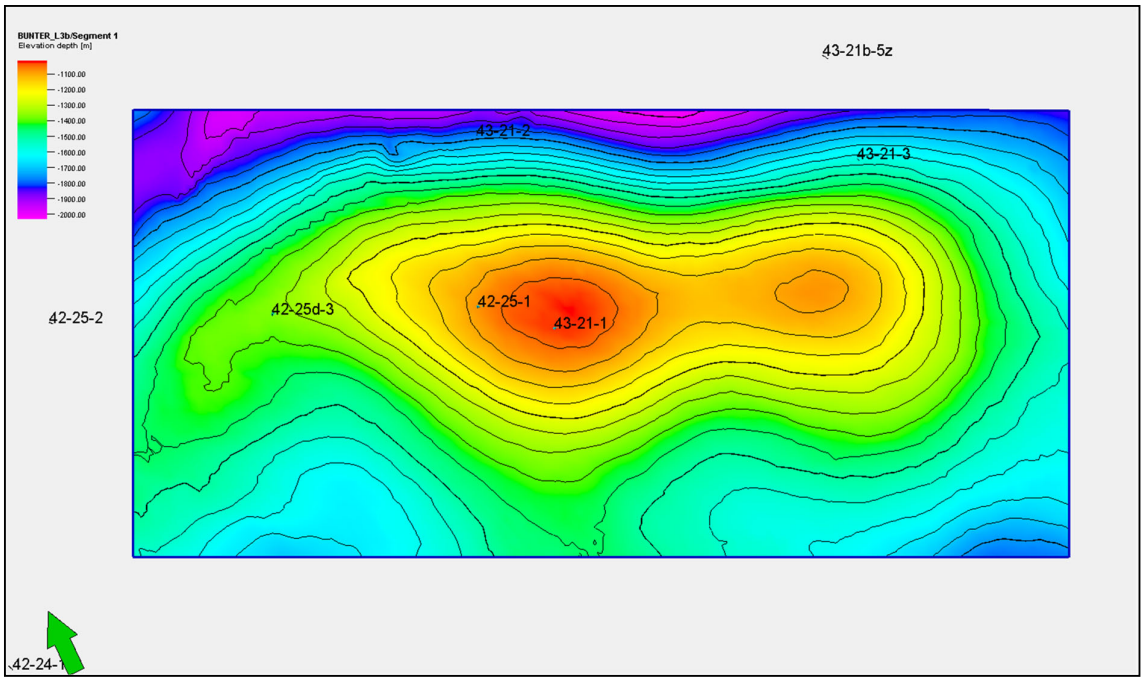

Figure 16 - Bunter L3b (Top Bunter Sandstone) surface in the overburden AOI Grid.

4.0 Geomechanical Modelling

This section describes the Petrel Reservoir Geomechanics and VISAGE modelling process adopted to create geomechanical grids and properties, initialise the geomechanical grid with in-situ stresses and perform geomechanical simulations on the supplied pressure cases. Seismic inversion products were not used for the geomechanical property modelling due to the unsuitability of the available volumes for seismic inversion processes. However, the Simulation Grid porosity property utilised a phase change boundary interpretation to model porous and cemented intervals in the Bunter Sandstone. This porosity property was used to condition the distribution of density and sonic data within the Bunter Sandstone.

A workflow diagram of the whole geomechanical modelling process is shown in **Figure 17**. As part of the geomechanical property modelling process, sonic and density logs were upscaled to and distributed within the Overburden Grid and then upscaled into the Geomechanical Grids. This was done because the Overburden Grid layering is more refined and the grid covers a larger area allowing most of the available well data to be used. These upscaled sonic and density properties are then used for the creation of the geomechanical properties.

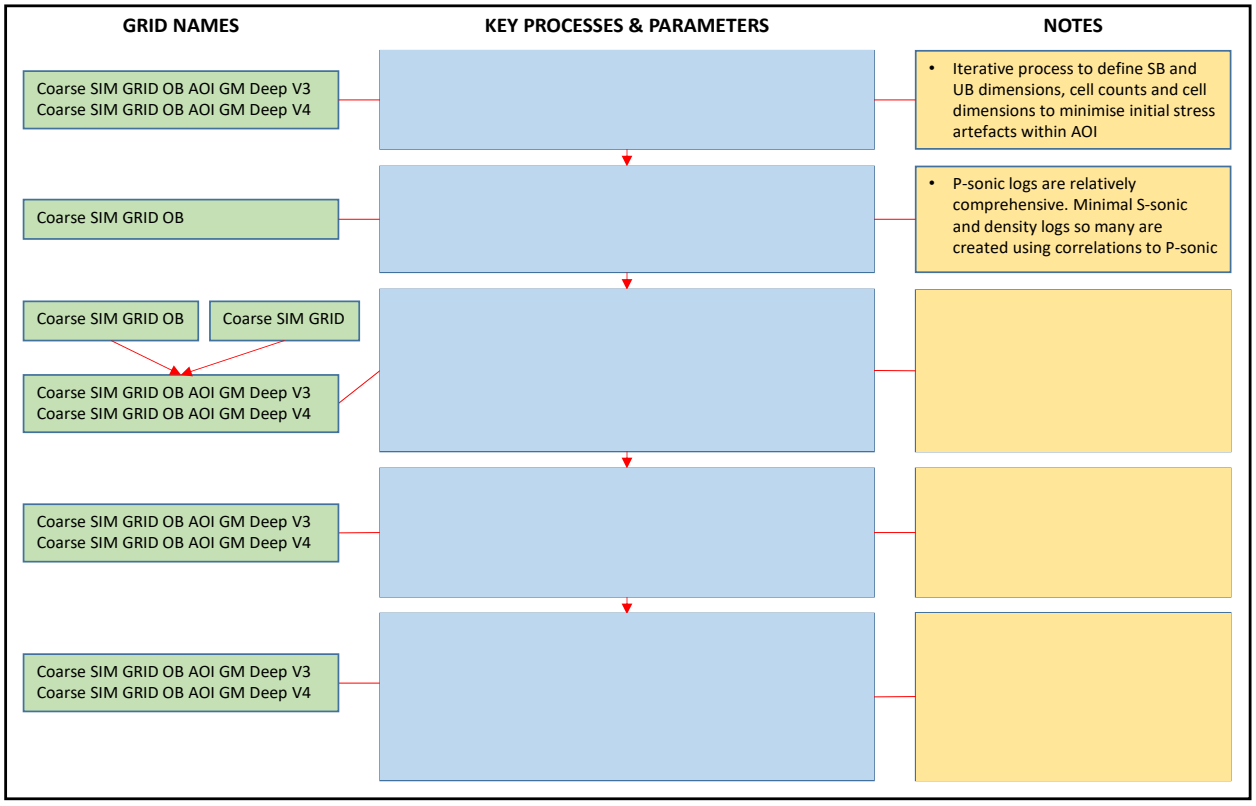

Figure 17 - Endurance geomechanical modelling workflow diagram.

The steps described below are in the required order to get to a matched stress initialisation. However, the process adopted was iterative with a number of Geomechanical Grid rebuilds, property redistributions and modifications and boundary condition adjustments required to get a satisfactory initial stress match. In particular, the presence of a large mass of Zechstein halite under the Endurance structure has proved challenging to model in such a way that the material properties and initial stresses are acceptable for all units.

4.1 Geomechanical Grids

The Geomechanical Gridding process tabs are shown below with the settings enabled for the Coarse SIM GRID OB AOI GM Deep V3 geomechanical (GM) grid (**Figure 18**). The process takes an input grid (the AOI grid – Coarse SIM GRID OB AOI) and creates a new larger grid with that AOI grid embedded within it.

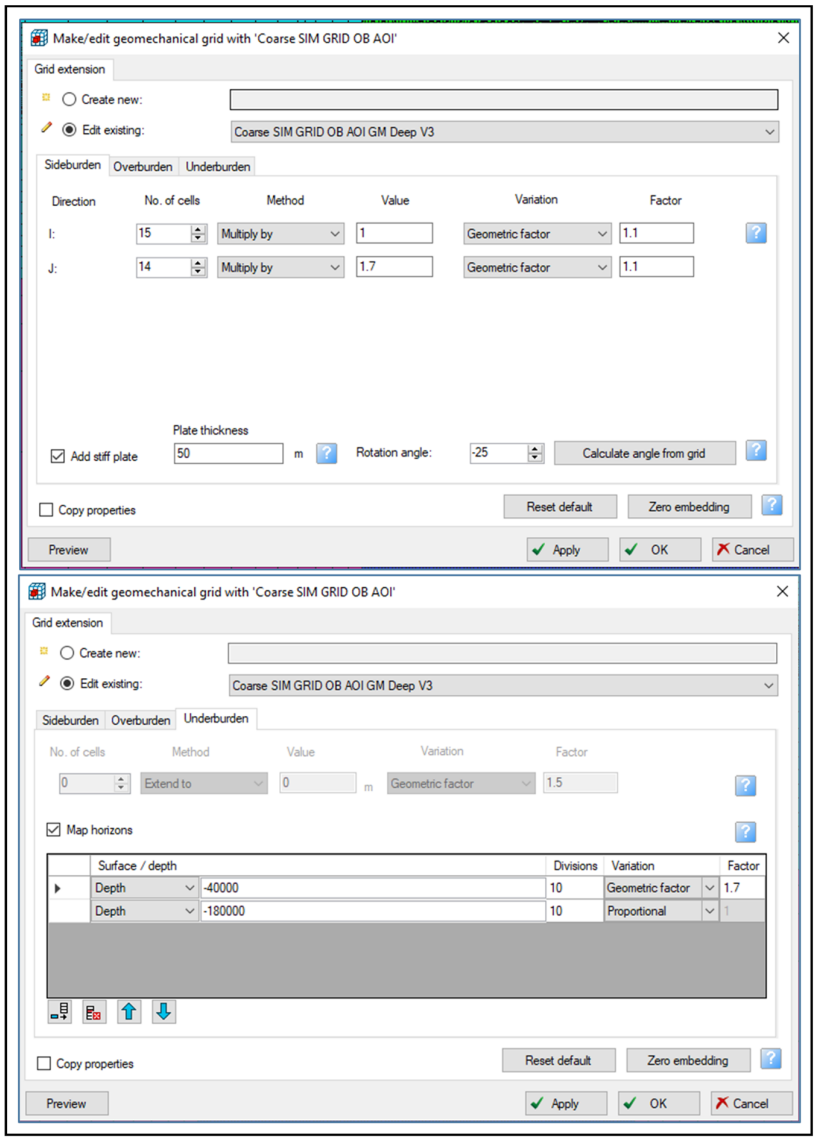

Figure 18 - Geomechanical gridding set-up.

The Sideburdens were defined with relatively small equidimensional cells to help the stresses equilibrate between the Sideburdens and the 200m x 200m cell size AOI grid embedded within them. The Overburden tab was not used as the AOI grid was defined with explicit zones from Seabed to Top Rötliegend. Stiff plates were enabled on this grid to help with stress boundary condition initialisation. The grid Rötation angle of -25 degrees aligns the GM grid with the AOI grid I direction of 115°. This is parallel to the Endurance structure crest and the reference case SHmax azimuth.

The Underburden was defined with map horizons set at -40000 and -180000 mTVDss. These depths are quite large compared to default values and were chosen to stabilise the initial stresses at shallow levels when initialising with strain gradient or stress gradient boundary conditions.

Figure 19 shows the Embedded area property for the Coarse SIM GRID OB AOI GM Deep V3 grid. Green is the AOI input grid, cyan is Sideburden and magenta and dark blue is the Underburden. Note the geometric expansion of cells in the Sideburden and the Underburden to minimise large changes in cell dimensions.

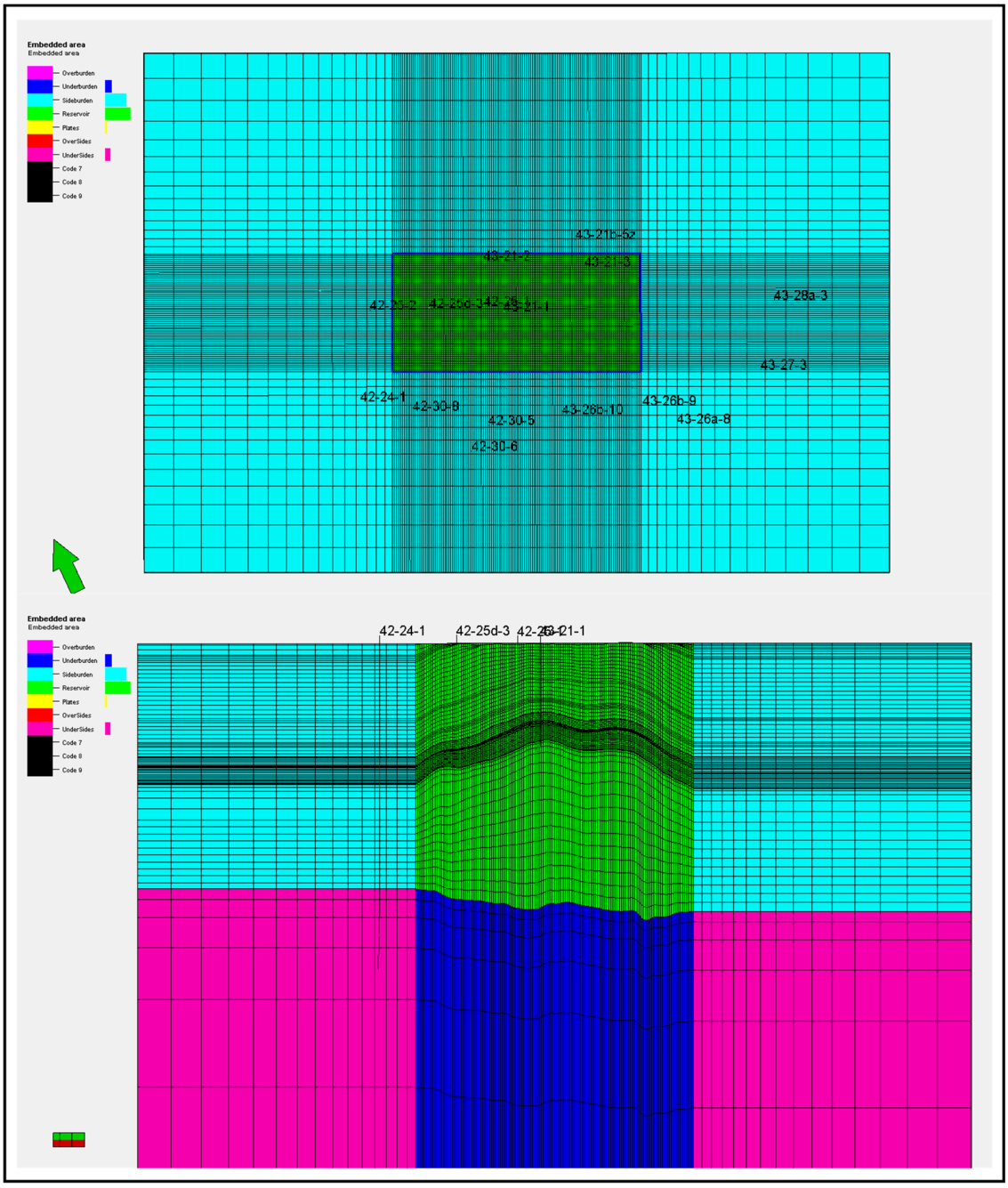

Figure 19 - GM grid Embedded area property.

Also, note that the grid layering in the Sideburdens is a horizontal extrapolation of the layers from the interface between the edge of the AOI and the edge of the Sideburdens. This is to create stable stress/strain/displacement relationships on the boundaries of the model.

4.2 Geomechanical Property Modelling

4.2.1 P-sonic and Density

The cleaned up P-sonic log and the combined density plus density from sonic log were upscaled into the Coarse SIM GRID OB grid. The Triassic and Lower Jurassic sequences do not generally display significant heterogeneity on the scale of the Endurance structure so the properties were distributed using kriging to provide smoothly varying trends. The only disadvantage to this approach is that the trends are sensitive to the location of the wells. The Bunter Sandstone was treated differently as some sedimentary and diagenetic heterogeneity is observed, particularly with respect to flank cementation.

The Bunter Sandstone net-to-gross (NTG), porosity and permeability was modelled using Sequential Gaussian Simulation (SGS) with a clear reduction in porosity and permeability within the cemented intervals in the deeper sections (Endurance flanks and structural lows). To ensure the geomechanical properties honoured these Bunter Sandstone trends, the P-sonic and density logs were distributed with moderate conditioning to porosity within this unit. The various steps taken to model the P-sonic and density properties are described in more detail below and shown in **Figure 20** (P-sonic) and **Figure 21** (density).

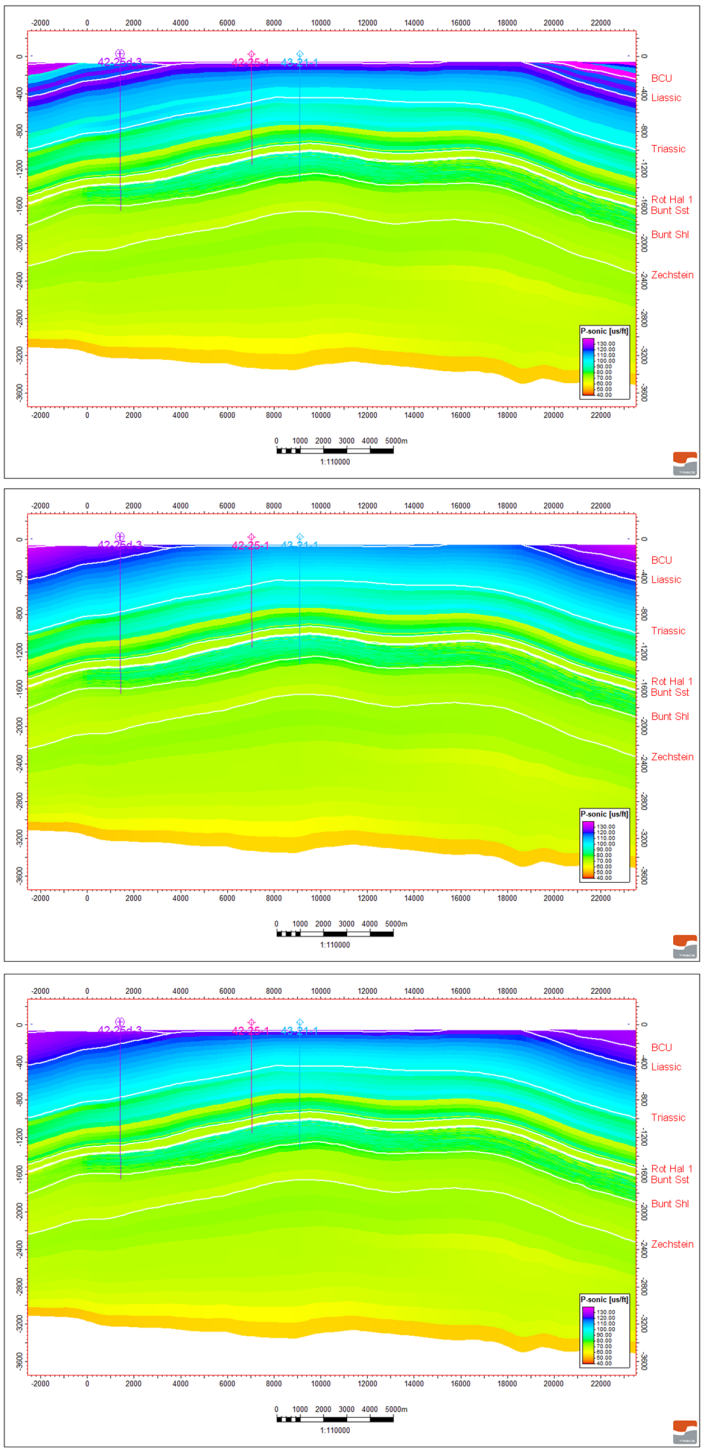

Figure 20 - P-sonic property DT_gm_V2_Merge in Coarse SIM GRID OB grid. Upper – as upscaled and distributed from logs. Middle – modified with Above Triassic Trend (ATT) applied. Lower – modified with Depth Trend (DT) applied.

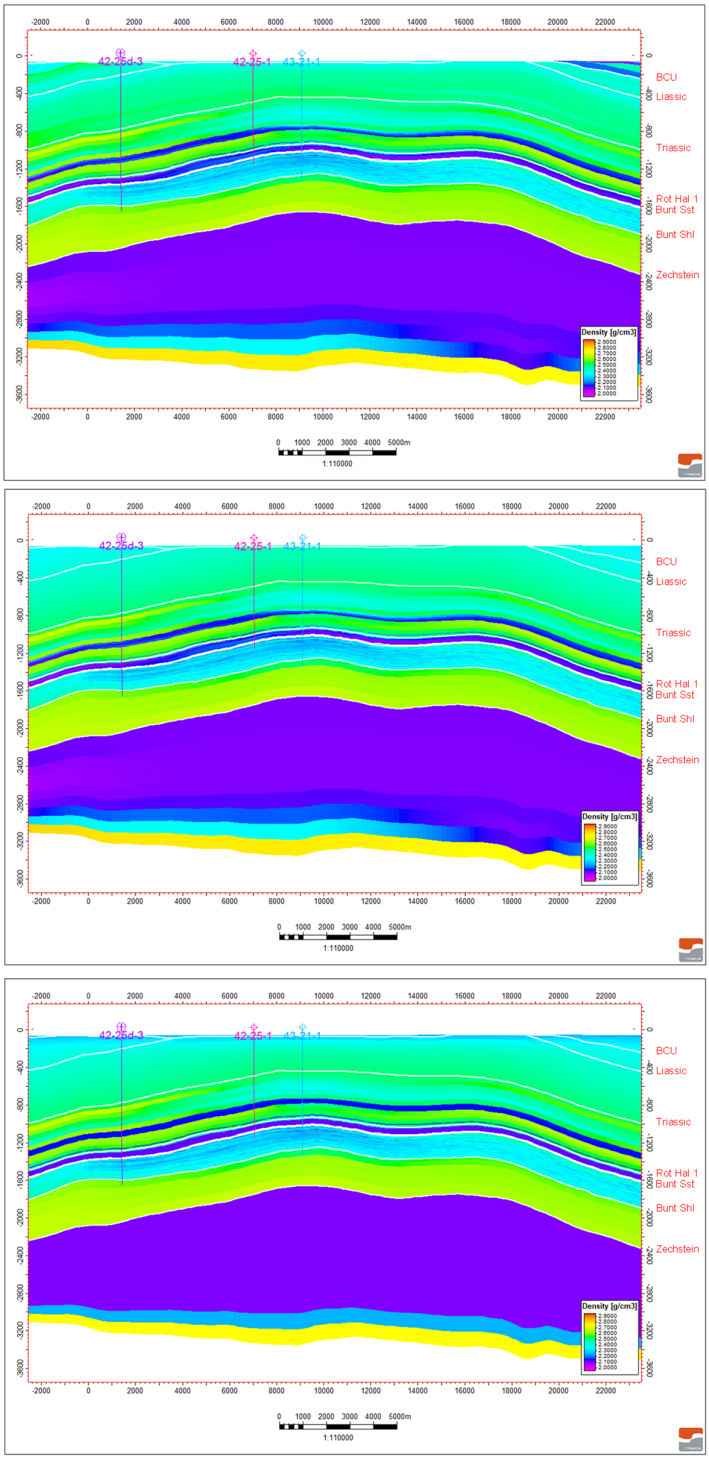

Figure 21 - Density property Dens_DTT_Cmb_Merge_V2 in Coarse SIM GRID OB grid. Upper – as upscaled and distributed from logs. Middle – modified with Above Triassic Trend (ATT) applied. Lower – modified with Depth Trend (DT) applied.

It can be seen from **Figure 20** Upper that there is a lot of P-sonic variability in the shallow units (Middle Jurassic to Quaternary). Only one well samples all these units (43/26b-9) with a further three wells containing additional samples. Therefore, whilst some of the variability is probably genuine, the log responses are not regarded as accurate or representative of this part of the sequence. In addition, the Liassic sequence, which reaches base Quaternary over much of Endurance, has variable amounts and quality of log data. Therefore, additional steps were undertaken to improve the property variability in the shallow sequence. The full sequence of steps and resulting properties are described below.

Upscale P-sonic log DT_gm_V2 to Coarse SIM GRID OB grid. Distribute with kriging in all units. Create copy (DT_gm_V2_PHIT_V02_Krig) and distribute using collocated co-kriging on the Bunter Sandstone supplied porosity property edited to remove spurious high values (Edit_PHIT_V02). Merge with the Kriged P—sonic from non-Bunter Sandstone units to create DT_gm_V2_Merge (**Figure 20** Upper)

Create an Above Triassic Trend (ATT) trend of increasing P-sonic travel time above Top Triassic. Merge with log property created in 1. as DT_gm_V2_Merge_V2_ATT. (**Figure 20** Middle)

Add a Depth Trend (DT) to re-impose the general trend of upwards increasing P-sonic travel time in all units in the shallow sequence above approximately -400 mTVDss. Merge with log and ATT derived property created in 2. as DT_gm_V2_Merge_V2_ATT_DT (**Figure 20** Lower)

The same upscaling, distribution and shallow modification process was applied to the density log data. The steps are described below and shown in **Figure 21**. Note that the density in the deepest two layers of the Zechstein was averaged to remove some of the variability in density associated with changes in anhydrite and carbonate thicknesses encountered at the base of this unit.

Upscale combined (real and Gardner sonic derived) density log DENS_DTT_Cmb to Coarse SIM GRID OB grid. Distribute with kriging in all units. Create copy (DENS_DTT_Cmb_PHIT_V02_Krig_V2) and distribute using collocated co-kriging on the Bunter Sandstone supplied porosity property edited to remove spurious high values (Edit_PHIT_V02). Merge with the Kriged density from non-Bunter Sandstone units to create Dens_DTT_Cmb_Merge_V2 (**Figure 21** Upper)

Create an Above Triassic Trend (ATT) trend of decreasing density above Top Triassic. Merge with log property created in 1. as Dens_DTT_Cmb_Merge_V2_ATT. (**Figure 21** Middle)

Add a Depth Trend (DT) to re-impose the general trend of upwards decreasing density in all units in the shallow sequence above approximately -400 mTVDss. Average density in deepest two K layers of Zechstein to average anhydrite and carbonate influences. Merge with log and ATT derived property created in 2. as Dens_DTT_Cmb_Merge_V2_ATT_DT_MH (**Figure 21** Lower).

The various steps described above and shown in **Figure 20** and **Figure 21** serve a series of objectives listed below:

1. Create a robust set of P-sonic travel time and density logs in as many wells as possible. Sonic and density are the two key measured plus calculated inputs to the log derived geomechanical property generation process.
2. Upscale and distribute the data per geological unit to capture sampled trends. Co-Krig P-sonic and density on porosity within the Bunter Sandstone to impose a geological trend in this key unit.
3. Modify the shallow sequence P-sonic and density properties above the Triassic to honour the general trends seen in logs but also remove sampling and log quality related artefacts. This is a particular issue in the shallow sequence above approximately -400 mTVDss where property variabilities in the partially eroded onlapping units can have a significant effect on the modelled stresses.

4.2.2 Upscaling to Geomechanical (GM) Grids

The final P-sonic and Density properties were both upscaled from Coarse SIM GRID OB to the geomechanical grid (Coarse SIM GRID OB AOI GM Deep V3). The grid sampling was via Zone Mapped Layers and Geometric Overlap as the zone boundaries were exactly the same in both grids and only the K layer cell count was coarser in the GM grid. These properties are scalar so were upscaled using arithmetic averaging with volume weighting. The same upscaling processes and settings were adopted for all the pressure case properties used in the simulations.

Figure 22 shows the comparison between the original density property in grid Coarse SIM GRID OB (upper picture) and the upscaled version in grid Coarse SIM GRID OB AOI GM Deep V3 (lower picture). There is no significant difference.

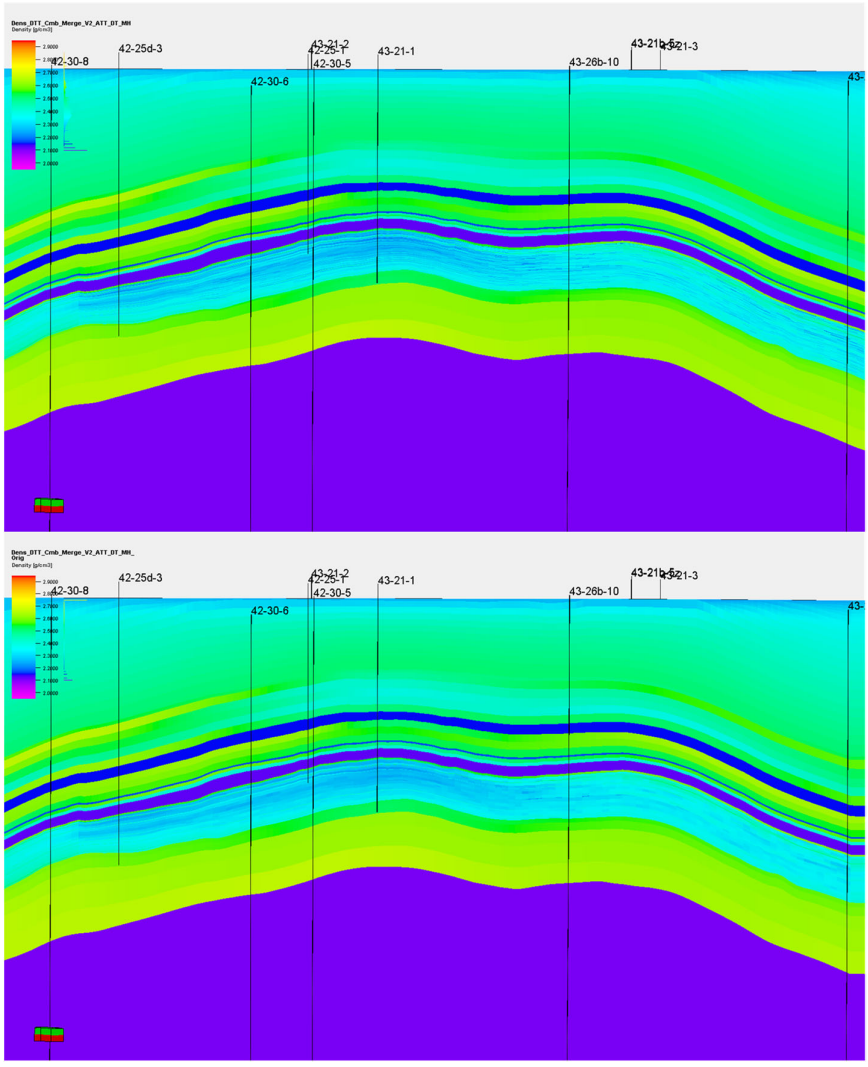

Figure 22 - Comparison of original (upper) and upscaled (lower) density properties.

4.2.3 Key Property Creation and Clean-up

The key properties from the GM grid described in this section are:

- Distance from edge of grid Area of Interest (AOI)
- Depth
- P-Sonic
- Density
- Flags defining salt presence

A distinction is required between properties defined in the Area of Interest (AOI) and those in the Sideburdens. A series of closely spaced vertical lines were defined that formed a ‘fence’ around the AOI (**Figure 23**). These are used to create a distance from property (Distance from AOI_Vert_Boundary).

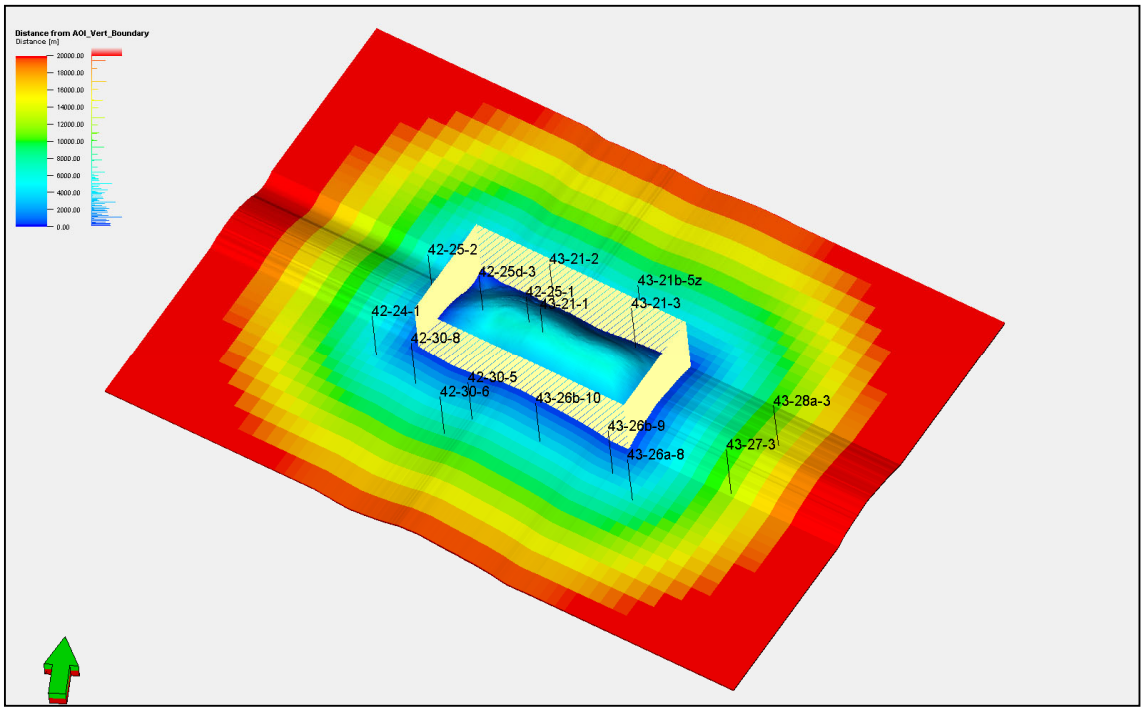

Figure 23 - Distance from AOI_Vert_Boundary property and vertical lines (yellow) used for defining it.

mTVDss (negative values) was assigned to each cell as the DP property using the Geometrical Modelling process. Both Distance from AOI_Vert_Boundary and DP are used for creating flag and gradational properties throughout the geomechanical modelling.

After upscaling to the GM grid, the density and P-sonic properties are renamed as:

- DT_gm_V2_Merge_V2_ATT_DT_Orig
- Dens_DTT_Cmb_Merge_V2_ATT_DT_MH_Orig

These were then copied and renamed as:

- DT_gm_V2_Merge_V2_ATT_DT_R3
- Dens_DTT_Cmb_Merge_V2_ATT_DT_MH_R3

The equations shown in **Figure 24** were used to create flags defining the where the salt properties occur, clean-up the upscaled P-sonic and density and then extrapolate the P-sonic and density into the Sideburdens. P-sonic and density (and any other upscaled property) require cleaning up as some cells outside valid zones are assigned values during upscaling (due to slight mismatches in grid geometry) and because the Coarse SIM GRID OB grid covers a larger area than the AOI of the Coarse SIM GRID OB AOI GM Deep V3 grid, these values need removing.

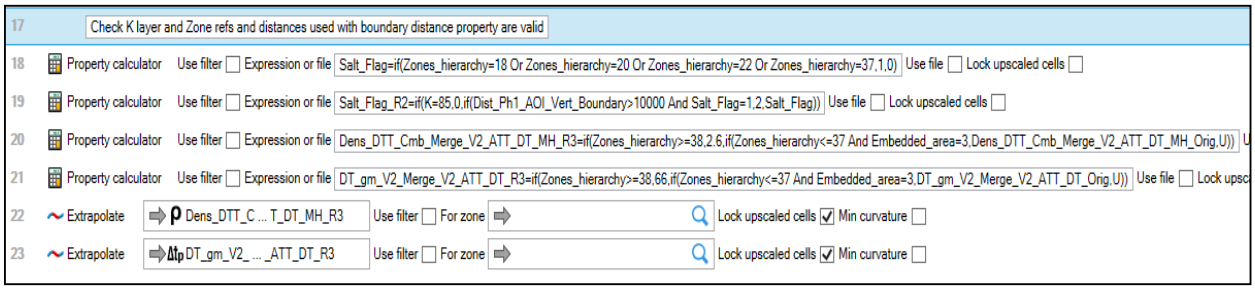

Figure 24 - Salt flag creation and P-sonic and density clean-up processes.

Figure 25 shows the upscaled density (Upper) and the cleaned up and extrapolated density (Lower) in the Coarse SIM GRID OB AOI GM Deep V3 grid. The AOI is shown within the red outline. It can be seen that after upscaling, the Underburden has been assigned high densities from the deepest Zechstein layer and some densities from the larger grid are showing variability in the Sideburdens (RH side of **Figure 25** Upper). As the Sideburdens exist to create a buffer to the AOI, they are assigned values by extrapolating out from the values at the edge of AOI to the edges of the model (**Figure 25** Lower). The Underburden is assigned a slightly lower density than that from upscaling to represent average properties. The same process was adopted for the P-sonic property.

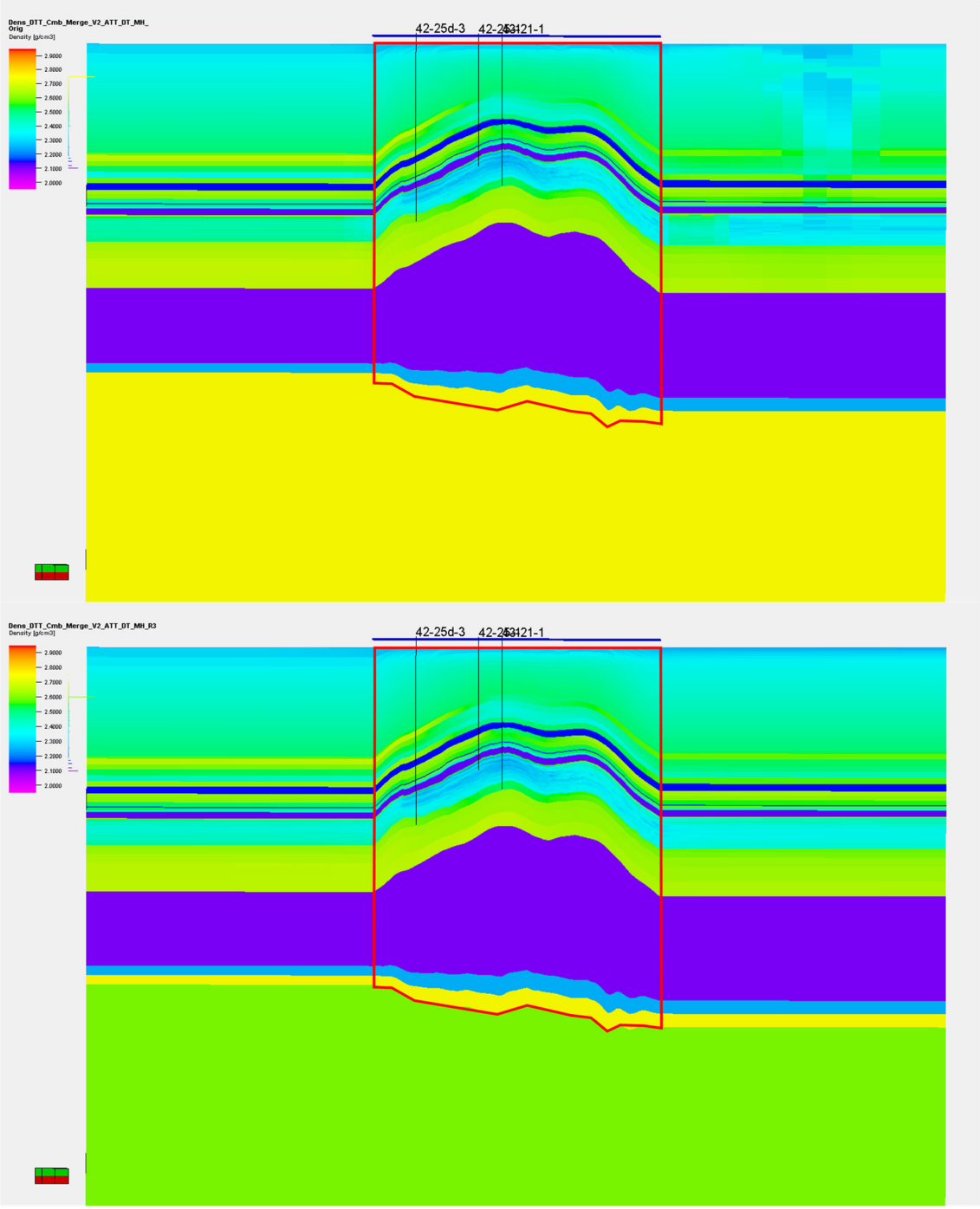

Figure 25 - Upscaled density (Upper) and extrapolated density (Lower) properties in GM grid Coarse SIM GRID OB AOI GM Deep V3.

The Salt_Flag_R2 property (**Figure 26**) was created to allow control on how salt was treated within the AOI (dark blue) and in the Sideburdens (purple). The selection of the interface location within the Sideburdens was based on extensive testing of a variety of different GM grid geometries and different salt property combinations.

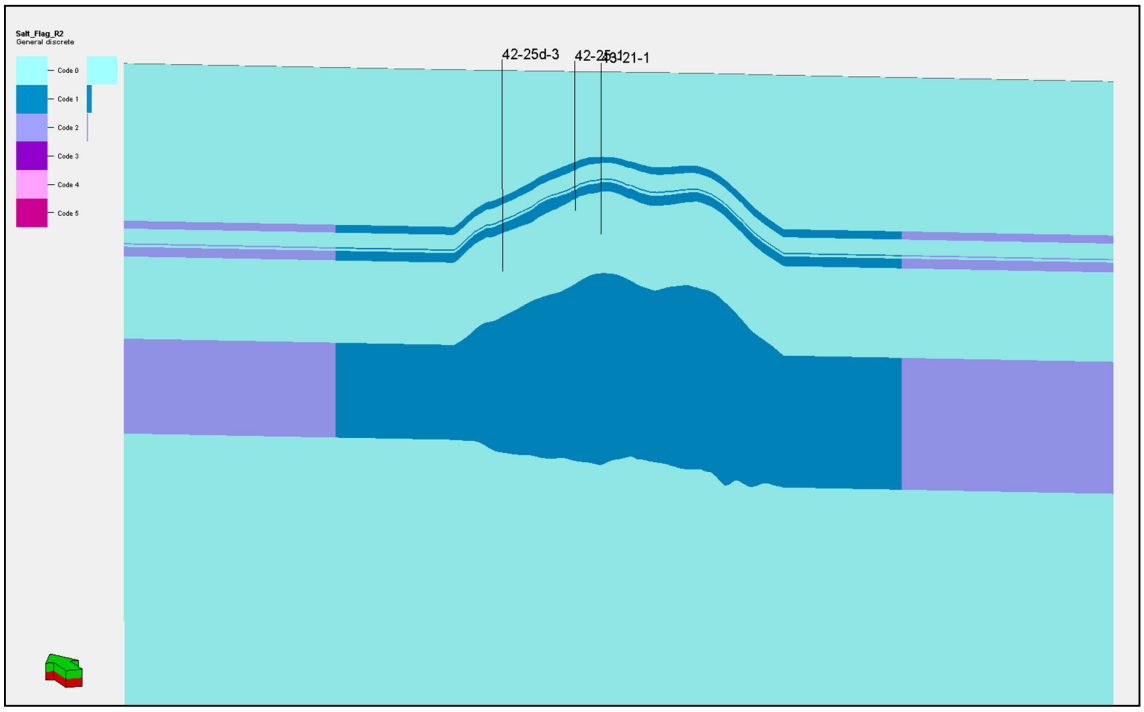

Figure 26 - Salt_flag_R2 property.

4.2.4 Pore Pressure Properties

Pore pressure properties were upscaled from Coarse SIM GRID to Coarse SIM GRID OB and modified to remove zero pressure cells within the Bunter Sandstone and to convert from psi to bar. The zero pressure cells occur where the NTG is zero and will create numerical problems if not removed. They are removed by nulling them and interpolating values from surrounding Bunter Sandstone cells.

These modified pore pressures were then upscaled to Coarse SIM GRID OB AOI GM Deep V3 and cleaned up using a similar process to that described for P-sonic and density earlier using a workflow loop instead (**Figure 27**).

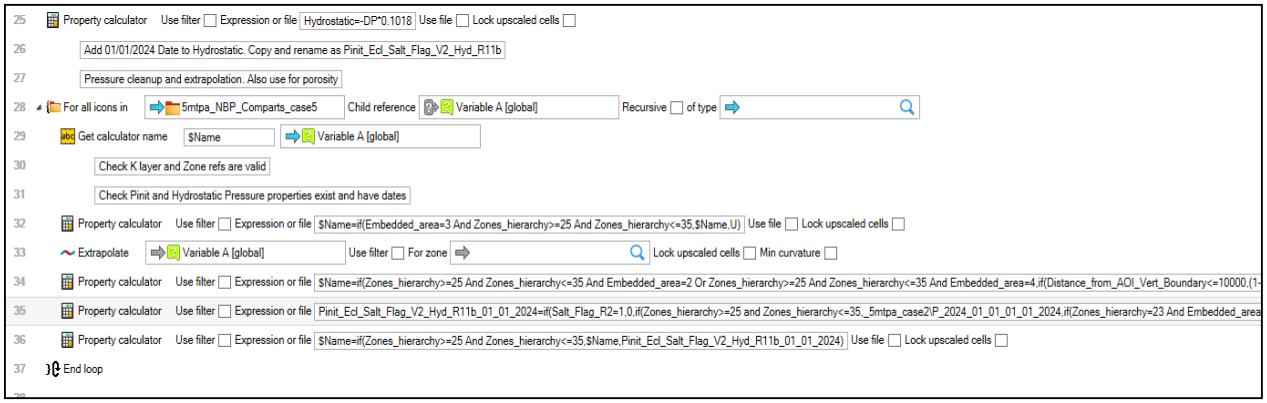

Figure 27 - Pressure property clean-up process.

Note that up to workflow step 32, the pressures are only defined within the Bunter Sandstone as that is how they are exported from Nexus. For geomechanical property modelling, pore pressures need to be defined in all units. The rest of the workflow adds these pressure properties in. The detailed steps are outlined below.

1. The Nexus Bunter sandstone initial pressures are slightly higher than typical hydrostatic due to the salinity. Workflow step 34 linearly blends the pressures from Nexus values at the edge of the AOI to hydrostatic (0.1018 bar/m) at 10,000m radius from the AOI within the Sideburdens
2. Workflow step 35 ensures the initial pressure property (Pinit_Ecl_Salt_Flag_V2_Hyd_R11b) zero values in the salt, Bunter sandstone values from one of the upscaled initial pressures and higher pressures of 0.106317 bar/m in the Röt Clay and Bunter Shale. A linear blend from 0.106317 bar/m on the edge of the AOI to hydrostatic (0.1018 bar/m) at 10,000m from the AOI is assigned in the Sideburdens within the interval from Röt Clay to Bunter Shale. All other units are given an initial pore pressure 0.1018 bar/m. This step does not need to be repeated within the workflow but it is placed here to ensure it is not left out.
3. Each Bunter Sandstone pressure step is combined with the initial pressure defined in step 2. This is to ensure the Bunter Sandstone simulated pressures change but those in the surrounding rocks remain the same.

Salt is effectively self-sealing, typically with very low porosities so pore spaces will tend to be isolated and surrounded by creeping salt with lithostatic pressures. This will create isolated pores that contain fluids at or close to lithostatic pressure. However, unlike most rocks they will not form part of a connected pore network so the pore pressures will not contribute to the effective stress calculation. Within the VISAGE calculations, this can be handled in two ways.

1. Set Biot's effective stress parameter as zero and assign salt pore pressure as lithostatic or some other pressure value
2. Set Biot's effective stress parameter as one and assign salt pore pressure as zero.

The results should be identical as one of the terms in the effective stress equation is zero. The latter approach was taken during this work. This has the added advantage of helping to visualise where the salt is when creating the pore pressures.

4.2.5 Matrix Geomechanical Properties

The equations in **Figure 28** define all the relevant equations used to create matrix geomechanical properties used in the stress initialisations and in the subsequent pressure case simulations. Sonic velocity is created first and then shear velocity using the trends. Notes below on elastic property creation:

1. G_dyn, K_dyn, E_dyn and v_dyn are dynamic (log derived) versions of the shear, bulk, Young's and Poisson's moduli respectively.
2. E_ref_R11b and v_Ref_R11d are static (42/25d-3 core matched) estimates of Young's modulus and Poisson's ratio respectively.
3. Dens_DTT_Cmb_Merge_V2_ATT_DT_MH_R3_R11 is the upscaled and cleaned up density with a further refinement of the Zechstein salt density.

Figure 28 - Geomechanical property equations used in GM grids.

The various R11 properties listed above are the reference elastic properties derived from multiple iterations of stress initialisation and property models. Additional variants are described in later sections.

It should be noted that Biot factor has been left at the default value of one in all units in all runs bar one sensitivity case where it was reduced in the Bunter Sandstone. This is because investigation of the full impact of pore pressure changes over the whole model were deemed more important than applying a range of Biot values relevant to the more porous matrix materials. Intact samples of a relatively strong but porous rock like the Bunter Sandstone are likely to have a Biot factor in the range of 0.7 to 0.95.

A Mohr Coulomb failure model was chosen as it is a robust and conservative failure criterion and useful in helping define the limits of the Endurance CCUS store integrity. Notes below:

1. UCS_Hors_Ref is log-derived strength using Vp data using the Horsrud rock strength equation. No adjustments were required with respect to core data
2. TSTR_Hors_Ref is the tensile strength cut-off derived from UCS_Hors_Ref
3. FANG and DANG are the friction and dilation angles respectively derived from Vp data

1. PHIT_V02_Ref. Reference case porosity used in simulations. Bunter Sandstone contains upscaled values from BP Petrel model out to 10,000m from edge of AOI, Salt set to 1% and all other units set as 20%. However, note that porosity is not directly used in the simulations.
2. Salt_MC_Flag_R3. Salt_Flag_R2 with salt set to zero, all units set to a Mohr-Coulomb material flag above top Zechstein to -100 mTVDss below seabed. This was done to avoid failure of very shallow units with very low strengths and potentially high stresses.

The flag listed in 2. above and shown in **Figure 29** is used to control the distribution of Elastic and Mohr coulomb properties in the Populate Properties geomechanical modelling process. Code descriptions given below.

1. Code 0. Elastic properties only, clastic rocks
2. Code 1. Elastic properties only, salt values & density. See text for details
3. Code 2. Elastic properties only, background values and salt density. See text for details
4. Code 3. Elastic and Mohr-Coulomb strength parameters, clastic rocks

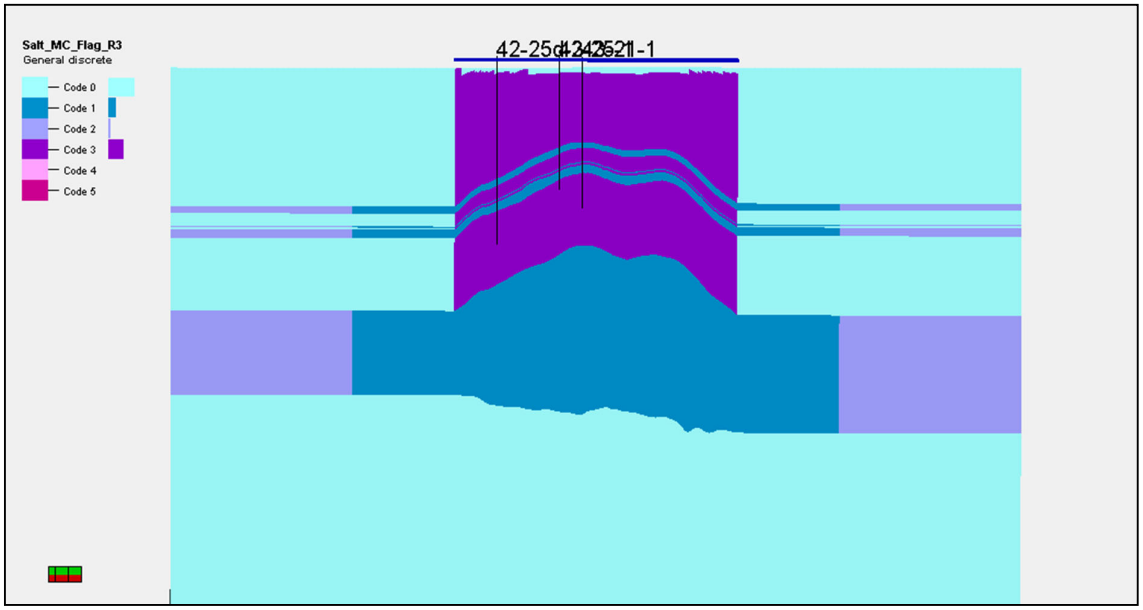

Figure 29 - Salt_MC_Flag_R3 property.

Elastic properties only means only elastic stress strain relationships are setup and no failure calculations are performed. The addition of strength parameters means that failure calculations are also performed so both elastic and plastic strains (where they occur) are estimated. Note that cells with centre depths of >= -100 mTVDss Endurance were set to elastic only. This is because the initial in-situ stress values and rock properties are difficult to constrain at these depths. Because the stress magnitudes are so low and strength properties likely to be weak, failure during initialisation is a common problem in the models when it is less likely in reality. This is discussed further in later sections.

Salts are difficult materials to model as they are typically less dense than surrounding rocks and deform by creep mechanisms on geological timeframes leading to lithostatic stress states. This creeping behaviour can be initiated by gravity instabilities and/or from external tectonic forces.

VISAGE versions since 2018 have primary (non-linear) and secondary (linear) Norton Bailey creep model functionality. However, these creep models require careful calibration to test data and the models take a considerable time to run. Whilst salt creep data does exist for the Röt Halite 1, the tests were conducted under limited time and temperature conditions and the results require detailed analysis to be converted to useful creep model parameters. Given these limitations, it was decided to model the halite using an equivalent elastic medium

approach. This assigns a Poisson's ratio of 0.495 to ensure a near lithostatic stress state and low shear stresses. The Young's Modulus of 0.75 GPa is then calculated from the measured bulk modulus of ~25 GPa (from logs) and the assigned Poisson's ratio of 0.495. This ensures consistency between the parameters in the stress-strain calculations. This approach has the benefit of being fast and robust but is only valid for low strain situations where the salt is not expected to move very much. This is believed to be the case for Endurance at the field scale and injection timeframes although a different approach will be required to capture near wellbore halokinesis and or longer term higher strain field scale salt deformation.

The Endurance structure is likely to have undergone several phases of Zechstein salt core movement leading to the uplift, erosion and faulting seen on the crest and flanks of the structure. Whilst the Endurance structure is likely to be in equilibrium at the present day, it is possible that the stress states in adjacent units reflect a combination of paleo stresses, salt buoyancy forces and in-situ tectonic stresses. This complex evolution is difficult to capture in VISAGE irrespective of the salt stress initialisation method as the grids only contain present day geometries. Therefore, the evolution of the structure (e.g. uplift, Rötation and erosion of beds) has not been modelled.

4.3 Faults

Faults occur as a series of normal or possibly oblique slip features situated on the crest of Endurance. The features have relatively low throws and appear to terminate at the Top Röt Halite 3 unit (**Figure 30**). Their detailed origins are unclear but likely to be related to one or more pulses of halokinesis and uplift causing stretching in the Endurance overburden (please see earlier faults section). Fault surfaces were imported from Earth Vision format grids and edited in a few places to remove edge artefacts.

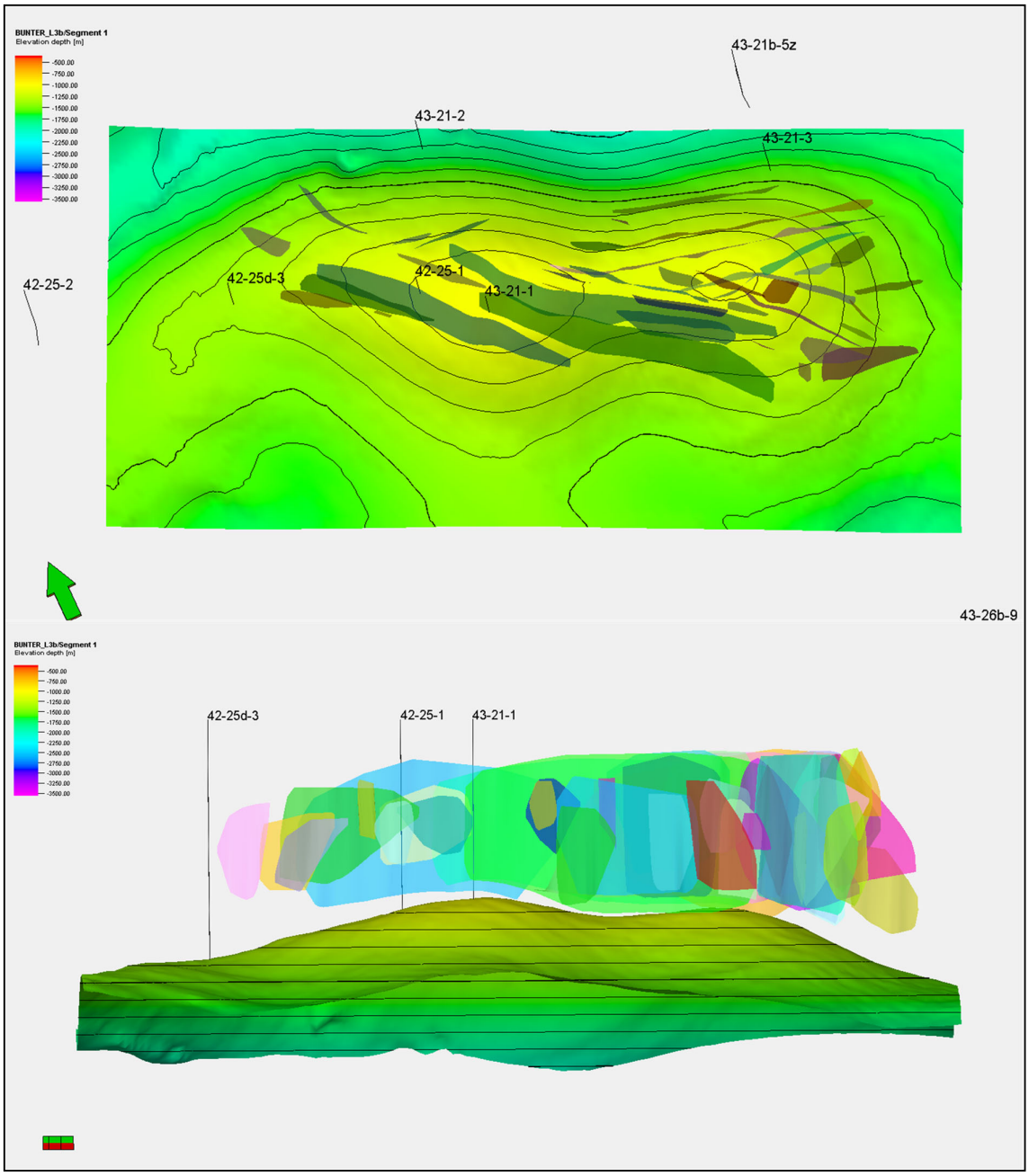

Figure 30 - Endurance overburden fault surfaces. Top Bunter L3b (Top Bunter Sandstone) also shown.

Faults extending down into the upper Bunter Sandstone are clearly observed to occur further east toward the outcrop so there is potential for sub-seismic faults or fault tips to extend deeper than mapped over Endurance. Therefore, five of the imported faults were copied and manually edited to extend down into the upper few layers of the Bunter Sandstone Z6 unit. These faults are shown in **Figure 31**.

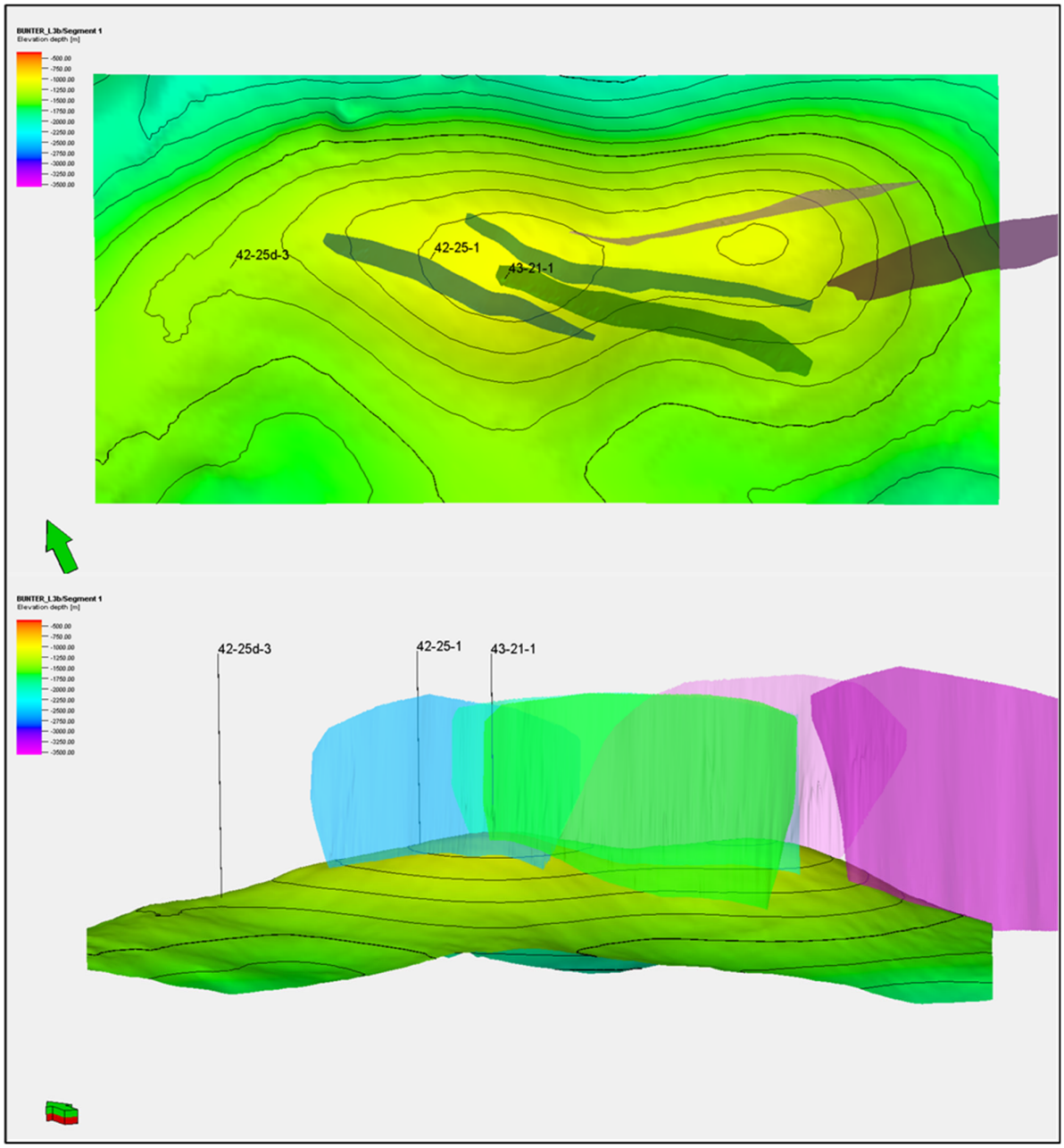

Figure 31 - Faults above Endurance. Bunter L3b (Top Bunter Sandstone) surface also shown.

Fault properties (in terms of cohesion, friction angle stiffness, etc.) are hard to define for these faults as there is no direct data and published data is sparse, particularly for fault rocks that may contain some halite. For the Endurance fault rock properties, a number of different fault property combinations were reviewed and tested during initialisation. Two were selected for further modelling. The parameter details are given below in Table 5.

Table 5 - Fault property cases and parameters.

Parameter	Weak Case	Ref Case	Units
Fault Material Name	Ref Fault Material 2020 V5	Ref Fault Material 2020 V6	-
Fault Property Name			
Fault Normal stiffness	10000	10000	bar/m
Fault Shear stiffness	5000	5000	bar/m
Cohesion	5	10	bar
Friction Angle	22	25	Deg.
Dilation Angle	5	10	Deg.
Tensile Strength	0.01	1	bar
Initial Opening	0.0001	0.0001	-

The Endurance structure is likely to be in a stable tectonic regime and active tectonic faults do not occur (or have not been detected to date). Therefore, the criteria for defining the weak fault properties case was for the parameters to be just strong enough to prevent plastic failure on initialisation. The initialisations were determined from with boundary stresses and matrix properties that match the available in-situ stress data from wells. The weak case listed in Table 5 incorporated changes to both cohesion and friction angle to increase the likelihood of failure during simulations. The Reference Case fault properties were defined from Zhang et al (2007) with the tensile strength cut-off reduced from 15.67 to 1 bar. The fault normal and shear stiffness's in both cases were reduced from the Petrel defaults of 40000 and 15000 bar/m respectively.

The two fault surface cases and two fault property cases described in this section were combined in the Discontinuity process to create the following Fault collections in Petrel (**Table 6**).

Table 6 - Discontinuity process fault collections.

Fault Property Collection Name	Fault Surfaces Folders	Fault Materials Collection Name	Notes
Ref20FltV6Mapped	Ref Case Sim (40 faults)	Ref Fault Material 2020 V6	Main run used with all pressure cases
Wk20FltV5Mapped	Ref Case Sim (40 faults)	Ref Fault Material 2020 V5	Sensitivity with 5.0 Mtpa case
Ref20FltV6ExtBuntV2	Ref Case Sim (36 faults)		
Ref Case Sim Extended (5 faults)	Ref Fault Material 2020 V6	Sensitivity with 5.0 Mtpa	

4.4 Stress Initialisation

This is one of the most important steps in the geomechanical modelling process, as it is where the model can be history matched to stress data obtained from wells. This step allows adjustments to be made to the model properties and boundary conditions (within reason) to obtain an initial in-situ stress match.

In-situ stresses can be initialised in VISAGE in a variety of ways. The methods are split into two groups:

- Imposed boundary conditions in the forms of strains or stresses imposed on the lateral edges of the model plus gravity loading (constants or gradients)
- Stress initialization where the in-situ stress state is defined for each cell. This may be defined by pre-existing stress properties or defined via ratios of the horizontal stresses to the vertical stress.

The Imposed boundary conditions group of methods were the primary choice used for the Endurance Phase 1 modelling. This is because the model properties and layer geometries are used with external stresses or strains (the imposed boundary conditions) to generate predictions of the initial in-situ stresses within the Bunter Sandstone and surrounding units. Assessing how well these initial stresses match with the available data is a good way of assessing the accuracy (and predictive usefulness) of the model. The drawback with this approach is that it works best for a relatively flat-layered system with consistent boundary conditions and a relatively gradual change in rock properties with depth. Whilst Endurance is

not a high amplitude fold feature it is cored by a thick sequence of Zechstein salt, it has variability in the basal layer (Rötliegend) geometry, it has been uplifted and eroded and it is overlain by Röt and Muschelkalk halites.

4.4.1 Salt Influence

Particular issues have been encountered when incorporating the Zechstein elastic properties of Young's (E) = 0.75 GPa and Poisson's Ratio (Nu) = 0.495. Whilst this method attains the lithostatic stresses within the salt units, it also leads to relatively large stretching (negative) strains in the overlying units (particularly above Röt Halite 3). This results in very low (sometimes negative) Shmin values, particularly in the shallow sequence. This effect occurs when stress gradient or strain gradient boundary conditions are imposed. Constant strain or stress gradient boundary conditions coupled with shallower Underburden can significantly improve the very low shallow stresses in much of the sequence. However, the opposite problem occurs in some parts of the very shallow layers where Shmin and SHmax become very large and both exceed Sv.

4.4.2 Stress Initialisation Process

To address these issues for this study, two separate imposed boundary condition initialisations were created that were then merged (spliced) to create a composite explicit stress initialisation used in subsequent simulations. This is shown in **Figure 32** and the detailed steps are listed below.

1. V155 Case. Create stress state valid for shallow sequence above Röt Halite 1 excluding Röt halite 3 and Muschelkalk Halite. Match FIT data in 42/25d-3, 42/25-1 and 43/21-1. Use Reference case elastic and density properties defined earlier. Boundary conditions defined as strain gradients of Eh = 3E-07 1/m and EH = 3.3E-07 1/m with Eh aligned with the Shmin direction of 25°.
2. V152 Case. Create stress state valid for deeper sequence below Top Röt Halite 1 plus Röt halite 3 and Muschelkalk Halite. Match Röt clay and Bunter Sandstone MicroFrac stress data in 42/25d-3. Use Reference case elastic and density properties earlier. Imposed boundary conditions defined as strain gradients of Eh = 2.7E-07 1/m and EH = 3E-07 1/m with Eh aligned with the Shmin direction of 25°.
3. V156 Case. After running cases V155 and V152, take the total stress outputs from the relevant layers in each case and combine as a set of total stress tensor components (XX, YY, ZZ, XY, YZ, ZX). Use these combined stresses in check initialisation (V156) and in subsequent simulations.

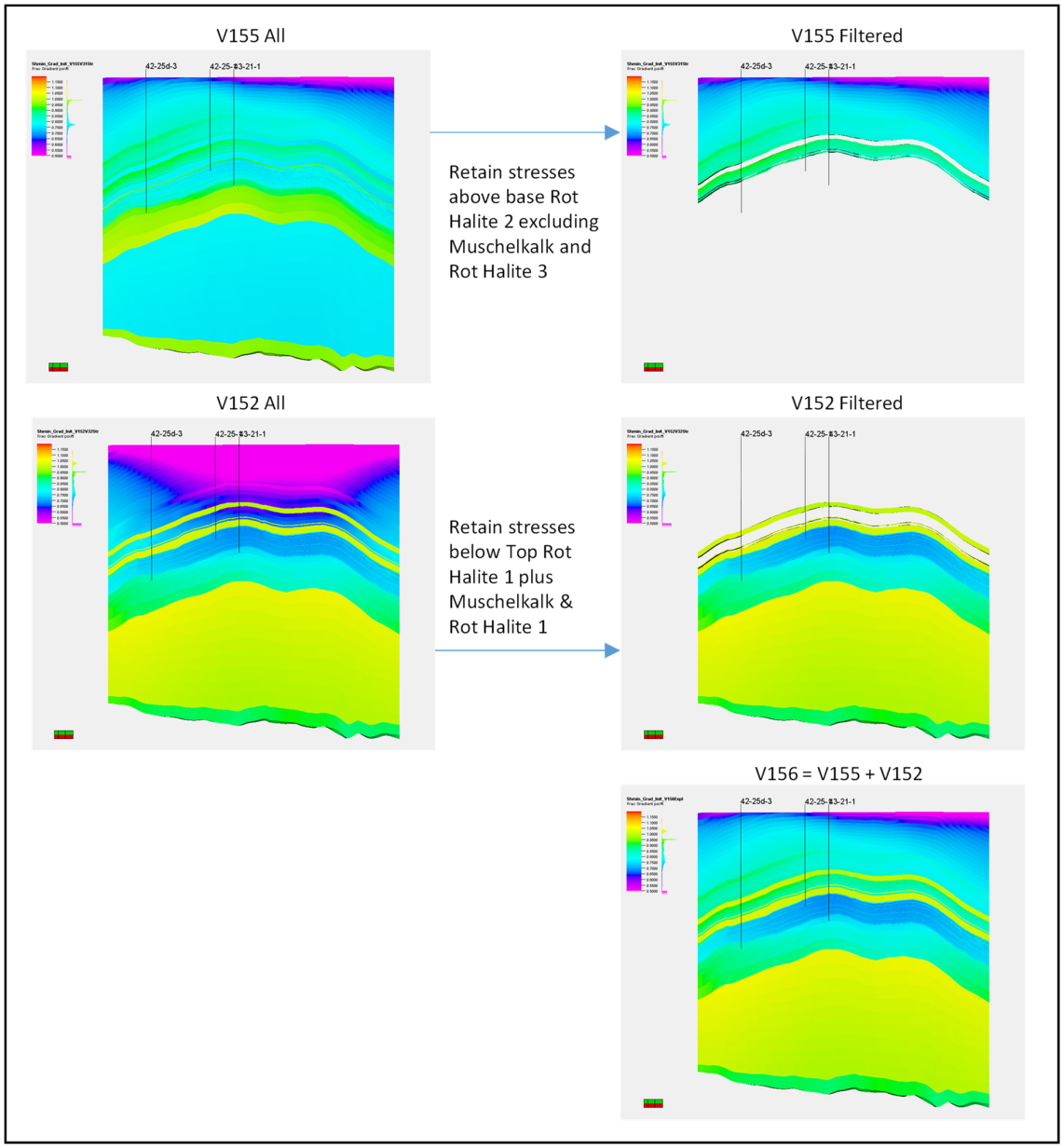

Figure 32 - Reference case stress state property construction. Shmin gradient in psi/ft shown.

4.4.3 Stress Initialisation Checks

The approach outlined produces a realistic initial in-situ stress distribution for Endurance, although it is not the only one possible. This initial in-situ stress model has been obtained by merging the results of two separate Imposed boundary condition initialisations and using that as an explicit Stress initialization. There is valid a concern that a model with simulated pressure steps that uses the Stress initialization process will not behave in the same way as a model where the stresses are initialised with an Imposed boundary condition.

To address this, a number of tests were performed where pressure steps were simulated with just the V152 or the V155 case initial stresses and various fault models to see if deformation

within the reservoir and immediate cap rocks (Röt Clay and Röt Halite 1) were significantly different to the cases utilising the V156 case initial stresses. The difference in results were minor.

5.0 Simulation Cases

With the V155 + V152 = V156 initial in-situ stress case as the starting point, a number of simulations were performed using the pressure steps outlined. These were designed to capture the behaviour of the Bunter Sandstone, overlying units and the overburden faults in response to Bunter Sandstone pressurisation during CO2 injection. As stated previously, thermal effects were not modelled during these simulations. In addition, any potential for geomechanical property changes resulting from chemical interactions between the injected CO2 and the formation brine, matrix or the faults were not considered. The full list of output properties from the simulations is given later. The key parameters investigated are given below in **Table 7**.

Table 7 - Key VISAGE simulation output parameters for evaluating Endurance integrity.

Parameter Name	Description	Relevance
ROCKDISZ	Vertical rock displacement (metres)	Could indicate seabed uplift and/or tilting relevant to seabed infrastructure including Hornsea windfarm
PLSTRNZZ PLSTRNXX PLSTRNYY	Plastic matrix + fault strains in vertical (ZZ) E-W direction (XX) and N-S direction (YY)	Could indicate permanent deformation that could create leak paths between Bunter Sst and cap rocks
FLT_PLSN FLT_PLSS FLT_PLDN FLT_PLDS	Fault related plastic normal strain (PLSN) and shear strain (PLSS) Fault related plastic normal displacement (PLDN) and shear displacement (PLDS)	
STRAINZZ STRAINXX STRAINYY	Total elastic + plastic strains in vertical (ZZ) E-W direction (XX) and N-S direction (YY)	Could indicate permanent deformation of faults that may create leak paths and/or seismic activity within or above the store

FLT_ELSN FLT_ELSS FLT_ELDN FLT_ELDS	Fault related elastic normal strain (ELSN) and shear strain (ELSS) Fault related elastic normal displacement (ELDN) and shear displacement (ELDS)	Could indicate recoverable deformation of faults. Probably not relevant for leak paths but indicates where strain and displacement are accumulating

5.1 Scenario Tree

Figure 33 shows the tree of Endurance model scenarios that were simulated with different combinations of injection pressures, faults (properties and extents) and matrix properties. All cases ran one initialisation step, five injection pressure steps from 2025 to 2050 and one post injection pressure recovery step. The tree is not an exhaustive combination of parameters but all the most likely variations have been simulated, in addition to some more extreme parameters. Other runs were completed for various checks but are beyond the scope of this document.

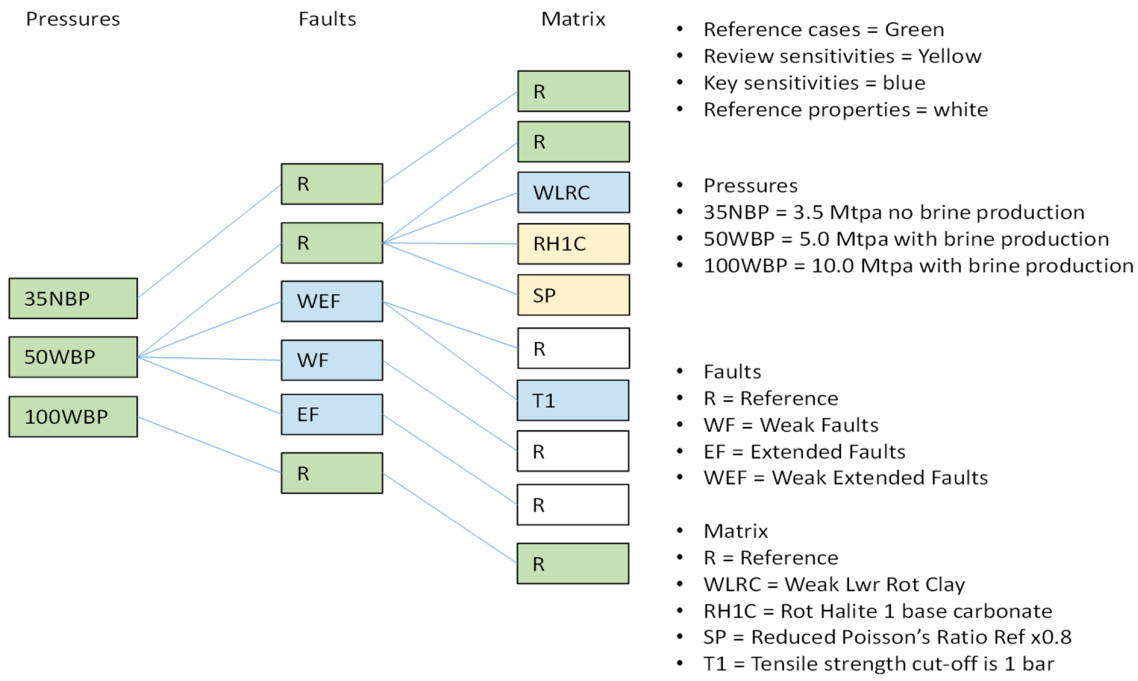

Figure 33- Endurance simulation scenario tree.

Selected cases and analyses are described in more detail below and contain the full range of behaviours observed in terms of matrix and fault related deformations. Other cases in the scenario tree exhibited behaviours within the ranges described and are therefore not covered in more detail.

To help understand the simulation results described below, **Figure 34** shows a 2D Mohr circle diagram of a notional failure envelope and Mohr circles for stress. Mohr diagrams are a useful way of defining the in-situ stress state at a given point and how that relates to the likelihood of failure at that point. The horizontal axis defines the normal stress (σn) and the vertical axis defines the shear stress (τ). Positive normal stresses are compressional and negative normal stresses are tensile. The three principal effective stresses are all normal stresses so plot on the horizontal axis. For a given pair of principal effective stresses such as σ1 = σ v = vertical effective principal stress and σ 3 = σ h = minimum horizontal effective stress, a circle can be drawn on the Mohr diagram that represents all combinations of normal and shear stress in a plane between these two principal stress values. 3D Mohr diagrams are also possible that represent all combinations of stress states between all three principal stresses but these are more complex and the 2D diagram captures all the essential elements.

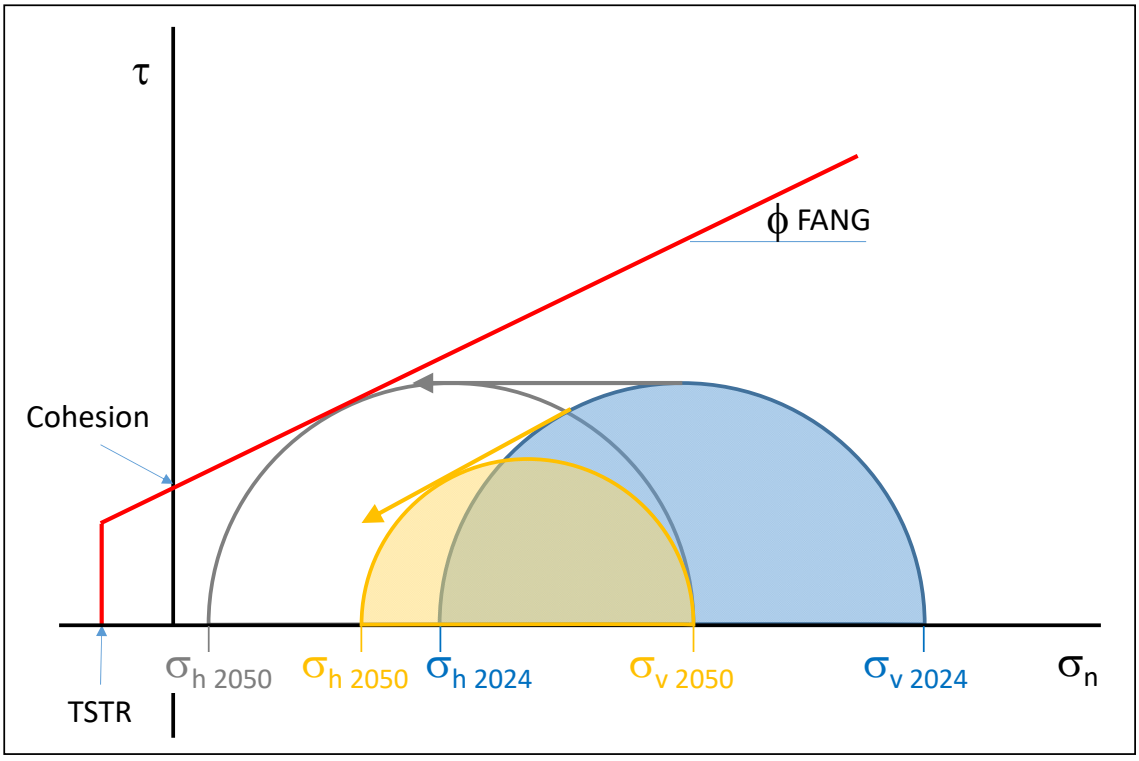

Figure 34 - Mohr diagram defining controls on failure.

Also shown on **Figure 34** is the failure envelope for intact rock. The input parameters in the model are Unconfined Compressive Strength (UCS) and Friction angle (FANG). In**Figure 34** , Cohesion can be calculated by:

Cohesion = UCS / (2*Tan(45 + FANG/2))

By changing the stress state via external forces or changing pore pressure, the Mohr stress circle can change size and/or position on the diagram. Increasing pore pressure will reduce the effective stress and the circles will move to the left on the diagram. If the failure envelope is touched by the circle in positive normal stress space, shear failure occurs (blue to grey in). If the initial circle shrinks and moves enough to the left then it will touch the vertical portion of the failure envelope in the negative part of the normal stress axis and tensile failure occurs (not shown in **Figure 34**).

Poroelasticity is a key characteristic of all the Endurance simulations. As the pore pressure increases, the effective stress is not just a function of Total stress – pore pressure x Biot, it is also coupled via Poisson's ratio. In summary, this poroelastic coupling will tend to shrink the principal effective stress Mohr circles via an increase in the horizontal minimum total stresses (SHmax and Shmin). This effect is shown schematically on **Figure 34** via the change in effective stress Mohr circle size from 2024 (blue) to 2050 (orange). If that poroelastic coupling is significant, the stress path tangent to the circles (orange arrow) will either be parallel to the failure envelope or will be steeper than the failure envelope. Therefore, failure in these models will tend to be via tensile failure but only where the pore pressure increases are significant and/or the tensile strength is low.

5.2 Reference Cases – 3.5,5.0 and 10 Mtpa Injection

These cases are regarded as the reference case scenarios as they include the reference case matrix properties and mapped faults (to Top Röt Halite 3) and initial in-situ stresses. Simulated injection schemes are 3.5 Mtpa no brine production, 5.0 Mtpa with brine production and 10.0 Mtpa with brine production. All injection simulations are for 25 years of injection from 2025 to 2050 with a monitoring step to 2500. One of the notable features of all these cases is that the pressures equilibrate very rapidly in the high permeability Bunter Sandstone. This means that differences in the number and placement of injectors is less important to Endurance Bunter Sandstone reservoir pressures than the total material balance of CO2 injected vs brine produced. None of these reference cases had any plastic failure during injection; only recoverable elastic strains were simulated.

5.2.1 3.5 Mpta no Brine Production

Figure 35 shows the vertical displacement (Upper) and vertical elastic strain (Lower) properties from the 3.5 Mtpa no brine production injection case at 2050. Vertical displacement is largely translated from the Bunter Sandstone (interval with red bars in **Figure 35**) to Seabed. The maximum values are approximately 0.185 m at Top Bunter Endurance crest and 0.170 m at Seabed above Endurance crest. It is possible that these vertical displacements are toward the high end of expectations as the relatively coarse layering in the overburden averages out the compliant lithologies that could otherwise absorb the vertical displacement via strain. However, by largely transmitting the Top Bunter displacements to Seabed, the model does provide an upper limit on expected Seabed uplift and associated tilting (see section 0 for tilt data).

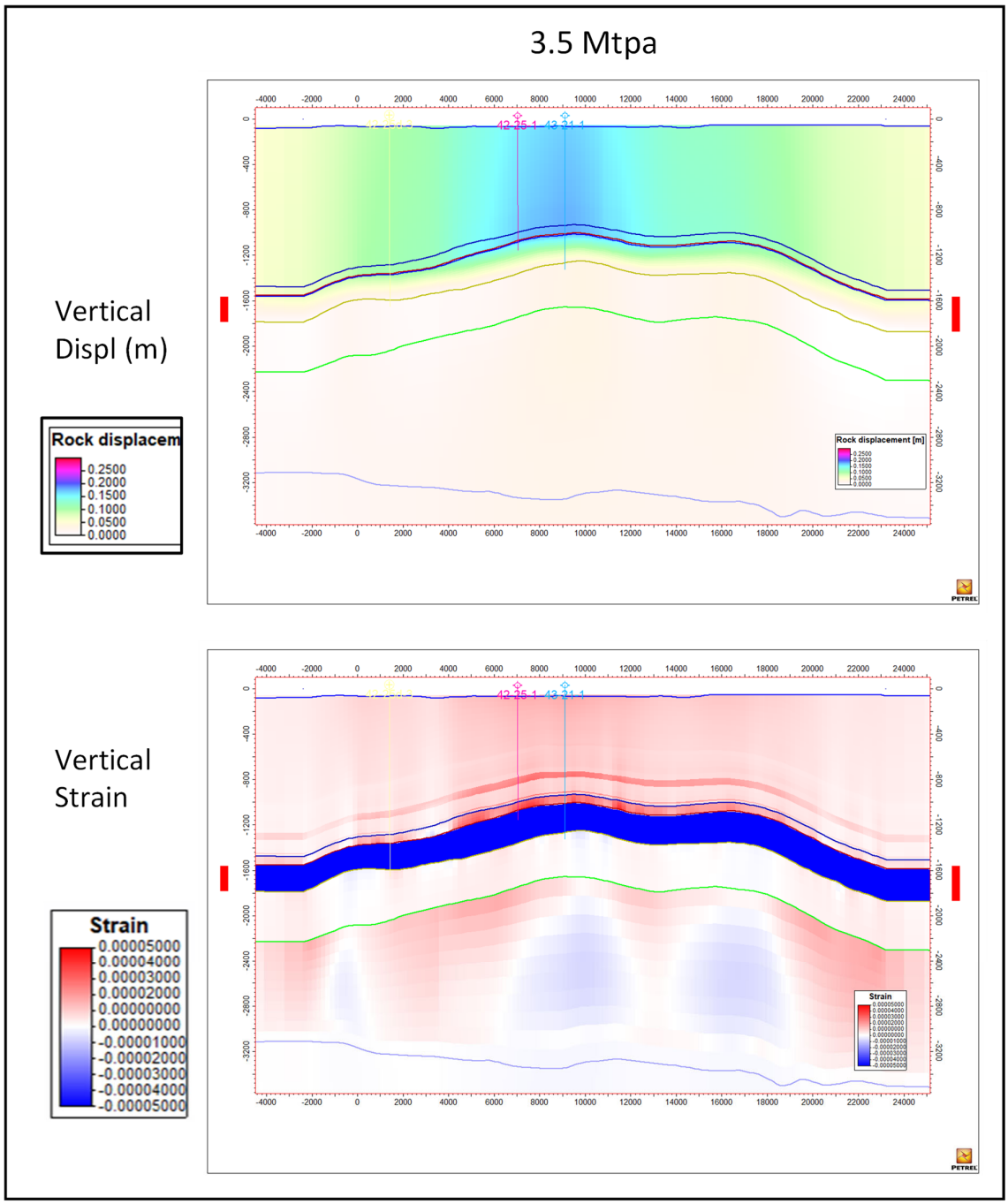

Figure 35 - Endurance 3.5 Mtpa no brine production vertical displacement and vertical strain properties in 2050.

There are minor compressive strains throughout the overburden that absorb the 0.015 m displacement difference. The largest compressive vertical strains in the overburden occur within the within the Röt and Muschelkalk halite units. Some minor stretching and compressive vertical strains also occur in the Zechstein salt. This is in response to the injection pressure strains in the overlying Bunter Sandstone.

Maximum lateral displacements (XX and YY) are under half the vertical displacement and increase toward the AOI edges. Lateral XX and YY strains are generally low and indicate stretching in both the XX and YY directions in the overburden. This horizontal stretching is also represented by a slight reduction in horizontal minimum total stress in the overburden compared with the strong poroelasticity related horizontal minimum total stress increase in the Bunter Sandstone (difference plot shown in **Figure 36**). Also, note that the total stresses stay the same (lithostatic) in the Röt Halite 1, Röt Halite 3 and Muschelkalk salt units. Faults do not have any plastic strain and fault shear and normal elastic strains are all less than about 1E-06 in absolute terms.

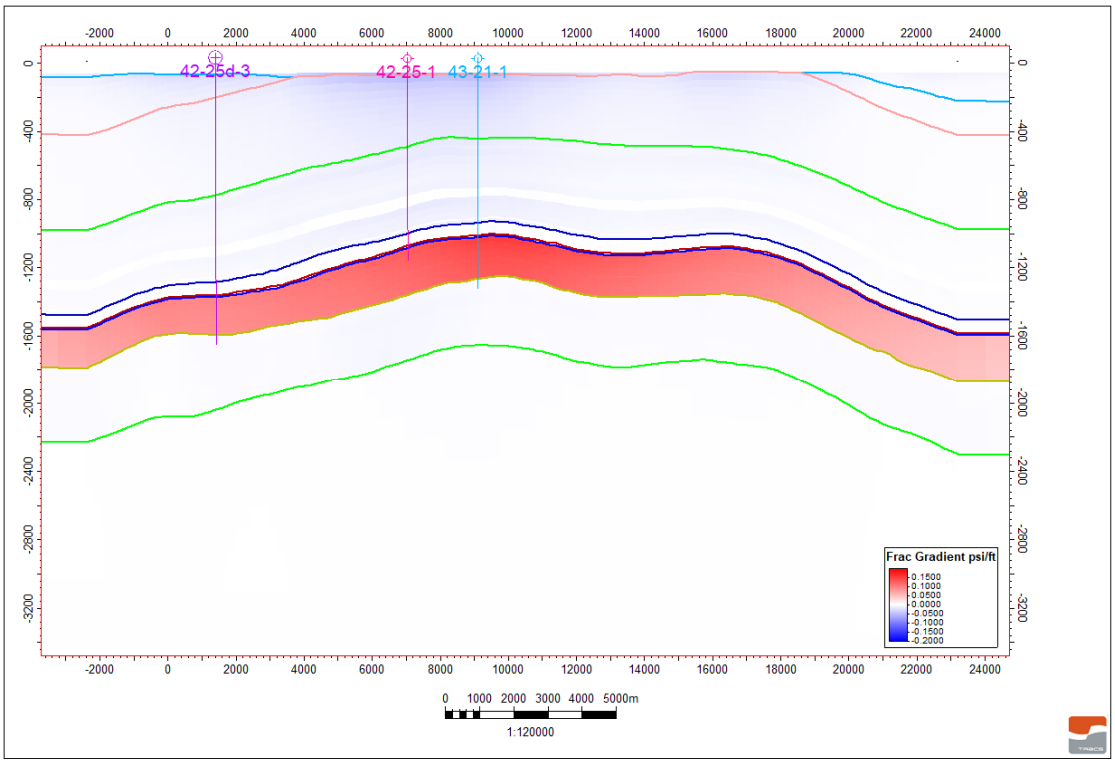

Figure 36 - Endurance stress gradient change from 2023 to 2050 3.5 Mtpa injection.

Stress paths are another way of investigating the impact of poroelasticity where the stress path (A) is defined as the difference in minimum horizontal total stress (Shmin) divided by the difference in pore pressure (Pp):

A = (Shmin 2050 – Shmin 2024) / (Pp 2050 – Pp 2024)

Figure 37 shows a variety of stress paths calculated for producing reservoirs from Zoback (2007). The diagram indicates that under producing conditions, stress paths of 0.67 or more will lead to production induced normal faulting. **Figure 38** shows the stress path histogram for the Bunter Sandstone with an average of 0.68 and approximately half the values above 0.68. The location of Bunter Sandstone stress path values calculated for the 3.5 Mtpa injection case are shown by the orange oval in **Figure 37**. However, the stress path values that would lead to faulting under depletion are less likely fail under injection because the Mohr circles at higher

reservoir pressures are moving away from the failure envelope rather than toward it, as would happen under depletion.

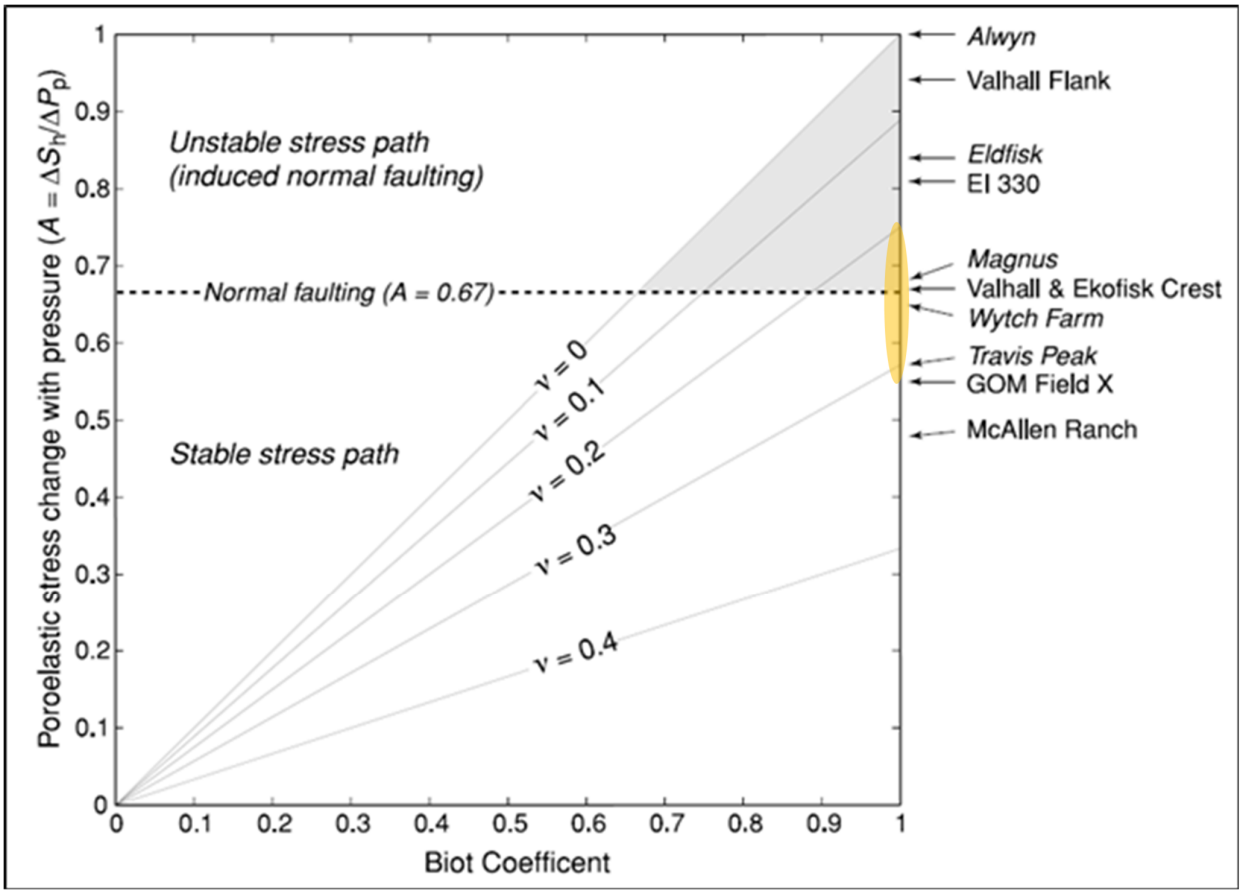

Figure 37 - Examples of stress paths from Zobak (2007). Orange ellipse represents 3.5 Mtpa case values.

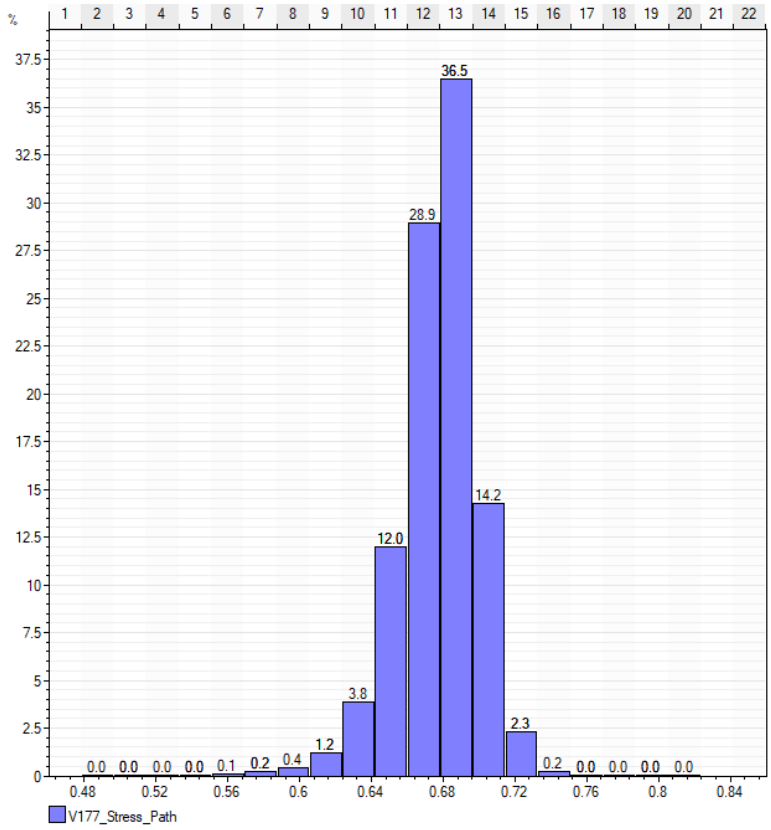

Figure 38 - Endurance 3.5 Mtpa injection case Bunter Sandstone stress path.

After 450 years of post-injection monitoring, the peak Bunter Sandstone total stress values reduce to values that are approximately 3% higher than the initial condition total stresses. This pressure and stress recovery is also reflected in the maximum seabed displacement in 2500, which is around 0.04 m.

5.2.2 5.0 Mtpa with Brine Production

The key difference to the 3.5 Mtpa case, other than injection volume per annum, is that brine production is activated to manage the reservoir pressures. Brine production can be a key mitigation to any potential geomechanical seal breach issues arising in the reservoir during injection. It should be noted that because of brine production in the 10.0 Mtpa case, the 5.0 Mtpa case with brine production has marginally higher pressures by 2050.

The vertical displacement and vertical strain properties are shown in **Figure 39**. The vertical displacement and vertical strain values are slightly larger than the 3.5 Mtpa case but have very similar distributions. Maximum displacement at Seabed is 0.187 m.

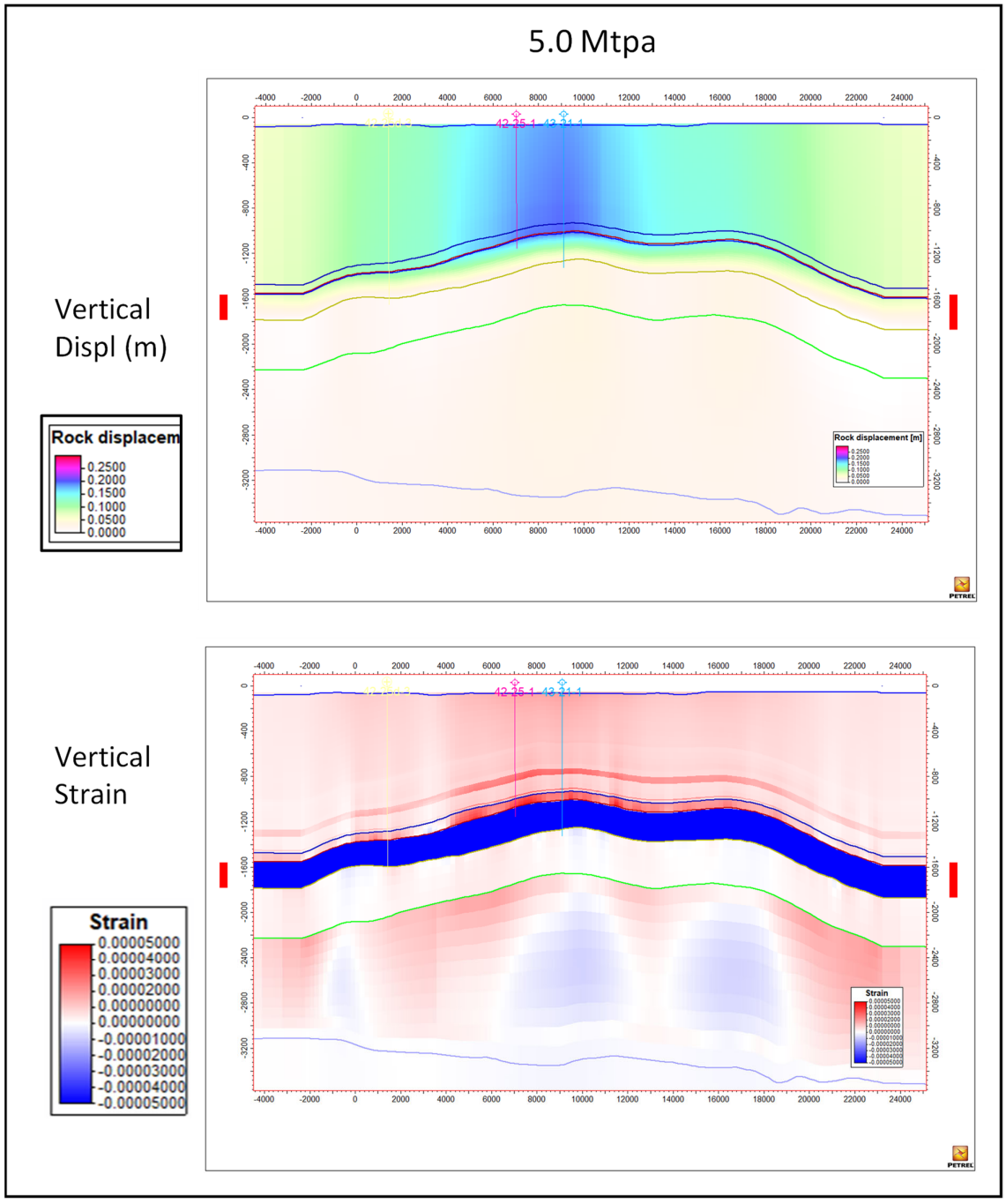

Figure 39 - 65 Endurance 5.0 Mtpa with brine production vertical displacement and vertical strain properties in 2050.

The 2050 to 2024 minimum horizontal total stress difference property is shown in **Figure 40**. The distributions and magnitudes of stress changes are very similar to the 3.5 Mtpa case, however, the overburden stress reductions above Röt Halite 1 to Seabed are discussed in more detail here. There is a slight decrease in the Röt Clay Shmin total principal in-situ stress of -0.01 to -0.03 psi/ft during injection in the 5.0 Mtpa Reference case. This stress reduction (expressed as a gradient) becomes more marked in the shallow levels reaching a maximum change of -0.078 psi/ft for the Shmin in the Quaternary over the Endurance crest. These stress drops are expected from the elastic inflation and stretching of the Bunter Sandstone during

injection. Some of these stress drops reduce shallow unit (>-200 mTVDss) Shmin values from positive to negative.

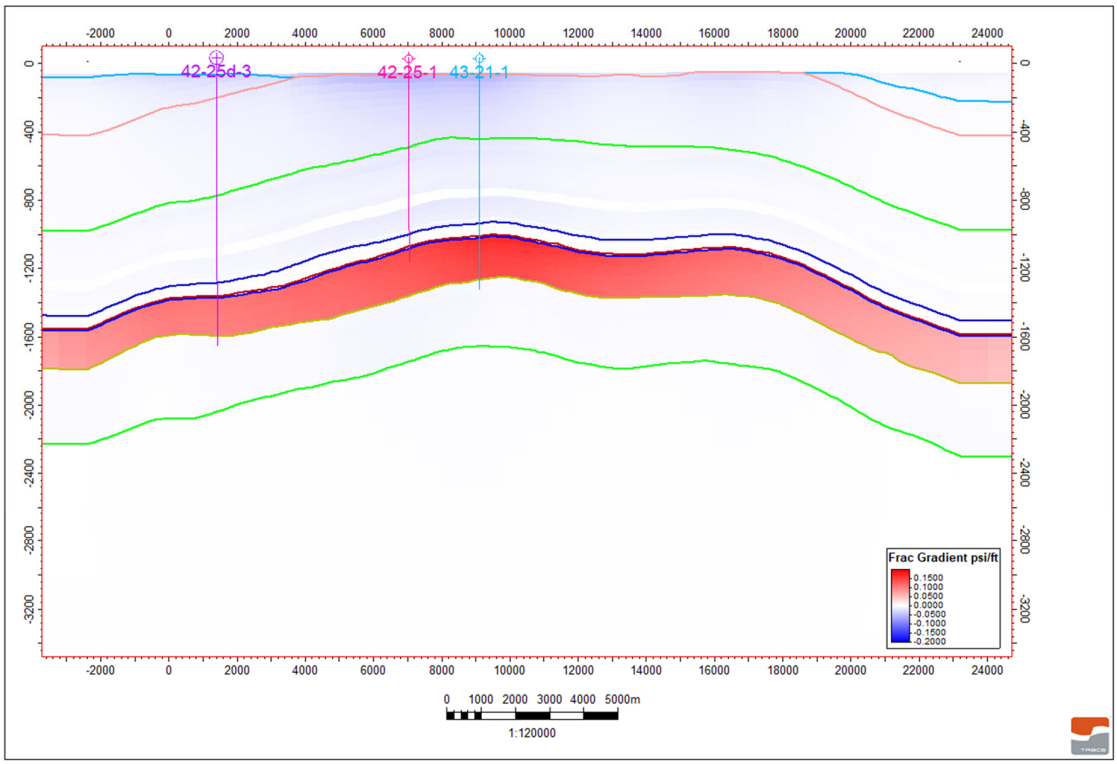

Figure 40 - Endurance stress gradient change from 2024 to 2050 5.0 Mtpa injection.

However, the shallow stresses and rock properties above about -500 mTVDss are very poorly constrained in the Endurance Phase 1 area. This is particularly true for the in-situ stresses in the interval above -100 mTVDss where the values are all likely to be small and very similar to Sv. Model layers >= -100 mTVDss have been set to elastic to prevent failure during in-situ stress initialisation and stabilise the model. Irrespective of the shallow layer modelling methods, absolute stress reductions in the interval above -200 mTVDss are typically 1 to 2 bar or less and Bunter Sandstone stretching related deformation will probably be largely absorbed within the overburden rather than applied throughout it. Therefore, shallow stress gradient reductions are not regarded as a significant issue in Endurance but should be accounted for in surface infrastructure designs and monitoring programs.

Faults do not have any plastic strain and fault shear and normal elastic strains are all less than about 1E-06 in absolute terms. The average stress path from 2024 to 2050 is 0.68 and the distribution of values is very similar to that shown earlier. Stress and displacement recovery by 2500 is similar to the 3.5 Mtpa case with a maximum seabed displacement in 2500 of around 0.04 m.

In addition to the stress path values described above and the stress changes, more detailed assessments can be made of the stress changes via the stress chart tool. The benefit of this approach is that a cell-by-cell evaluation can be made of the stress changes with respect to the failure envelopes. **Figure 41** shows the Shmin gradients (psi/ft) in 2024 and 2050 on the crest

of Endurance. Total stress Mohr circles and their associated failure envelope projections (red lines) are shown for a crestal basal Röt Clay cell (Upper) and a crestal shallowest Bunter Sandstone cell (Lower). A number of points can be made.

1. Shmin in the Bunter Sandstone increases significantly from 2024 to 2050 due to injection pressure related poroelasticity. This is why the Mohr circles shrink with increasing pore pressure in **Figure 41**.
2. The Röt Clay Shmin values and Mohr circles only change very slightly from 2024 and 2050. This is because there are no modelled pore pressure changes in this unit and the underlying Bunter Sandstone stress and strain changes impart a small external strain on the Röt Clay. This accounts for the minor Röt Clay Mohr Circle changes.
3. The Bunter Sandstone poroelastic stress changes shrinks the Mohr circle sizes meaning they stay a significant distance from the failure envelopes (red lines) even at end injection. The factors that would cause these circles to approach the failure envelopes more closely or to touch them are:

a. Increased Mohr circle size at initial conditions, i.e. smaller Shmin values
b. A different stress path such that the circles shrink less and/or move more to the left during injection. This would require a different Poisson's Ratio.
c. Weaker rock with a lower tensile strength and/or lower cohesion and/or a lower friction angle. The dashed red line shows the scenario where the Röt Clay and Bunter Sandstone have zero tensile strength and cohesion. Failure still would not occur unless the friction angle is also reduced.

4. The Röt Halite 1 and Röt Halite 2 units above the Röt Clay show virtually no change in their lithostatic stress state. This is expected from a geological standpoint given the relatively low strains in this case and from the way the salts are treated in these models as compliant elastic materials.

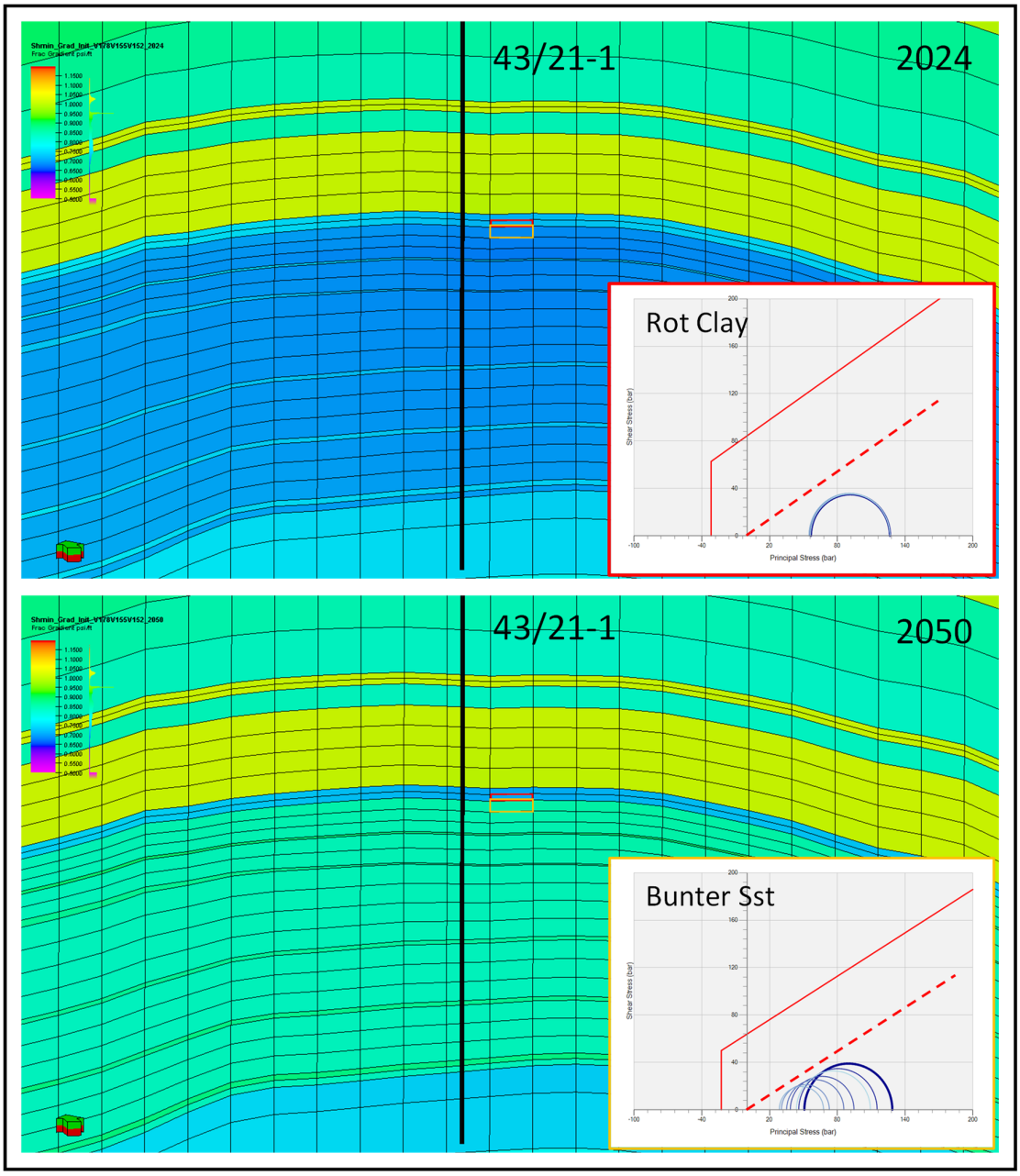

Figure 41 - 5.0 Mtpa case Shmin psi/ft gradient property on Endurance crest with Mohr circles for basal Röt Röt Clay cell (red outline) and upper Bunter Sandstone cell (orange outline).

A critical question arising from the situation illustrated is why the Röt Clay shows no failure in 2050 with a pore pressure of 108 bar and Shmin value of 163 bar when the underlying Bunter Sandstone has a pore pressure of 168 bar and Shmin of 197 bar. Reasoning is described below but it should be noted that pore pressure in the Bunter Sandstone will be managed to ensure it does not exceed Shmin of the Primary Seal which is set as part of reservoir pressure limit guidelines.

1. The simulation model that generated the pressures used in VISAGE does not directly couple any pore pressure changes in the Bunter Sandstone with the overlying Röt Clay.

2. One way coupled VISAGE simulations treats adjacent cells with different pore pressure histories as separate entities. Their stresses and strains are only coupled by the changes in cell displacements and strains at the common cell boundaries. No pore fluid diffusion effects are modelled in VISAGE as occurring from the increasing pore pressure Bunter Sandstone cells into the matrix of the adjacent Röt Clay cells. Therefore, any potential open fractures within the Röt Clay are not connected to the pore pressure changes in the underlying Bunter Sandstone.

The situation described above is at least partly a function of the modelling methodology (one way coupled). To address the potential for failure in these situations, a number of approaches could be taken.

1. Assume that any pore pressure in the Bunter Sandstone that exceeds the overlying Röt Clay in-situ minimum total stress will cause leakage via zero tensile strength or zero cohesion fractures. This is the classic analytical approach taken in say seal breach analyses for exploration targets and provides a conservative assessment of cap rock integrity.
2. Create two way coupled models where some criteria for changes in the Bunter Sandstone reservoir pressures and stresses leads to a revised permeability and pore pressure in adjacent Röt Clay cells. That way the leak path is defined and modelled explicitly.

This was tested to a degree but could be taken further.

5.2.3 10.0 Mtpa with Brine Production

This is the higher rate case considered as part of the group of reference scenarios. Brine production largely mitigates the higher reservoir pressures that would otherwise be expected so the reservoir and overburden stress strain behaviour is very similar to the 5.0 Mtpa case.

The vertical displacement and vertical strain properties are shown in **Figure 42**. The vertical displacement and vertical strain values are slightly larger than the 3.5 Mtpa case but very slightly lower than the 5.0 Mtpa case. All cases have very similar vertical displacement and vertical strain distributions. Maximum displacement at Seabed is 0.182 m.

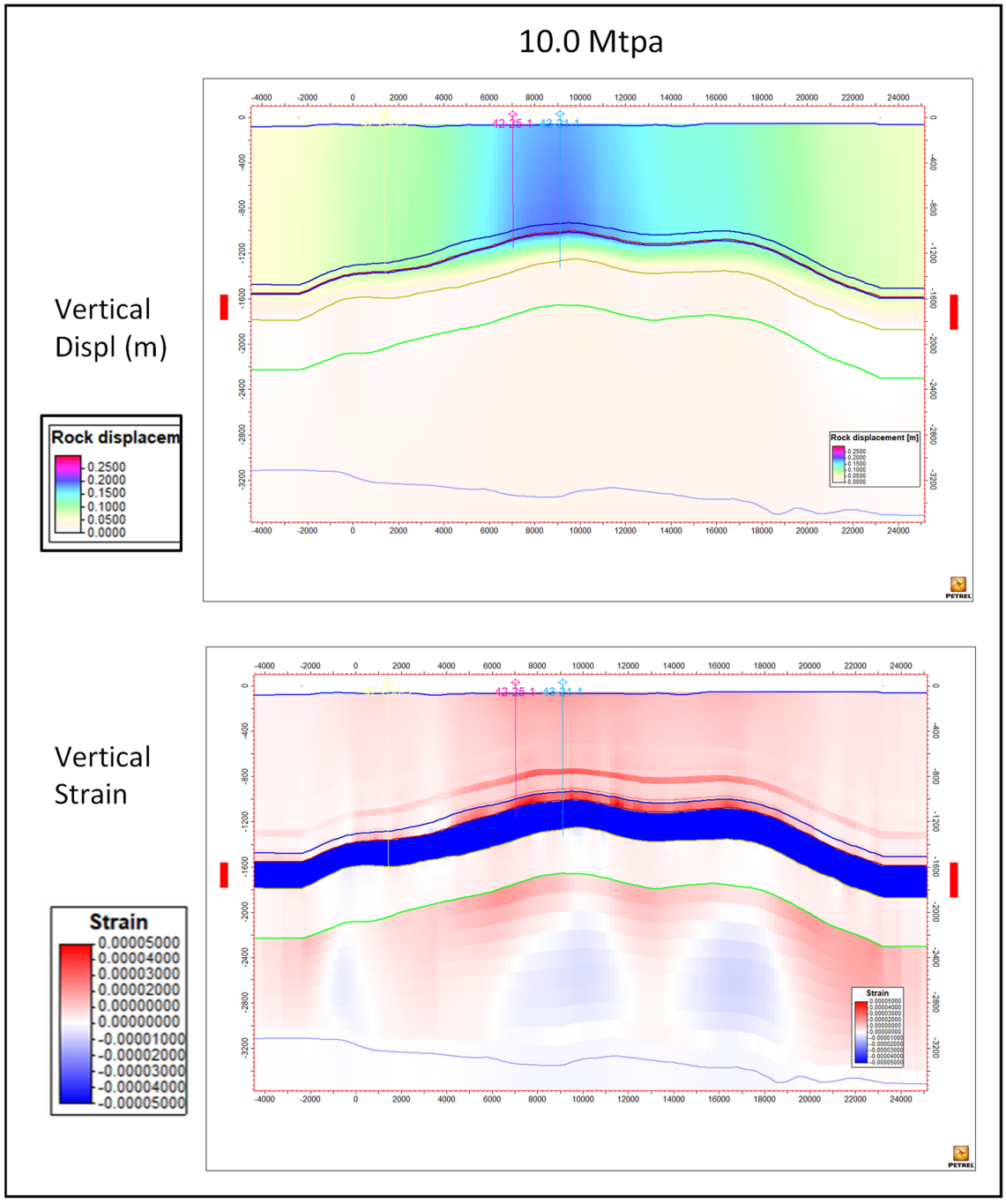

Figure 42 - Endurance 10.0 Mtpa with brine production vertical displacement and vertical strain properties in 2050.

The 2050 to 2024 minimum horizontal total stress difference property is shown in Figure 69. The distributions and magnitudes of stress changes are very similar to the 3.5 Mtpa case.

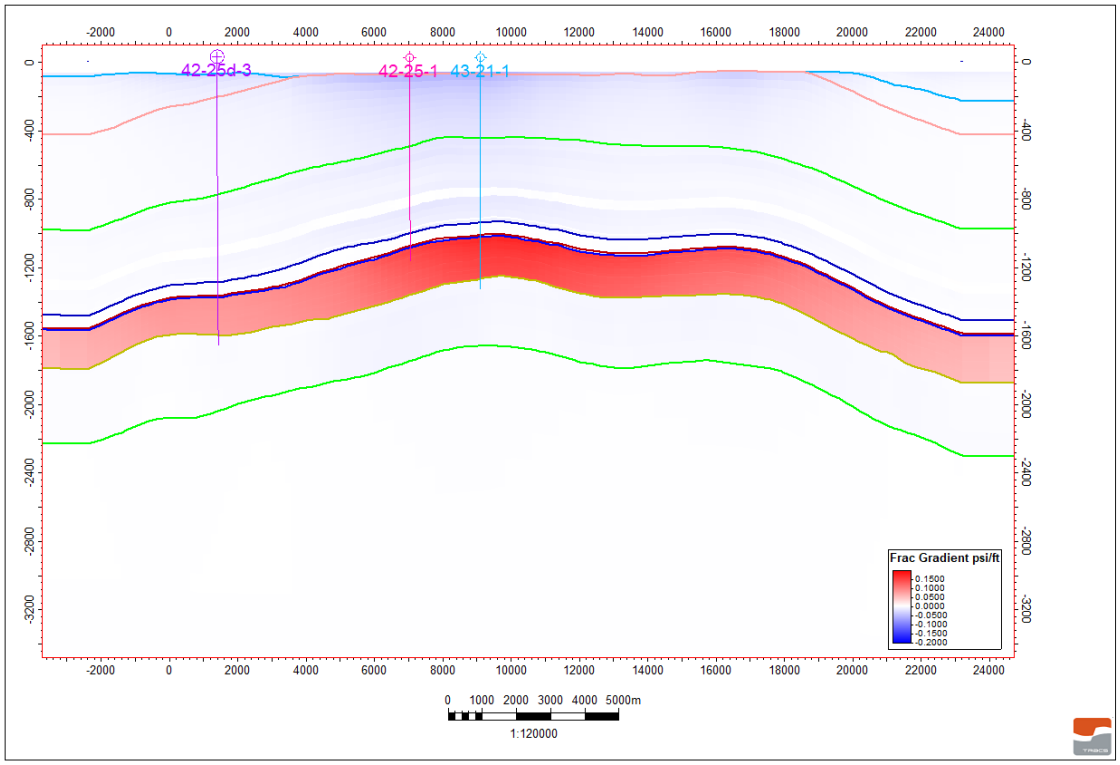

Figure 43 - Endurance stress gradient change from 2024 to 2050 10.0 Mtpa injection.

Faults do not have any plastic strain and fault shear and normal elastic strains are all less than 1.3E-06 in absolute terms. The average stress path from 2024 to 2050 is 0.70 and the distribution of values is very similar to that in the 3.5 Mtpa case. Stress and displacement recovery by 2500 is similar to the 3.5 Mtpa case with a maximum seabed displacement in 2500 of around 0.05 m.

5.3 Seabed Iplift and Tilts – All Cases

5.3.1 Seabed Uplift

The magnitude of seabed uplifts have been described in previous sections for all the pressure cases. The uplift magnitudes in these models are not sensitive to the matrix and fault strength properties and whether failure has occurred on matrix or faults. Modelled vertical displacement at seabed is controlled by the elastic strain within the Bunter Sandstone, which is largely transmitted upwards to the overburden as vertical displacement with only minor compressive strain occurring within the overburden.

The seabed uplift values associated with the Reference case injection schemes are all less than 0.19m. The Reference case estimates may be at the upper end of expected Seabed uplift values for each case due to the lack of absorption within the overburden of the Bunter Sandstone vertical stretching (and Top Bunter Sandstone upward displacement) via compressive vertical strains. However, compared to many offshore scenarios overlain by Mesozoic and Cenozoic sediments, Endurance is overlain by relatively well-lithified Triassic

sediments so less compressive strain would perhaps be expected than potential analogues. Even if the modelled seabed uplift magnitudes are close to reality, they are unlikely to cause significant issues to seabed infrastructure.

5.3.2 Seabed Tilts

It is possible that injection in Endurance could cause some seabed uplift and also tilting. This has been assessed and discussed with engineering regarding the planned Hornsea windfarm.

Figure 44 shows the seabed tilts over Endurance along with the Hornsea windfarm potential Phase 4 area. These tilt maps were calculated by deriving the vertical displacement values at the shallowest model layer (usually Quaternary) and creating a map of these values. These mapped values were then used in dip calculations to determine the surface tilts over the Endurance structure. Key points are listed below:

These tilt calculations are independent of the absolute amount of vertical displacement and they assess the rate of change of vertical displacement across the structure.

The Endurance Phase 1 area model has 200m x 200m grid cell dimensions. Any changes in surface displacement occurring over smaller distances (such as associated with a fault that is close to surface) may cause larger displacement gradients and therefore locally larger tilts than modelled here.

All reference case modelled seabed tilts reported here are below 0.002° meaning seabed tilting is unlikely to cause significant issues with the planned windfarm and other infrastructure.

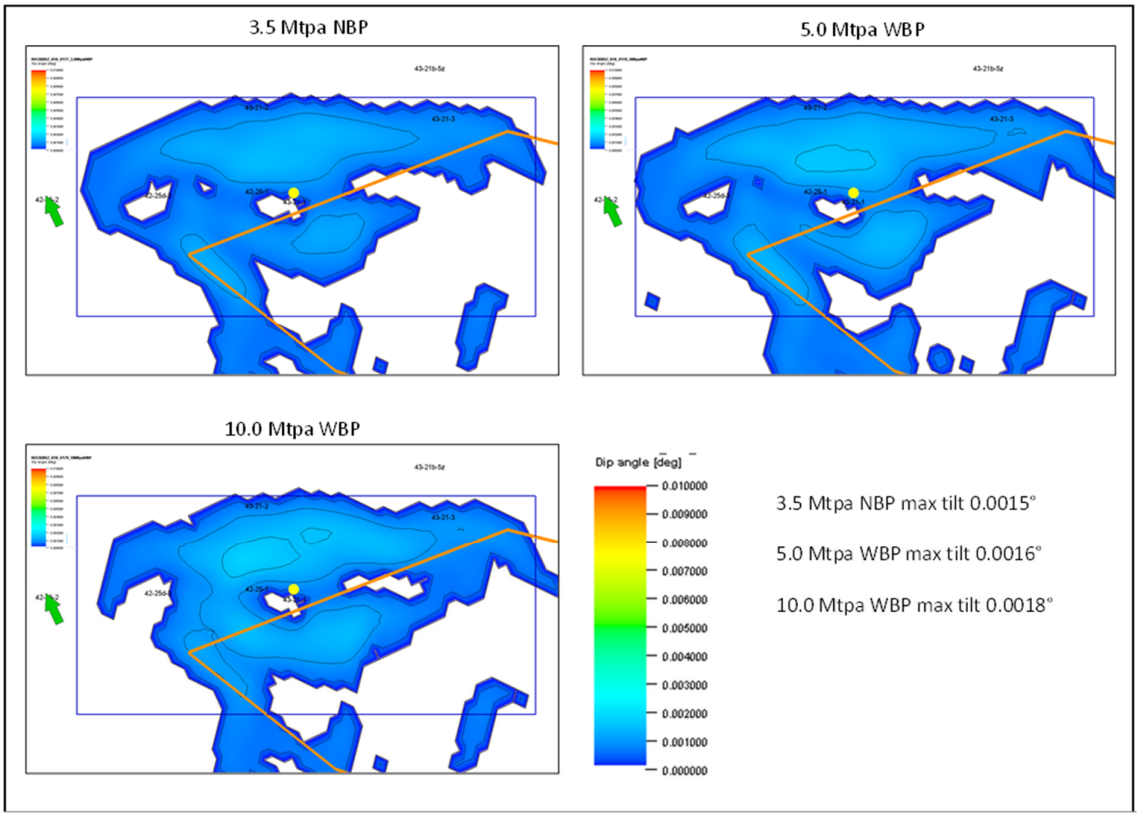

Figure 44 - Endurance Seabed tilts in 2050 for all injection cases with reference properties. Yellow dot marks Endurance Crest location NE of well 43/21-1. Orange outline is potential Hornsea windfarm Phase 4 area.

6.0 Conclusions and Recommendations

Containment is a fundamental component of successful long-term storage of CO2 and geomechanical modelling a key tool for assessing the stress / strain changes from the injection pressure increases and the potential for failure of primary sealing units. This study sought to obtain best estimates honouring available data, applying engineering judgement to sense check results where appropriate and testing sensitivity to key parameters.

Key risks that were assessed include:

- Failure of Röt Halite 1 and Röt Clay sealing units via tensile or shear failure.
- Tensile or shear reactivation of faults mapped in the overburden of Endurance down to Top Röt Halite 3 and some tests of extended faults
- Uplift and tilt of seabed
- Tensile or shear failure of Bunter Sandstone

Three key pressure cases (3.5, 5 and 10 Mtpa) were supplied from the dynamic model and simulated in VISAGE cases utilising different combinations of fault and matrix properties. None

of the simulations using the key pressure cases displayed any plastic failure or reactivation of faults.

The Röt Clay initial in-situ stress is approximately 0.15 psi/ft lower at the crest just North of 43/21-1 (~0.71 psi/ft) compared to the flank location at 42/25d-3 (0.86 psi/ft). It is possible that the crestal initial in-situ stress is higher and in the range of 0.75-0.80 psi/ft. However, all the models indicate that crestal Röt Clay initial in-situ stresses will be lower than the measured values at 42/25d-3. Because of the likely crestal reduction in Röt Clay initial in-situ stress values plus the possibility for weak discontinuities within the Röt Clay, the Röt Halite 1, modelled with high lithostatic in-situ stresses, is also treated as part of the seal system over Endurance.

Modelled maximum uplift at seabed occurs over the Endurance structure crest and ranges from 0.17m to 0.19m. Uplift values decrease onto Endurance flanks. These uplift values are regarded as toward the high end of expectation as they are similar to the uplift values at Top Bunter Sandstone. It is likely more uplift will be absorbed within the overburden although these values provide a useful reference point for Seabed infrastructure design.

Tilting of the seabed calculated from the gradient of vertical uplift was evaluated regarding the planned Hornsea windfarm. Modelled maximum tilt values in all cases reported here were below 0.002° and generally found on the flanks of the structure. The geomechanical model cell dimensions are 200m x 200m, which will tend to reduce lateral strain and displacement gradients and therefore reduce average tilt values compared to a more refined grid. Seabed tilting is unlikely to cause significant issues with the planned windfarm and other infrastructure.

Horizontal in-situ stress drops above the Bunter Sandstone are expected from the elastic inflation and stretching of the Bunter Sandstone during injection. There is a slight decrease in the Röt Clay Shmin total principal in-situ stress of -0.01 to -0.03 psi/ft during injection in the 5.0 Mtpa Reference case. This stress reduction becomes more marked in the shallow levels reaching a maximum change of -0.078 psi/ft for the Shmin in the Quaternary over the Endurance crest. In absolute terms, these stress reductions near Seabed are 1 to 2 bar or less. It is likely that in reality the modelled injection related shallow in-situ stress reductions would be largely absorbed by the overburden. However, although these shallow stress reductions are not regarded as a significant issue in Endurance, surface facility and monitoring system designs should account for them.

The Bunter Sandstone unit in the models displays a clear poroelastic response with the total horizontal principal stresses increasing during CO2 injection. This reduces the likelihood of failure in this unit by reducing the differential stress and keeping it below the modelled failure envelopes despite the effective stresses decreasing. Further work on the reservoir was carried out in Reveal (please see next section).

The geomechanical model provides a useful exploration of the possible rock mechanics properties and in-situ stresses expected within and above Endurance including the overburden fault system. With planned injection schemes of up to 10 Mtpa (with brine production where necessary) coupled with a comprehensive data gathering and monitoring program, risks of seal

breach or adverse Seabed uplift and tilting effects are regarded as low. However, the elastic strain estimates reported here can be used as input to surface facility designs, data gathering and monitoring program design or for further modelling to provide more detailed characterisation. In particular, the potential for Röt Clay failure could be investigated by dual porosity / dual permeability models that explicitly couple the geomechanical effects with the potential for fluid ingress from the Bunter Sandstone to the Röt Clay via joints or small faults. This has been tested to an extent with this work but could be developed further.

7.0 References

White Rose, 2016. K40: Subsurface geoscience and production chemistry reports. Capture Power Limited, 300pp., https://assets.publishing.service.gov.uk/government/uploads/system/uploads/attachment_data/file/531045/K40_Subsurface_Geoscience_and_Production_Chemistry.pdf

Williams, J.D.O., Fellgett, M.W., Kingdon, A, Williamson, J.P., 2015. In-situ stress orientations in the UK Southern North Sea: Regional trends, deviations and detachment of the post-Zechstein stress field. Marine and Petroleum Geology, 67, 769-784.

Zhang, X., Koutsabeloulis, N.C., Heffer, K.J., Main, I.G and Li, L., 2007. Coupled geomechanics–flow modelling at and below a critical stress state used to investigate common statistical properties of field production data. In: S.J. Jolley, D. Barr, J.J. Walsh and R.J. Knipe (eds) Structurally Complex Reservoirs. Geological Society, London, Special Publications, 292, 453–468.

Zoback, M. D., 2007. Reservoir Geomechanics, University Press, Cambridge, 452pp.

Annex A – VISAGE Simulation Output Property Key

The table below is the full list of dynamic simulation outputs from VISAGE after importing into Petrel via the Results tab. Note: The parameters available depend on the type of simulation being performed (e.g. linear – elastic or non-linear – plastic or creep) so some outputs are unavailable. Detailed table key below.

^ are calculated at nodes in the simulation and are then averaged to a cell value for visualization in Petrel.

* are calculated at Gauss points in the simulation and are then averaged to a cell value for visualization in Petrel.

Compression is positive in Petrel for stress and strain results.

All strains are output as mathematical strains. This is so that the Petrel tensor calculations work correctly for the calculation of principal values.

Output Parameter	Description
ROCKDISX^	X component of total displacement vector.
ROCKDISY^	Y component of total displacement vector.
ROCKDISZ^	Z component of total displacement vector.
EFFSTRXX*	XX component of effective stress tensor.
EFFSTRYY*	YY component of effective stress tensor.
EFFSTRZZ*	ZZ component of effective stress tensor.
EFFSTRXY*	XY component of effective stress tensor.
EFFSTRYZ*	YZ component of effective stress tensor.
EFFSTRZX*	ZX component of effective stress tensor.
TOTSTRXX*	XX component of total stress tensor.
TOTSTRYY*	YY component of total stress tensor.
TOTSTRZZ*	ZZ component of total stress tensor.
TOTSTRXY*	XY component of total stress tensor.

Output Parameter	Description
TOTSTRYZ*	YZ component of total stress tensor.
TOTSTRZX*	ZX component of total stress tensor.
STRAINXX*	XX component of total strain tensor (mathematical).
STRAINYY*	YY component of total strain tensor (mathematical).
STRAINZZ*	ZZ component of total strain tensor (mathematical).
STRAINXY*	XY component of total strain tensor (mathematical).
STRAINYZ*	YZ component of total strain tensor (mathematical).
STRAINZX*	ZX component of total strain tensor (mathematical).
PLSTRNXX*	XX component of plastic strain tensor (mathematical).
PLSTRNYY*	YY component of plastic strain tensor (mathematical).
PLSTRNZZ*	ZZ component of plastic strain tensor (mathematical).
PLSTRNXY*	XY component of plastic strain tensor (mathematical).
PLSTRNYZ*	YZ component of plastic strain tensor (mathematical).
PLSTRNZX*	ZX component of plastic strain tensor (mathematical).
YIELDMOD*	Invariant yield criteria yielding mode. 1 = tension, 3 = shear, 5 = cap
YLDVAL_I*	Initial invariant yield value at the first iteration of load step.
YLDVAL_F*	Final invariant yield value at the convergence of load step non-linear.
???_YLDV*	Discontinuity yield value at convergence, where ??? is either DFN for DFNs, or FLT for faults. The results are unified for all DFN or faults, and take the maximum value for cells with multiple discontinuities.
???_MODE*	Discontinuity yield mode, where ??? is either DFN for DFNs, or FLT for faults. The results are unified for all DFN or faults and take the maximum value for cells with multiple discontinuities. —2 = elastic shear,—1 = elastic tension, 1 = yielding tension, 2 = yielding shear.

Output Parameter	Description
???_PLSN*	Discontinuity plastic normal strain, where ??? is either DFN for DFNs, or FLT for faults. The results are unified for all DFN or faults, and take the maximum value for cells with multiple discontinuities.
???_PLSS*	Discontinuity plastic shear strain, where ??? is either DFN for DFNs, or FLT for faults. The results are unified for all DFN or faults, and take the maximum value for cells with multiple discontinuities.
???_ELSN*	Discontinuity elastic normal strain, where ??? is either DFN for DFNs, or FLT for faults. The results are unified for all DFN or faults, and take the maximum value for cells with multiple discontinuities.
???_ELSS*	Discontinuity elastic shear strain, where ??? is either DFN for DFNs, or FLT for faults. The results are unified for all DFN or faults, and take the maximum value for cells with multiple discontinuities.
???_ELDS	Discontinuity elastic shear displacement, where ??? is either DFN for DFNs, or FLT for faults. The results are unified for all DFN or faults, and take the maximum value for cells with multiple discontinuities.
???_ELDN	Discontinuity elastic normal displacement, where ??? is either DFN for DFNs, or FLT for faults. The results are unified for all DFN or faults, and take the maximum value for cells with multiple discontinuities.
???_PLDS	Discontinuity plastic shear displacement, where ??? is either DFN for DFNs, or FLT for faults. The results are unified for all DFN or faults, and take the maximum value for cells with multiple discontinuities.
???_PLDN	Discontinuity plastic normal displacement, where ??? is either DFN for DFNs, or FLT for faults. The results are unified for all DFN or faults and take the maximum value for cells with multiple discontinuities.
PRESSURE	Pore pressure, given as input to simulation (not calculated).
TEMP	Temperature, given as input to simulation (not calculated).
SWAT	Water saturation, given as input to simulation (not calculated).
PERMX	Updated permeability X direction (two-way coupling).
PERMY	Updated permeability Y direction (two-way coupling).
PERMZ	Updated permeability Z direction (two-way coupling).

Output Parameter	Description
PERM_M??	Component of the matrix permeability tensor, where ?? is the X, Y, Z, XY, YZ, or ZX component.
PERM_F??	Component of the fracture permeability tensor, where ?? is the X, Y, Z, XY, YZ, or ZX component.
PP_MATRX	Pore pressure for the matrix.
PP_FRACT	Pore pressure for the fracture.
CRSTRNXX	XX component of creep strain tensor.
CRSTRNYY	YY component of creep strain tensor.
CRSTRNZZ	ZZ component of creep strain tensor.
CRSTRNXY	XY component of creep strain tensor.
CRSTRNYZ	YZ component of creep strain tensor.
CRSTRNZX	ZX component of creep strain tensor.

This publication is available from: www.gov.uk/beis

If you need a version of this document in a more accessible format, please email enquiries@beis.gov.uk. Please tell us what format you need. It will help us if you say what assistive technology you use.